Send Orders for Reprints to reprints@benthamscience.ae

Current Medicinal Chemistry, 2019, *Volume, Page Enation*

REVIEW ARTICLE

Looking for SARS-CoV-2 therapeutics through computational approaches

Marian Vincenzi, Flavia Anna Mercurio, Marilisa Leone*

Institute of Biostructures and Bioimaging, National Research Council of Italy (CNR-IBB), Naples, Italy

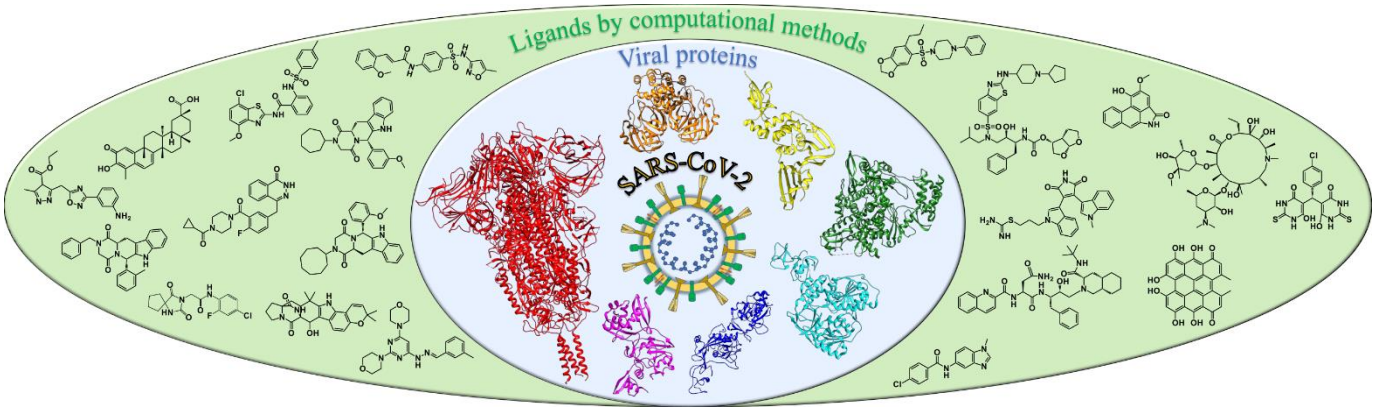

The review presents a survey of the main computational approaches that have been explored during the last few years to quickly identify potential therapeutic agents against COVID-19.

0929-8673/19 $58.00+.00

Looking for SARS-CoV-2 therapeutics through computational approaches

Marian Vincenzi, Flavia Anna Mercurio, Marilisa Leone

Institute of Biostructures and Bioimaging, National Research Council of Italy (CNR-IBB), Naples, Italy

ARTICLE HISTORY

Received:
Revised:
Accepted:

DOI:

Abstract

Background: In the last few years *in silico* tools, including drug repurposing coupled to structure-based virtual screening, have been extensively employed to look for anti-COVID-19 agents. **Objective:** The present review aims to provide readers with a portray of computational approaches that could conduct more quickly and cheaply to novel anti-viral agents. Particular attention is given to docking-based virtual screening. **Method:** The World Health Organization website was consulted to gain the latest information on SARS-CoV-2, its novel variants and their interplay with COVID-19 severity and treatment options. The Protein Data Bank was explored to look for 3D coordinates of SARS-CoV-2 proteins in their free and bound states, in the wild-types and mutated forms. Recent literature related to *in silico* studies focused on SARS-CoV-2 proteins was searched through PubMed. **Results:** A large amount of work has been devoted thus far to computationally target viral entry and search for inhibitors of the S-protein/ACE2 receptor complex. Another large area of investigation is linked to *in silico* identification of molecules able to block viral proteases -including Mpro- thus avoiding maturation of proteins crucial for virus life cycle. Such computational studies have explored the inhibitory potential of the most diverse molecule databases (including plant extracts, dietary compounds, FDA approved drugs). **Conclusion:** More efforts need to be dedicated in the close future to experimentally validate the therapeutic power of *in silico* identified compounds in order to catch, among the wide ensemble of computational hits, novel therapeutics to prevent and/or treat COVID-19.

Keywords: SARS-CoV-2, COVID-19, structure-based drug design, virtual screening, drug repurposing, molecular modelling, drug-discovery

1. INTRODUCTION

The past sixty years were characterized by the appearance of many zoonotic coronaviruses (CoVs) [1]. CoVs zoonotic pathogens originate in animals and can be transmitted to humans through direct contact [2]. During the last two decades large-scale pandemics triggered by coronaviruses, like Severe Acute Respiratory Syndrome (SARS) and the Middle East Respiratory Syndrome (MERS) emerged [3]. SARS and MERS outbreaks occurred in 2002 and 2012, respectively [4]. More recently, on 30 January 2020, the new coronavirus disease-19 (COVID-19) was established by the World Health Organization (WHO) as a public health emergency with international relevance that turned into pandemic on 11 March 2020 [5].

Thus far COVID-19 has brought terrible outcomes worldwide leading the whole world into an economic recession, destroying health-care systems, causing prolonged schools and communities' closures [6].

1.1. COVID-19: A BRIEF OVERVIEW

Since December 2019, many cases of pneumonia-like conditions of unknown etiology were revealed among people having a history of contact to the Huanan Seafood Wholesale Market in Wuhan, capital of Hubei province in China [4]. The new pneumonia cases were attributed to a CoV that the International Committee on Taxonomy of Viruses denominated on 11 February 2020 "Severe Acute Respiratory Syndrome Coronavirus 2" (SARS-CoV-2) [7]. The name SARS-CoV-2 was chosen due to its similarity with the SARS-CoV virus genome [7]. At the same time, the disease associated to SARS-CoV-2 was called by the World Health Organization (WHO) as Coronavirus Disease-19 (COVID-19) [8]. Presently, COVID-19 still represents a public international health emergency requiring the highest level of attention.

Coronaviruses owe their name by the crown-like spikes that are present on the virion surface [1]. CoVs are enveloped viruses provided with positive-sense single-stranded RNA (+ssRNA). Four principal subgroups of coronaviruses exist: alpha, beta, gamma, and delta. Alpha and beta classes might have originated from bats and rodens whereas, gamma and delta subgroups may have originated from birds [1]. Coronaviruses infecting humans (HCoVs) belong to two of these genera (alpha and beta coronaviruses) [9]. Up until 2020, six HCoVs were known [4] and, according to the aggressiveness, they were classified into highly and low invasive subclasses. HCoV-NL63, HCoV-229E, HCoV-OC43 and HCoV-HKU1 belong to the low aggressive

category and are principally responsible for infections affecting the upper respiratory tract and minor respiratory diseases [2, 3, 10]. In contrast, CoVs belonging to the highly aggressive subclass, like SARS-CoV and MERS-CoV, mostly attack lower airways and induce life-threatening pneumonia [3, 11]. SARS-CoV-2 was added as the seventh affiliate to the HCoV group; it belongs to the same lineage of CoVs responsible for SARS. However, from a genetic point of view SARS-CoV-2 is different from SARS-CoV (79% similarity) and MERS-CoV (nearly 50%) [4, 12]. As indicated by whole-genome sequencing SARS-CoV-2 presents 96% sequence identity with bat coronavirus RaTG13 whereas, 88% sequence identity was revealed between SARS-CoV-2 and the two SARS-like bat coronaviruses bat-SL-CoVZC45 and bat-SL-CoVZXC21 [3]. Nevertheless, SARS-CoV-2 shares at amino acid level over 90% sequence identity with another coronavirus from Malaya pangolins, while just a single amino acid difference was found at the receptor-binding domain (RBD) of their S (=Spike) proteins. Because the pandemic originates in a Seafood market, it has been supposed that bats and pangolins could indeed represent natural reservoirs and intermediary hosts of SARS-CoV-2, respectively [3]. SARS-CoV-2 employs as cellular receptor the Angiotensin-converting enzyme 2 (ACE2), thus, a recent investigation of ACE2 receptor amino acid sequences from diverse species proposed a possible SARS-CoV-2 transmission flow across nineteen different species [13]. However, SARS-CoV-2 is characterized by continuous human-to-human transmission and general susceptibility to humans [14, 15].

The SARS-CoV-2 pandemic represents probably the largest global public health disaster after the influenza epidemic of 1918. COVID-19 patients show the following canonical and early clinical symptoms: fever (87.9%) and cough (67.7%), moreover, 15% of patients also suffer of gastrointestinal diseases, including diarrhea, nausea and vomiting [3]. COVID-19 clinical evolution includes three principal phases: a) early infection stage, b) pulmonary phase, and c) hyperinflammation, with clinical characteristics fluctuating from slight or no symptoms to acute respiratory distress syndrome (ADRS) and multi-organ failure. Although the lungs are the principal organs targeted by COVID-19, the disease may also attack the heart, kidneys, genitals, and liver [16, 17]. In fact, as mentioned before and as will be better detailed later within this review, SARS-CoV-2 interacts with the ACE2 receptor employing the spike (S) protein to assault alveolar epithelial cells and induce straight toxicity and extreme immune responses. The resulting systemic inflammation produces in turn a cytokine storm, leading lung injury, and patients with severe disease might develop respiratory failure and even die [8, 18, 19]. The overall pathological appearance of the lungs resembles the one in SARS and MERS [8, 20]. However, as ACE2 is similarly expressed in the kidneys, heart, lung, and intestines, SARS-CoV-2 can attack cells in these tissues too thus flourishing and destroying these organs [8]. In patients suffering from severe COVID-19 conditions, the levels of several interleukins (i.e., IL-2, IL-6, IL-7, IL-10), tumor necrosis factor-α, macrophage inflammatory protein 1, granulocyte colony-stimulating factor, interferon gamma-induced protein 10, and monocyte chemoattractant protein-1 are significantly high thus possibly leading to poor outcomes [8, 21]. Patients with COVID-19 presents massive activation of lymphocytes while increased levels of pro-inflammatory CCR4+, CCR6+, and Th17 cells favors immune mediated injury [8]. Elderly people along with patients possessing defective immune systems or presenting comorbidities are more inclined to SARS-CoV-2 infection [22]. COVID-19 is found to increase the risk of venous and arterial thromboembolic events too [23].

SARS-CoV-2 is highly infectious and can last in the air for 2 hours [9]. Transmission of SARS-CoV-2 happens mainly from face-to-face contact through respiratory droplets and, to a lower extent, by interactions with contaminated surfaces [24]. The faecal-oral route represents another possible mode of transmission. Nevertheless, certain studies excluded the vertical transmission of SARS-CoV-2 from infected mothers to the newborns [25]. Because the conjunctival epithelium can be easily contaminated, transmission may occur via the conjunctiva [9]. The incubation time for SARS-CoV-2 is approximately 4-8 days after-infection [21]. Virus carriers may be provided by people who are infected but are asymptomatic and by person being in the incubation timeframe of the virus [14].

More than 6,196,243 people have died from the coronavirus COVID-19 outbreak ([26] accession date 08/04/2022).

Nowadays the health emergency situation is somehow improving due to the development of several vaccines against COVID-19 (See relevant paragraph below). In fact, during 2020 COVID-19 vaccines were successfully implemented within extraordinarily short timeframes that could not even be conceivable before [27]. In spite of massive vaccination campaigns all over the world, 2021 was a challenging year too due to the emergence of multiple SARS-CoV-2 variants [27]. In fact, unfortunately, coronaviruses exhibit ability to mutate and recombine. The genomic sequence of SARS-CoV-2 has varied since it was first identified and many variants have been reported. The battle to vaccinate the whole world will need to face also the pathogen's constant evolution to escape immunity [6]. In fact, since the beginning of 2022 it has been necessary to adapt COVID-19 vaccines to newly emerging virus lineages [6].

That said, it is evident that the scientific community cannot lower the guard and is constantly invited to discover original routes to find novel compounds targeting SARS-CoV-2 old and future variants and able to prevent viral infection and/or cure COVID-19.

During the last couple of years, the structural biology community has spent tremendous efforts to solve 3D structures of SARS-CoV-2 crucial proteins. Nowadays the structural features of many proteins relevant for different steps of virus life cycles (described in paragraph 1.2) have been elucidated. In this context computational approaches played a pivotal role to support structure-based drug design strategies, drug repurposing and the identification of novel potential anti COVID-19 therapeutic agents though virtual screening of large compound libraries.

The present review intends to stress out the importance of these computational tools in the fight against COVID-19.

1.2. SARS-CoV-2 and its proteins

SARS-CoV-2 is an enveloped virus with a spherical shape (~80–120 nm in diameter) (Fig. **1A**). The name “CoVs” is related to the amazing virus appearance similar to a solar corona that is produced by multiple glycosylated homotrimeric S proteins projecting outwardly from the virion

surface. The lipid bilayer envelope encloses nucleocapsids embracing complex of RNA and capsid proteins (Fig. **1A**) [28].

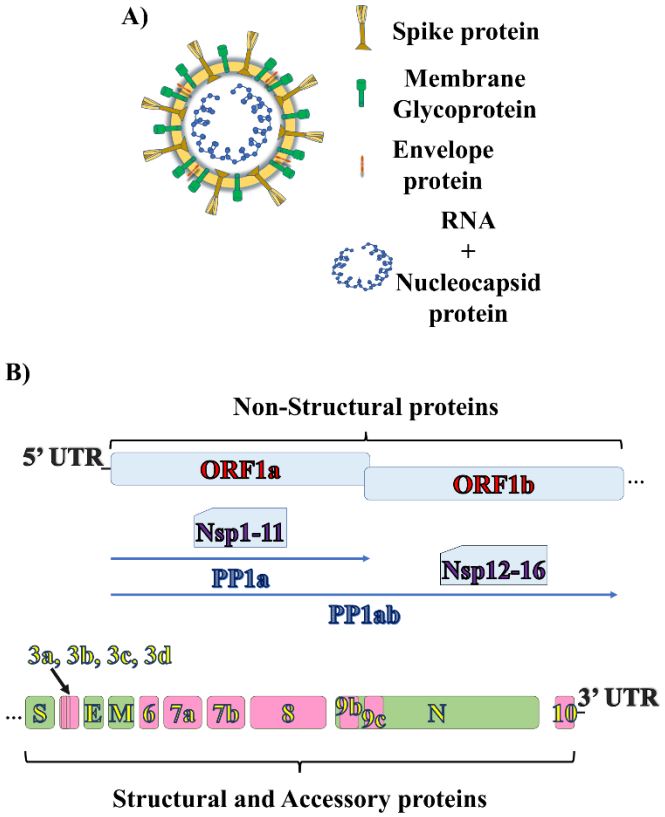

Fig. (1). A) Schematic view of SARS-CoV-2 virion and its structural proteins. **B)** SARS-CoV-2 genome arrangement. Non-structural, structural and accessory proteins are indicated by cyan, green and pink boxes, respectively. Structural and Accessory proteins are encoded by genes located towards the 3' UTR following ORF1a and ORF1b.

SARS-CoV-2 genome (~29.9 kb) (Fig. **1B**) consists of a ss +RNA (single-stranded, positive-sense RNA) [29]. Fourteen open reading frames (ORFs) are included in the SARS-CoV-2 genomic RNA (gRNA). ORF1a and ORF1b represent the two principal ORFs; they overlap with a (-1) ribosomal frame-shift and cover two-thirds of the genome. The polyproteins pp1a and pp1ab are the translation products of ORF1a and ORF1b, respectively. Viral proteases (i.e., main-protease and papain-like protease) are responsible for the processing of pp1a and pp1ab finally generating the non-structural proteins (NSPs), NSP1 to NSP16 [30]. A replication-transcription complex (RTC) is made up inside double-membrane vesicles (DMV) by a few host factors together with some of the NSPs [29]. The core of viral genome replication and transcription is represented by the RTCs. The four principal structural proteins (Spike (S), Membrane (M), Envelope (E) and Nucleocapsid (N)), and a few accessory proteins are encoded by other ORFs encompassing the rest of the genome (Fig. **1B**) [28, 30].

During viral infection, SARS-CoV-2 genome is injected into the host cell through endosomes or directly by fusion of the viral envelope to the host cell membrane, arbitrated by interaction of the human angiotensin-converting enzyme 2 (ACE2) at the cell surface with the spike (S) protein [30]. Epithelial cells of the lungs and small intestine along with heart, kidney, and additional tissues express principally ACE2 receptor. However, computational studies speculated that SARS-CoV-2 S protein might also interact with nicotinic acetylcholine receptors (nAChRs), thus pointing out a great and diverse binding potential that could explain the multi-organ pathogenesis [28, 31]. The S protein possesses a RBD (Receptor Binding Domain) region in its S1 subunit, that is actually responsible for the interaction with ACE2. It has been reported that the dissociation constant (K_D) for binding of SARS-CoV-2 S protein to human ACE2 is 14.7 nM whereas, that related to the interaction with SARS-CoV S is 325.8 nM, thus indicating the higher affinity of SARS-CoV-2 to ACE2 with respect to SARS-CoV [32]. Interestingly, a ~24% dissimilarity exists between S proteins of SARS-CoV-2 and SARS-CoV, with ~23% divergence associated to the RBD region [32].

After the virus has entered into the host cell, the viral gRNA is uncoated and released into the cytoplasm of the host and is next translated by the host ribosomes [30]. The pp1a and pp1ab polyproteins are thus produced and undergo a proteolytical cleavage that generates the nonstructural proteins (NSP1 to 16) through the action of the PLpro and Mpro viral proteases. Inside the infected host cell, the RTC is formed by the assembling of several NSPs (NSP2-16) and other factors. Within the RTC NSP12-16 provide the enzymatic machinery that is needed for viral genome replication/transcription. Initially, the RNA (+) strand is replicated to the RNA (-) strand and next the RNA (-) is employed either for generation of the RNA (+) strand necessary for the assembly of new virions or for the transcription of sub-genomic mRNAs. The structural proteins (S, M, E, N) along with the accessory proteins are generated by translation of sub-genomic mRNAs [30]. The S, M, and E proteins pass in the endoplasmic reticulum (ER), while the N protein binds to the genomic RNA (+) strand to form the nucleoprotein complex. Next the nucleoprotein complex together with the structural proteins pass to the ER Golgi intermediate compartment (ERGIC) [30, 33]. In ERGIC the virions are assembled, undergo maturation, and next, under the shape of small vesicles, bud off from the Golgi. These vesicles move towards the host cell membrane where *via* exocytosis are released into the extracellular space. The disease can spread as the newly released virions attack a novel group of cells [33].

Knowledge of structural and functional features of viral proteins allows a more rational route to designing efficacious antiviral drugs. Thus, a brief description of the diverse non-structural, accessory and structural proteins of SARS-CoV-2 is given below.

1.2.1 Non-structural proteins

NSP1

NSP1 is generated by proteolysis operated by the protease PLpro and derives by the N-terminal cleavage of pp1a and pp1ab. NSP1 interacts with the 40S ribosomal subunit and induce inhibition of endonucleolytic cleavage of host mRNA thus obstructing the protein synthesis machinery of the host cell [34]. Due to the translational slowdown several host factors cannot be adequately expressed to properly face the viral attack. NSP1 interferes with the expression of host proteins but it does not block expression of viral proteins. In the fight against SARS-CoV-2 targeting the interaction

between NSP1 and the 40S ribosomal subunit represents a clever way to help the innate immune system [30].

NSP2

The exact functions of SARS-CoV-2 NSP2 have not been fully clarified [35]. NSP2 is conserved in SARS-CoV where it has been reported to bind to two host proteins prohibitin 1 and prohibitin 2 (PHB1 and PHB2) [36]. PHB1 and PHB2 are related to several phases of cell life cycle including cell cycle progression, cell migration, cellular differentiation, as well as apoptosis, and mitochondrial biogenesis. Thus, interactions involving NSP2 let speculate this non-structural protein may function to disrupting the host cell environment [37].

NSP3/PLpro

NSP3 consists of 1945 amino acid residues thus representing the largest protein encoded by the coronavirus genome. It is a membrane-bound protein made up of several domains. NSP3 contributes to form the viral replication-transcription complex (RTC) by working as a membrane-anchored scaffold that interacts with the other NSPs and host proteins. The PLpro domain is encoded within NSP3 [38]. As the protease function is crucial to release key proteins for viral action, blockade of NSP3 protease activity represents a significant goal of antiviral drug discovery [37].

NSP4

NSP4 is a member of the CoV replication complex; 80% sequence identity exists between SARS-CoV-2 and SARS-CoV NSP4 [37]. In SARS-CoV NSP4 interacts with NSP3 and possibly other proteins from host playing a function linked to membrane rearrangement. The association between NSP4 and NSP3 is crucial for viral replication [37].

NSP5/Mpro/3CLpro

NSP5 is also identified as 3C-like protease (3CLpro, name derived from the 3C proteases of the Picornaviridae) or the main protease (Mpro). NSP5 is a cysteine protease with a molecular weight of 33 kDa, NSP5 from SARS-CoV-2 and SARS-CoV share 96% sequence similarity. NSP5 cleaves viral polyproteins, pp1a and pp1ab, at 11 distinct loci characterized by cleavage pattern LQ↓(S/A/G) thus producing twelve functional proteins. Mpro is an important target in anti-CoV drug design as inhibitors of its protease activity interfere with the viral replication machinery [30].

NSP6

NSP6 of SARS-CoV-2 has not been very well investigated, however, it is a transmembrane protein, possessing a few portions outside the membrane [37]. NSP6 function in SARS-CoV-2 may be related to autophagosome formation. In detail, NSP6 from the avian coronavirus was related to formation of autophagosomes from the endoplasmic reticulum (ER). The assembly of replicase proteins resulted enhanced by autophagosomes. On the other side, NSP6 reduced autophagosome/lysosome expansion thus avoiding autophagosomes mediated delivery of viral components in lysosomes for degradation [37].

NSP7, 8, 12

NSP12 is a RNA-dependent RNA polymerase (RdRp) [37]. A replicase complex is generated by NSP12 with NSP7 and NSP8, and is involved in the replication and transcription of viral RNA genome. Moreover, RNA primase activity is played by the NSP7-NSP8 complex throughout the viral RNA synthesis [30].

NSP 9

NSP9 function is linked to virulence. It is a single-stranded RNA-binding protein [30].

NSP10

NSP10 represents a small protein made up of 139 amino acid residues and a single domain. NSP10 works as a scaffold protein that together with NSP14 (exonuclease and N7-methyltransferase) and NSP16 (2'-Omethyltransferase) compose the mRNA cap methylation complex [30, 37].

NSP11

Further studies are needed to clarify NSP11 function [28]. This protein consists of thirteen amino acids; interestingly, the -SADAQSFLN- sequence composing the first nine residues is identical to the corresponding one in NSP12 [37].

NSP13

NSP13 represents a superfamily 1B helicase; its functions include: NTPase, duplex RNA/DNA unwinding, and 5'-RNA capping activities [30].

NSP14

NSP14 possesses a dual function as it includes an N-terminal exonuclease (ExoN) domain provided with proofreading activity and a C-terminal guanine-N7 methyl transferase (N7-MTase) domain responsible for the methylation of viral RNA cap. The evolution and maintenance of such a wide genome in coronaviruses is possibly related to the proofreading function of NSP14. Moreover, NSP14 mRNA capping activity is crucial for maintaining the stability of viral mRNA by avoiding the destruction operated by the host immune answer [30].

NSP15

NSP15 works as an endoribonuclease and is responsible for specific cleavage of RNA at the 3'-end of uridylates. Through its endonuclease function NSP15 supports the virus to escape the host immune system. Mutations in NSP15 affect viral replication highly weakening the disease in mice [30]. Consequently, original molecules able to regulate NSP15 activity and/or stability might function as antiviral agents [39].

NSP16

NSP16 is a 2′-O-methyltransferase that is crucial in immune evasion [40]. NSP16 is an enzyme responsible for the 5'-methyl capping of viral mRNA. The 5'-methyl capping avoids that the viral RNA is degraded by host 5'-exoribonucleases and provides supports to elude the triggering of innate immune answer [30]. Hence, NSP16 represents another amazing drug target for COVID19.

1.2.2 Accessory proteins

Thus far eleven SARS-CoV-2 accessory proteins have been described: ORF3a, 3b, 3c, 3d, 6, 7a, 7b, 8, 9b, 9c, and 10, whose roles during infection have still not been fully clarified [41].

Interestingly, mutations in accessory proteins including ORF3a, ORF6, ORF7a, ORF8 or ORF10 have been identified

in a few *"variants of concern"* thus possibly pointing out a certain linkage to increasing pathogenesis and transmissibility in these SARS-CoV-2 strains [41].

The accessory factor 3a represents the largest accessory protein (~274 amino acid residues) of SARS-CoV-2 and is encoded by the ORF3a gene that is positioned between the S and E genes (Fig. **1B**) [28]. This is an integral membrane protein that acts like a viroporin, forming an ion channel that could favor virus release. The accessory factor 3a is thus important to achieve maximal replication and virulence [42].

ORF3b protein is made up of 22 residues and is definitively shorter than the corresponding SARS-CoV protein, that consists instead of ~153 a.a.. Despite its small size, SARS-CoV-2 ORF3b protein works as a potent interferon (IFN) antagonist, blocking the induction of type I interferon more proficiently than the SARS-CoV ortholog. Interferons (IFNs) are secreted cytokines provided with large antiviral functions that play a key role in the first line of defense against pathogens attack [43].

ORF3c protein possesses a predicted largely conserved transmembrane domain, thus letting speculate its interactions within the lipid bilayer connected to membrane-associated and membrane-disrupting signaling roles. However, more studies are necessary to better comprehend ORF3c function during SARS-CoV-2 infection [41].

ORF3d has been more recently designated in SARS-CoV-2 as a new overlapping gene encoding a protein made up of 57 amino acids. It is now known that ORF3b and ORF3d are distinct proteins positioned in different genomic regions. ORF3d is positioned at the 5' side of the ORF3a sequence overlying the 3' half of ORF3c [41].

The protein encoded by SARS-CoV-2 ORF6 gene is 61 a.a. long and has been confined to membrane of vesicles - including autophagosomes and lysosomes- and at the endoplasmic reticulum [28]. SARS-CoV-2 ORF6 protein has strong IFN antagonistic activity [41].

ORF7a and ORF7b accessory proteins are synthesized from the bicistronic subgenomic RNA 7 of SARS-CoV-2 [29].

SARS-CoV-2 ORF7a is a type-I transmembrane protein made up of 121 a.a. residues and is another SARS-CoV-2 protein provided with capacity to antagonize the IFN-I response [41].

Little is known about ORF7b. This is an integral membrane protein of 44-amino acids and it might form stable multimers *via* leucine zipper. ORF7b could possibly affect a few cellular mechanisms that trigger certain canonical symptoms of SARS-CoV-2 infection related to leucine zipper formation and epithelial cell-cell adhesion, like heart rate dysregulation [41].

ORF8 consists of 121 amino acid residues, and it possesses a shape similar to an immunoglobulin (Ig)-like fold with a β-strand core (18–121 residues). The first seventeen residues encompass an N-terminal signal sequence, required for transport to ER. Several roles have been suggested for ORF8. Interestingly, when in cells ORF8 expression is exogenously upregulated, it destroys IFN-I signaling. Nevertheless, differently from SARS-CoV ORF8a/b, SARS-CoV-2 ORF8 downregulates MHC (Major Histocompatibility Complex)-I in cells [30]. In COVID-19 patients ORF8 is provided with a great immunogenic potential and consequently, can be employed for a precise diagnosis of COVID-19. Interestingly, along with N protein and ORF3d, it provokes the largest and most specific antibody answer among the SARS-CoV-2 antigens at different infection stages [43].

ORF9b consists of 97 amino acid residues. It tends to associate with an adaptor protein, TOM70, thus inhibiting IFN-I mediated antiviral response [28, 30]. Therefore, targeting the ORF9b/TOM70 interaction with small molecules or peptides could provide a clever anti COVID19 strategy.

ORF9c presents 94% sequence identity with bat SARS-coronavirus ORF14, and 74% with SARS-CoV ORF14 [41]. Experimental studies have shown that ORF9c SARS-CoV-2 plays a role in suppression of antiviral response. In major details, ORF9c expression was shown to impair interferon signaling, processing and presentation of antigen, and favor IL(InterLeukin)-6 signaling [41].

ORF10 protein derives from a gene located downstream of the N gene. ORF10-related sgRNA is infrequently found, even if ORF10 protein has been detected into infected cells [28]. It has been demonstrated that ORF10 is not crucial for human SARS-CoV-2 infection. SARS-CoV-2 replication capability and transmission do not vary significantly following deletion of ORF10. ORF10 sequence is diverse with respect to other coronaviruses, and precise biological roles have not been defined thus far [41].

1.2.3 Structural Proteins

SPIKE protein

As mentioned in the previous paragraphs, the entry of SARS-CoV-2 into host cells is arbitrated by the transmembrane spike glycoprotein (Fig. **1A**). The surface of SARS-CoV-2 virion is decorated by homotrimers formed by the S protein. Glycosylation of the S protein is high, in fact, it possesses 66 potential N-glycosylation loci per trimer [44, 45]. The S protein undergoes a post-translational cleavage, operated by the mammalian protease furin, that generates the two S1 and S2 subunits. The receptor-binding domain (RBD) along with an amino-terminal domain is included in the S1 subunit. The RBD is in charge of the interaction with the ACE2 host cell-surface receptor. On the other side, the trimeric core of the protein is part of the S2 subunit that intervenes in membrane fusion. Infectivity and virulence are linked to the occurrence at the S1-S2 edge of the polybasic furin cleavage site (680SPRRAR↓SV687-cleavage motif RxxR-), that is absent in other group-2B coronaviruses [46, 47]. The global stability of SARS-CoV-2 S protein is decreased by the furin-cleavage site and the proteolytic event indeed favors the adoption of the open state that is responsible for binding of S to the ACE2 receptor [48].

The RBD of S-protein represents an important target for antiviral strategies including antibody-arbitrated neutralization and vaccine development [30].

Nucleocapsid protein (N)

The Nucleocapsid (N) protein of SARS-CoV-2 is made up of 419 a.a., it presents 49 and 91% similarity to MERS-CoV and SARS-CoV, respectively [49]. The N represents a crucial structural protein that packages the viral RNA forming helical ribonucleocapsid (RNP) (Fig. **1A**) and binds other structural proteins during virions' assembly bringing to encapsidation of

the genome [30]. The nucleocapsid (N) protein by interacting straight with viral RNA provides also stability [37].

Two largely conserved domains are present in the SARS-CoV-2 N protein: the N-terminal and C-terminal domains. The N-terminal one (residues 46–174) is an RNA binding domain (N-NTD) whereas, the C-terminal (a.a. 247–364) is a dimerization domain (N-CTD) [50]. A linker region, that is provided with a large number of serine and arginine residues, highly phosphorylated and also intrinsically disordered, is positioned in between the N- and C-terminal domains [30]. The N- and C-terminal ends of the N protein are disordered too [50]. During infection a large amount of N protein is formed and being extremely immunogenic, it represents a powerful target for generating novel vaccines.

Furthermore, the N protein of SARS CoV-2 plays also the role of antagonist of antiviral RNAi [37].

Membrane (M) and Envelope (E) proteins

Coronaviruses assembling/budding occurs at the lumens of the ERGIC and new virions are released *via* exocytosis. Virion's assembly is highly orchestrated by the M and E proteins. In β-coronaviruses M and E proteins are conserved and present more than 90% sequence identity in comparison with the SARS-CoV homologs [30].

M, E and S structural proteins gather in the ER as they are provided with the trafficking signal sequences. The effective integration of these proteins along with the ribonucleoprotein complex is crucial to achieve maturation and budding of novel virion particles [51].

The SARS-CoV-2 M protein is the most abundant structural protein, it consists of 222 amino acids and is a long transmembrane glycoprotein. Three main domains compose the M protein. In detail, the ectodomain is localized at the N-terminus and is followed by three transmembrane helices (TMH1-TMH3) whereas, the endo-domain is positioned at the C-terminal side [30]. The M protein participates in homotypic interactions with itself and into heterotypic complexes with diverse structural proteins (i.e., S, E and N). These interactions provide a sort of platform for new virions assembly [52].

The E protein contributes to form the outer capsid in coronaviruses (Fig. **1A**) [52]. The E protein of SARS-CoV-2 is the smallest transmembrane structural protein and consists of 75 amino acids [53]. Its domain organization includes an N-terminal hydrophilic ecto-domain, a hydrophobic transmembrane domain (TMD) preceding a long hydrophilic endo-domain that is instead positioned at the C-terminal side. Structural studies revealed a viroporin-like arrangement of the TMD of SARS-CoV-2 E protein composed by a pentameric helix bundle arrangement surrounding a cationic hydrophilic central channel [54]. These ion channels cause generally loss of membrane potential and trigger activation of host inflammasome [30].

The E protein has been shown to play multiple roles in the viral replication cycle: viral assembly, virion release, and viral pathogenesis [37]. In fact, recombinant CoVs lacking E protein represent good vaccine candidates as they exhibit decreased viral titres, weakened viral maturation and incompetent viral propagation [30].

1.3. COVID19 vaccines and therapies

Most of the treatment opportunities and strategies that are being explored against COVID-19 derives from the preceding experience acquired in fighting other emerging viral diseases like SARS and MERS [4]. Vaccines, immune-therapeutics, and antiviral drugs are at the heart of a few of the therapeutic routes that were undertaken against the earlier SARS-CoV and MERS-CoV outbreaks [4, 55]. Commercial and approved vaccines against these two previous CoVs do not exist as SARS-CoV and MERS-CoV attracted much less attention than SARS-CoV-2. The reason lies largely in the fact that SARS-CoV and MERS-CoV infected a lower slice of human population worldwide while causing not much disorder, global hazard, and panic in contrast to those induced by the SARS-CoV-2 pandemic [4].

Vaccines and drugs are crucial weapons to fight against the SARS-CoV-2 outbreak. Vaccines are linked indeed to a successful tale while it is being really challenging to develop anti-SARS-CoV-2 drugs [56]. Vaccination and therapeutic treatments represent potential routes to protect human population along with the public health plan to lower transmission. Infections can be opposed with prophylaxis; prophylaxis (=protection generally due to an antimicrobial therapeutic agent) decreases the morbidity and mortality loads, and the socio-economic aspects connected to the pandemic, but it is usually inefficient for those patients that have already been infected or stay in the days just before [56]. In order to avoid infection during a pandemic, vaccines are crucial whereas, antimicrobials are useful to rescue those who develop the infection. Generally, vaccines are characterized by large specificity towards an infectious agent, so there's a need to generate a new vaccine for each novel virus. On the contrary, drugs may possess much larger efficacy, and so can be soon accessible and ready to be employed against new infections. Currently, drug repurposing of the existing therapeutics, that have been previously developed to battle further viral diseases can be considered a good route to alleviate the present-day pandemic condition.

Soon after SARS-CoV-2 appeared at the end of 2019, the spike protein (principally in its native/prefusion state) was recognized as the main immunodominant antigen of the virus [57]. Analyses of patients infected with SARS-CoV-2 demonstrated that neutralizing antibodies primarily target the receptor-binding domain positioned in the spike S1 subunit [58]. After this potential vaccine target was recognized, next it was necessary to understand how to produce an effective immune answer against SARS-CoV-2. The immune response would comprehend generation of neutralizing antibodies, production of a T-cell answer, and evasion of immune-enhanced disease [58]. To fight the present outbreak, several strategies were verified simultaneously. Consequently, motivated by the urgency of the outbreak and the support afforded by numerous funding agencies, several preclinical candidates for the anti-Covid-19 vaccine were generated in a manner never seen before [58-61]

The main vaccination strategies that were undertaken to fight against SARS-CoV-2 included mRNA vaccines, viral vector and inactivated virus vaccines, protein subunits vaccines.

mRNA vaccines comprehend those produced by Pfizer-BioNTech and Moderna [59]. In these vaccines, lipid nanoparticles are employed to protect the mRNA encoding for the prefusion-stabilized S protein in its route towards the intracellular space. This mRNA is used by the host to produce

the target S protein, which generates a synchronized immune answer. During clinical trials Pfizer-BioNTech and Moderna mRNA-based vaccines showed more than 90% efficacy against SARS-CoV-2 disease [58].

However, in spite of a rather good efficacy, RNA vaccines present intrinsically small stability, moderately short shelf-life and often their storage or transport necessitate dedicated equipment [62]. This kind of vaccines presenting low stability requires to be stored under very cold temperatures, thus their distribution may be really challenging. Pfizer's vaccine needs to be stored at −70 °C and it cannot be refrigerated for more than 5 days whereas, Moderna's vaccine can be kept at −20 °C and be refrigerated for just 30 days [63, 64]. The new SARS-CoV-2 variants that have more recently been developed possess certain mutations, a few of which are positioned in the RBD, that theoretically could decrease a vaccines' capacity to induce immunity against such novel variants [62, 65].

Astra-Zeneca, Johnson & Johnson, Reithera and Sputnik produced viral vector (adenovirus) vaccines. Viral vector vaccines rely on a virus, that has been genetically engineered so that it is unable to induce an infection but, produces an immune response through generation of coronavirus proteins [59]. Such replication-incompetent adenoviruses were in the past also settled for different viruses such as malaria, Ebola, HIV, tuberculosis [58].

Inactivated virus vaccines represent another kind of vaccines obtained from a virus, that was grown in culture and next chemically deactivated, but able to distribute stably expressed, conformationally native antigenic epitopes. This kind of vaccine is being produced by manufacturers like Sinopharm and Sinovac [58, 59].

Protein subunits vaccines were instead produced by Novavax. Protein-based vaccines induces a safely immune answer through employment of pieces of proteins or protein shells that mimic SARS-CoV-2 external coat [59, 66]. For example, an additional way to generate a vaccine consists in the delivery of the S protein, in the form of recombinant protein subunit inside a certain cell-based platform able to support protein expression. The formulation of most protein-based COVID-19 vaccines includes adjuvants to gain a better immune response [67]. Novavax, through the saponin-based Matrix-M adjuvant, lately described its late-phase clinical trials in the UK, indicating 89% vaccine efficacy against COVID-19. Many vaccines, that are presently in development rely on the protein subunit strategy [58, 59].

Overall, the presence of variants of SARS-COV-2 virus - like the Delta one - produced a decrease of vaccines efficacy although Pfizer, Moderna and Janssen maintained a rather decent level of protection [59].

Even if vaccines demonstrated high potentials, they may be accompanied by "*troubles*". In fact, the production of a few vaccines has been slowed down or completely halted, like the V590 and V591 vaccine candidates produced by Merck [56]. On March 15, 2021, the AstraZeneca vaccine was withdrawn after having been employed for rather a long time in both the UK and in a few European countries, and this event generated a large confusion in the population. Moreover, on April 13, 2021, the Janssen vaccine was also paused by the FDA, due to the occurrence of a few cases of severe blood clots thus bringing the vaccination campaign to be delayed. Nowadays many diverse vaccines have been or are being produced around the world [59].

Vaccines of future generation will hopefully defend the population from virus variants containing spike mutations through production of larger and more efficient T-cell responses with respect to the currently available vaccines. Apart from the spike protein that generally plays a pivotal function in provoking the immune answer during the progression of viral infection [68], other proteins, like the N protein, M protein, non-structural and accessory proteins, could possibly work as antigens. Indeed, as explained in the previous paragraphs, viral proteins alone and in complex with host factors are linked to dysregulated host immune answers, including decreased IFN-I and IFN-III levels, and increased pro-inflammatory cytokine amounts [68].

As several COVID-19 vaccines are accessible but, their trustworthiness among people of different age groups and their long-term "guard" ability remains still dubious, it is important looking for anti-SARS-CoV-2 drugs. A few antiviral drugs demonstrated some positive outcomes in treated patients and were related to reduced risk of disease along with decreased adverse clinical manifestations [69]. Nevertheless, thus far, no antivirals resulted to be completely efficacious. Antiviral agents work through diverse routes like inhibition of viral particle's entry, blockage of virus-encoded enzymes, attack towards a specific host that is important for viral particle formation, or inhibition of viral replication [69].

Along with antivirals (i.e., favipiravir, remdesivir) other different classes of drugs have been tested or are being tested against COVID-19 including antibodies (i.e., hyperimmune immunoglobulins and convalescent plasma), antifibrotics - like tyrosine kinase inhibitors-, anti-inflammatory agents -like dexamethasone-, targeted immunomodulatory therapies for example employing tocilizumab, anticoagulants - like heparin - [24]. It is possible that a variety of treatments might possess divergent efficacies when the infection is at diverse stages or is accompanied by a particular clinical state. It is to be expected that viral blockage through drugs would be most efficacious at the early disease stage, whereas, in hospitalized patients, immunomodulatory therapeutic agents may be convenient to stop illness progression. On the other side, anticoagulant agents may be employed during infection to avoid thromboembolic complications [24].

Original strategy to find novel antiviral therapeutics against SARS-CoV-2 might employ natural products (NPs) and peptides. NPs gained a lot of attention in drug design as crucial scaffolds [70]. To search for new bioactive compounds with anti-SARS-CoV-2 activity, a group of scientists looked in literature for compounds with inhibitory activity against coronaviruses, their target proteins and other viruses, like HIV, Influenza A virus, human simplex virus or their target proteins and thus identified 42 NPs that they suggest to test against SARS-CoV-2 virus [70].

Peptides (generally made up of <5–100 amino acid residues) can be also considered to develop novel therapeutics as they possess several advantages with respect to traditional small molecule drugs and large biologics for anti-SARS-CoV-2 therapies. In fact, peptides present large specificity and affinity, little toxicity, low immunogenic activity [62]. Nevertheless, many peptide delivery strategies have been already established; in addition, peptides could in principle

been developed in a relatively short time lapse and possess rather good long-term stability upon storage under mild conditions [62, 71, 72].

1.4. Computational approaches in antiviral drug discovery

Starting two years ago to alleviate the pandemic and fight COVID-19, many efforts are being devoted to implement therapy and vaccination strategies. Knowledge of the molecular machinery governing SARS-CoV-2 pathogenesis has been fast acquired and progresses have been as well made as concerning vaccines developments [62]. However, an efficacious therapy to treat patient affected by COVID-19 is still lacking. For example, one good strategy to lighten the difficult situation appears drug repurposing of established therapeutic agents that have been previously developed to fight different viruses [62]. In this context, computational approaches are crucial to support the identification of SARS-CoV-2 original drugs and have assumed a great relevance during the pandemic. FDA (Food and Drug Administration)-approved drugs and compounds, currently in clinical trials for several diseases, are being employed in target-based or ligand-based approaches through docking or other computational techniques to investigate possible interactions with SARS-CoV-2 proteins [73]. In addition, large compound databases are being implemented in artificial intelligence (AI) strategies to identify therapeutic agents with known antiviral properties that could be exploited in drug repurposing. AI methods can be employed to analyze combinations of drugs but also remote linkages relating drugs to specific human and viral protein targets thus highlighting previously unknown biological activities. All these investigations stress out the relevance of *in silico* approaches to support drug discovery by providing a platform to evaluate a large volume of accessible biomedical data [73].

Similarly, specific bioinformatic tools have been developed quickly, right after the COVID-19 pandemic hit the world, to support SARS-CoV-2 research and enhance the detection, knowledge and treatment of COVID-19 [74]. Nowadays there are established bioinformatics roadmaps and tools to detect routinely SARS-CoV-2 infection, to analyze sequencing data, to track COVID-19 pandemic and evaluate actions able to contain it, to investigate SARS-CoV-2 evolution, to identify possible drug targets and design therapeutic routes [74].

UniProt (Universal Protein resource) is a bioinformatic resource [75] from which one can gain access to cutting-edge data related to viral or host proteins relevant to the disease. The COVID-19 UniProt roadmap supports research on SARS-CoV-2 by providing latest knowledge on proteins relevant to the disease for both the virus and human host. In addition, COVID-19 Uniprot offers the advantage to allow visualization of sequence features through the ProtVista tool [76], and provides access to several sequence analysis tools, along with COVID-19 publications provided by the scientific community.

Large-scale functional annotation of proteins can be retrieved by the Pfam (Protein families) database that is widely employed by the molecular biology community [77]. Lately the Pfam version 33.1 has been updated to include a subset of models that broadly cover SARS-CoV-2 encoded proteins.

CoV-GLUE database [78] is rather useful to SARS-CoV-2 research as it focuses on variations occurring in the SARS-CoV-2 genome. In fact, while the pandemic is moving forward, SARS-CoV-2 RNA genome is naturally gathering nucleotide mutations. CoV-GLUE collects all amino acid substitutions, insertion and deletions in SARS-CoV-2 viral genome.

In order to discover novel potential therapeutic agents, it is of utmost importance to understand the molecular machinery governing virus life cycle. A pivotal function during the course of a viral infection is attributed to the interaction network linking viral and host proteins. Drug repurposing, as mentioned before, by focusing on well-established drugs and PPI (Protein-Protein interactions) represents a much cheaper and easy route to identify antiviral agents with respect to a canonical drug-design strategy. As concerning SARS-CoV-2, an advantage relies on the virus genus that has already been widely investigated. In fact, by searching data on other beta-coronaviruses, particularly SARS-CoVs, much information can be extrapolated for example about potential therapeutic targets. In this context, databases exist where to look for virus host PPIs and virus-drug interactions on different viruses from which to get hypothesis about possible therapeutic agents and target PPI for SARS-CoV-2 and eventually set up drug-discovery strategies [74].

A wide-ranging collection of PPIs linked to several coronaviruses (i.e., MERS-CoV, SARS-CoV and SARS-CoV-2) is for example contained in the database VirHostNet (Virus Host Network) [79]. The VirHostNet SARS-CoV-2 offers indeed a systems virology platform useful for ranking repurposing of potential drugs. Similarly, CORDITE (CORona Drug InTERactions) database contains info, collected from published articles and preprints, on possible SARS-CoV-2 targets along with therapeutic agents and their interactomes [80]. CoVex (CoronaVirus explorer) is an interesting database to support drug repurposing for SARS-CoV-2 and from which to look for previously approved drugs [81]. On the other side the P-HIPSTer (Pathogen-Host Interactome Prediction using STructure similarity) databank [82] can help advancing SARS-CoV-2 studies by 1-furnishing potential molecular interactions connected to viral infection and pathogenesis to be tested and, 2-suggesting possible drug targets (including pathways and host factors) to treat infection provoked by diverse coronaviruses [74].

Inhibition of enzymes important for viral replication provides a route to fight SARS-CoV-2 [83]. Thus, to facilitate the drug discovery process, the drug database DockCoV2, focused on SARS-CoV-2, was generated. [83]. DockCoV2 can predict the interaction affinity of FDA-approved and Taiwan National Health Insurance (NHI) drugs with crucial SARS-CoV-2 related proteins (i.e., five viral proteins -spike protein, 3CLpro, RNA-dependent RNA polymerase (RdRp), PLpro, and N protein- and two human host proteins -ACE2 and the protease devoted to S protein priming TMPRSS2 (Transmembrane protease serine 2-)). A set of 3,109 drugs are comprised in this database. DockCoV2 is cross-linked to other databases, allows users to download docking results with the protein of interest and analyze several information concerning the drugs [83]. For example, DockCoV2 permits to gain knowledge on drugs that have already been demonstrated useful to fight against MERS or SARS-CoV [83].

Computational and knowledgebase strategies were also employed to gain insights in the host signaling pathways linked to virus-host relationship by combing data on experimentally corroborated host proteins interaction-

networks and host genes differentially expressed in SARS-CoV-2 infection [84]. Such a study searched for signaling pathways involving interactions between viral and host-proteins, and led to identification of several routes connected to antiviral immune answer including HIF-1 (Hypoxia-Inducible Factor 1) signaling, IL-17 pathway, Toll-like receptor signaling. The virus could use its proteins to manipulate many of the discovered signaling routes and strengthen its life cycle and survival. The same study revealed as well that genes, whose regulation resulted messed-up during SARS-CoV-2 infection, could also play a role in development of heart and kidney and in signaling routes involved in diabetic complications thus explaining the higher health risks connected to COVID-19 in patients with comorbidities. This work, supported by a computational approach, indicates that SARS-CoV-2 develops an efficacious immune escape strategy by letting its proteins to take part in diverse immune and other cellular signaling routes thus generating in the host a relevant illness state [84].

Another interesting field in the SARS-CoV-2 research concerns with multiepitope vaccine design [85, 86], to this aim several computational drug design tools are employed to predict antigenic epitopes able to induce a strong immune answer starting from SARS-CoV-2 structural proteins. The identified epitopes are linked together as suggested by *in silico* design and a combination of docking studies, molecular dynamic simulations and homology or ab-initio modelling is used to gain 3D models of the vaccine along with structural and dynamic features characterizing them in isolation or in complex with host receptors.

In summary we have widely described bioinformatic tools flourished during the last years bringing to generation of several useful databases, that are constantly upgraded, to support SARS-CoV-2 research. Other computational tools include homology or ab initio modelling, virtual screening, molecular dynamics simulations that, combined with the support also of bioinformatic resources, favor the drug discovery process.

In the next paragraphs these tools and their applications will be described separately in major details.

2. HOMOLOGY/MOLECULAR MODELLING

In absence of experimental structures of SARS-CoV-2 proteins, once the SARS-CoV-2 genome was made publicly available, many homology models were generated especially exploiting the sequence similarity between proteins of SARS-CoV, MERS-CoV and, SARS-CoV-2 [54, 87, 88]. In absence of experimentally derived structures, homology models of proteins with known templates potentially allow to identify ligand-binding pockets and get insights in the likely antiviral properties of these protein-ligand complexes.

CASP (Critical Assessment of Structure Prediction) aims to bring advance in the field of computing protein structure from sequence. In 2020, CASP started a community project focused on building structures of the most structurally challenging proteins encoded in the SARS-CoV-2 genome. Forty-seven research groups participated to the project by submitting more than 3,000 3D models and also worked to define local and global accuracy of these models. The models were next released to the public [89].

Moreover, to support researchers to employ quickly evolving structural data and to obtain further understanding into the molecular machinery governing COVID-19 infection, a study was conducted based on protein sequences related -according to UniProt definition- to the viral proteome. In detail, each SARS-CoV-2 protein sequence was compared with 164,250 PDB entries representing all accessible protein 3D structures from any organism [90]. Initially, 872 sequence-to-structure alignments produced meaningful structural similarity and provided 3D models. To make the gained structural data available and useful to other scientists, the 3D structural models were arranged in a structural coverage map, i.e., a kind of original visualization summarizing known and unknown information related to the 3D structure of the viral proteome. The derived Aquaria-COVID resource is available online (https://aquaria.ws/covid19, accession date 08/04/2022 [91]) and to date it contains 2,060 structural models built by identifying all sequence areas with obvious similarity to any published 3D structure [90].

In another work detailed comparison of sequences of each crucial protein from SARS-CoV-2 and other bat SARS-CoVs was conducted, and differences were pointed out. After building homology models the authors analyzed also if the new sequence changes in SARS-CoV-2 could influence protein function. This study showed that the sequences along with structures of the E, M and N SARS-CoV-2 structural proteins are mostly consistent with those of the bat SARS-CoV. Similarly, no relevant differences could be detected as concerning the main proteases PLpro and 3CL hydrolase. The predicted protein structures resulted highly reliable and the homology model of PLpro was further employed in docking studies with a tri-peptide library. The same study highlighted the major differences related to S proteins. Nevertheless, docking studies with ACE2 let speculate similar binding capacity of SARS-CoV-2 and SARS-CoV [87]. For the M protein of SARS-CoV-2 an interesting study also reported on the generation of protein models with a template-free approach (de novo or ab initio modelling) employing Robetta [92] and trRosetta [93] servers. The model was next implemented in 100 ns molecular dynamics simulations executed by incorporating a membrane milieu [94].

To date many structures of relevant SARS-CoV-2 proteins have been experimentally solved and deposited in the PDB (Protein Data Bank) (see paragraph 4) and of course the reliability of an experimentally determined structure is higher than that of a homology model. However, as described above molecular modelling techniques helped a lot the scientific community at the beginning of the SARS-CoV-2 pandemics by exploiting the similarities in between proteins from different coronaviruses. For nowadays studies, having in hand many experimentally derived structures of SARS-CoV-2 proteins and their complexes, structure-based drug design relying on computational strategies has flourished.

3. MOLECULAR DYNAMICS

Molecular dynamic (MD) simulations centered on SARS-CoV-2 proteins and their complex with small molecules or other protein interactors have also been largely described in literature.

Many such studies analyzed the most relevant viral protease 3CLpro (=Mpro) that, as described in paragraph 1.2.1,

represents a well-established target for antiviral drug discovery.

Somboon and collaborators studies investigated 3CLpro structural and dynamic features, along with the binding efficiency of a few peptidomimetic inhibitors, that have been previously co-crystalized with the protease, through all-atom molecular dynamics simulations and solvated interaction energy-based binding free energy calculations [95]. The gained insights could be exploited in future for generating original and highly potent SARS-CoV-2 3CLpro inhibitors to fight COVID-19.

Similarly, Suarez and Diaz in their work analyzed diverse configurations of the SARS-CoV-2 3CLpro protease by focusing on different enzyme states: monomeric/homo-dimeric forms, in the free state or in complex with a peptide substrate [96]. Tertiary and quaternary structures, inter-residue contacts in the active site or at the protomer interface were studied in detail through 2.0 s MD simulations thus obtaining key structural and dynamic features [96].

Another work reported on the design of new protease ligands by employing previously described small-molecule inhibitors of the SARS-CoV Mpro protease to generate a pharmacophore model. Different approaches and scaffolds were investigated *in silico* and ten novel compounds were designed. Next, the newly designed molecules were analyzed by molecular docking and dynamics simulations to evaluate the fitting in the SARS-CoV-2 Mpro active site [97].

Likewise, in an attempt to identify new and potential therapeutic agents able to target and inhibit SARS-CoV-2 Mpro, a multi-step *in silico* strategy was set up by employing a few N-aryl amide/aryl sulfonamide-based fragments. Several commercially available compounds from the database ZINC15 [98] were retrieved by a sub-structure query of co-crystallographic fragments. To identify the binding topology of fragments within the Mpro active site, molecular docking studies were first conducted to shed light on intermolecular contacts and interaction modes. Next, the best scoring docking solutions were re-evaluated based on the time-dependent stability that was analyzed through 50 ns molecular dynamic simulations. MD simulations highlighted that a specific fragment (i.e., ZINC_252512772) provided a more stable interaction with Mpro active site. MD results were further strengthened by quantum chemical calculations that also revealed a crucial H-bond (persisting for 98% of MD simulations time) involving Mpro conserved residue Glu166 and ZINC_252512772. Results from this study accompanied by good drug-like physicochemical properties let speculate that ZINC_252512772 could be an ideal starting candidate from which to generate SARS-CoV-2 inhibitors [99].

Another interesting study described canonical and mixed-solvent MD simulations of SARS-CoV-2 Mpro, and a comparison was carried out between the obtained results and those gained for SARS-CoV Mpro [100]. Even if there is a high sequence homology between SARS-CoV and SARS-CoV-2 Mpro, the size and shape of Mpro active site is rather diverse in these proteins thus indicating that repurposing of SARS drugs against COVID-19 could not bring to positive outcomes. MD simulations pointed out important factors that could be exploited to design novel compound inhibitors and potential COVID-19 therapeutics. First of all, the flexibility and plasticity of SARS-CoV-2 Mpro binding site, that was characterized by conformational movements during time, should be kept into account for drug design. Nevertheless, when mutations were inserted into the flexible loops, a certain structural stability was revealed thus letting speculate that a major challenge when designing novel therapeutics could be linked to the virus' mutability. Finally, MD simulations shed light on crucial stabilizing Mpro residues that could be considered as anchoring point for drug design [100].

The Amaro lab performed instead intensive molecular dynamics simulations suggesting original routes for the development of novel SARS-CoV-2 vaccines [101, 102]. In detail, all-atom MD simulations of the glycosylated full-length model of the SARS-CoV-2 spike protein were carried out in a membrane/aqueous background. MD simulations were performed by focusing on several conformations of the spike protein, i.e., open and closed states. This revealed the structural role of two N-linked glycans (N165 and N234) that resulted important to regulate the conformational dynamics of the RBD, apart from exclusively "protecting" the spike protein. A complete picture of the glycan shield around the spike protein was obtained in the time scale of nanoseconds to microseconds. Interestingly, the work also revealed that the stalk of the spike protein represents the region that is most efficiently shielded by glycans, with a coverage equal to ~90%; whereas, the head of the spike protein presents only ~62% of shielding by glycans. In summary, this work interestingly points out the weak points of the spike's glycan protection thus suggesting protein regions that could be more easily attacked by drugs or be exploited for vaccine design [101, 102].

Molecular dynamics simulation coupled to amide hydrogen-deuterium exchange mass spectrometry, were as well used to get insights into the binding interface between the S protein and ACE2 receptor and revealed long-range allosteric spread of ACE2 binding to loci crucial for host-mediated proteolysis of S protein, a key event for virus entry into the host cells. This work remarkably pointed out that protease docking sites nearby the S1/S2 cleavage position may provide different allosteric target hotspots for the development of potential therapeutics [103].

MD simulations were employed as well to study the changes induced in the spike protein by increasing temperature [104]. Following 200 ns of simulations at diverse temperatures, it was revealed that the S1 domain (i.e., the solvent exposed domain) was more mobile than the S2 (i.e., the transmembrane domain). Structural studies highlighted the presence of several charged residues on the surface of N-terminal domain of S1 which resulted to be optimally oriented at 10-30°C. Instead, around 40°C, it was found that the receptor binding motif (RBM), contained in the RBD of S1, started to assume a closed conformation that was completely achieved at 50°C. The closed conformation by masking receptor binding residues hampers the capacity of the virus to interact with the ACE2 receptor. Nevertheless, this S protein dynamics was not affected by glycan moieties. Thus, these molecular dynamics simulations, by revealing that at diverse temperatures there were different active and inactive conformations of the S protein, provided interesting insights to better understand molecular mechanism at the bases of SARS-CoV-2 functioning. At the same time these findings could also support the development of novel therapeutic agents and/or vaccines [104].

At the earliest stages of the SARS-CoV-2 pandemic when there was an urgent need for a vaccine, immuno-informatic approaches were employed to design multi-epitopic subunit vaccines. Predictions suggested the most efficient antigenic epitopes that could generate the strongest immune response. One study reported on the design of a vaccine by joining all these putative antigenic epitopes, that derived from SARS-CoV-2 structural proteins crucial for virus survival and pathogenicity, with *ad hoc* chosen linkers in order to achieve the largest stability and immunogenicity. The structure of the resulting vaccine was predicted and docking studies were conducted with the human TLR-3 (Toll-like receptor 3) receptor. Molecular dynamic simulations of the TLR-3 receptor/vaccine complex allowed a better understanding of dynamic motions and binding stability [86].

The nonstructural protein 16 (NSP16) is a 2'-O-methyltransferase (MTase) that catalyzes the transfer of a methyl group from its S-adenosylmethionine (SAM) cofactor to the 2′ hydroxyl of ribose sugar of viral mRNA thus favoring immune evasion by avoiding that the mRNA is recognized and degraded by host pathogen recognition machinery [105]. NSP16 however works by binding NSP10. To better comprehend the interaction between these two non-structural proteins and clarify the molecular mechanisms linking NSP10 to the MTase activity, molecular dynamic simulations in conjunction with the Molecular Mechanics Poisson-Boltzmann Surface Area (MM/PBSA) method were employed to study the conformational dynamics and energetics governing the binding of SAM to NSP16 alone and in complex with NSP10. This study revealed that favorable van der Waals and electrostatic interactions between SAM and NSP16 are increased when NSP10 is present. Therefore, NSP10 works to ensure a stronger binding of SAM to NSP16. This represents a further example of how molecular dynamics can provide structural information that could next be exploited for the design of peptide inhibitors of the NSP10/NSP16 heterocomplex with antiviral potential [105].

MD simulations of SARS-CoV-2 membrane protein in a membrane mimetic environment have been reported as well [94].

The variety of topics treated with MD simulations and described above clearly demonstrates how this computational approach is able to reveal the most dynamic features of SARS-CoV-2 proteins and their complexes and provides precious information on their structural stability in different environments. MD not only shows structural insights to be exploited in the design of novel drugs but also represents a useful tool to further validate results from docking.

4. VIRTUAL SCREENING & DRUG REPURPOSING

Starting early 2020 to date thousands of experimental structures of SARS-CoV-2 proteins have been characterized. A search within the PDB (https://www.rcsb.org/ accession date 08/04/2022 [106]) using SARS-CoV-2 as a keyword indicated 2,238 structures. Mainly X-ray diffraction and cryo-electron microscopy were employed to gain structural features of diverse viral proteins (i.e., non-structural, structural, and accessory proteins in the unbound and complexed states) [30]. NMR structural studies related to SARS-CoV-2 flourished as well [107].

Structural data are fundamental to understand the intricate mechanisms governing viral machinery at the atomic level and to better comprehend the different phases of the viral life cycle including attachment/entry to the host cell, reproduction of the viral genome, transcription, genome wrapping and assemblage of the virion. Many of the structurally characterized proteins are indeed also targets for the development of drugs to treat COVID-19 [30].

Structure-based drug design driven by docking studies and virtual screening strategies constitute a fundamental step to find out original lead compounds with therapeutic potentials against several diseases including viral infections [108]. In fact, computational Virtual Screening (VS) is particularly useful to face the challenges linked to antiviral drug discovery. *In silico* approaches including docking [109], pharmacophore-based screening [110] along with ligand-based similarity searches [111] are routinely employed to look at very large libraries of virtual molecules and identify the potential best drug candidates thus reducing the number of compounds under investigation to be next experimentally validated [112]. Interactions between ligands and biological macromolecules can be well described through computational VS by *in silico* models. There are indeed 2D and 3D *in silico* methodologies [113]. 2D methods represent descriptor-based approaches in which scalar molecular features are calculated and compared with the goal to discover compounds that present similarities respect to the considered molecular characteristics. 3D methods have been more widely used recently in most computational strategies aiming to identify anti-viral agents. 3D methods generally intend to define the complementarity (from a steric and chemical point of view) between the 3D conformations of the interacting compound and the chosen target (i.e., a protein or other biological macromolecule). 3D models can be generated through two main strategies: 1-the structure-based design relies on the 3D structure, that has been obtained by a specific experimental technique, of a therapeutically relevant macromolecular target; 2-the ligand-relying design is based on an ensemble of ligands, which binds the same macromolecules at an identical binding site [109]. In the best-case scenario, the binding site is known as the 3D structure of the complex between target and ligand has been determined for example by co-crystallization (i.e., X-Ray methodology). If this kind of structural information is missing, it is better to employ ligand-based design. Ligand-based design requires that biologically active molecules are known, but their shared binding site needs in this case to be experimentally proved for example through mutagenesis approaches. It is thus possible to look for original putative interactors that present a similar 3D profile as concerning either molecular shape/volume or chemical features (including charges, hydrogen bond donors/acceptors, lipophilic regions). At the lead optimization stage, when chemical modification of compounds is being achieved to improve target affinity and consequently biological activity, structure-relying 3D methods are most informative as, by positioning the possible active compounds in the specific binding locus, let speculate the best chemical modifications to be realized. Protein-ligand docking represents the most widely employed structure-based 3D strategy; its goal is to predict the binding topology of a compound for a specific target whose 3D structure is available, and it is generally based on the assumption that the ligand is flexible while the protein binding site is largely rigid [114]. As already mentioned before, another approach consists in 3D pharmacophore modelling that assumes that a few chemical characteristics (for example

lipophilic regions, charges, hydrogen bonds) can be arranged three-dimensionally to generate a model able to represent the interaction between a target macromolecule and a ligand [115]. 3D pharmacophore models are indeed generated by looking at well chemically defined sets of interactions characterizing the bioactive conformation of a ligand. The accurate 3D spatial arrangement of chemical properties to identify compounds able to meet the needed interactions is among the most fruitful VS strategies and has provided crucial hints to explain ligand affinity and drive ligand design. 3D analogs of a single molecule can be identified through shape-based similarity screening as well [116].

All the briefly described VS methods have been employed lately to find out anti-viral agents through screening of large and varied molecule databases even by focusing on compounds with previously unidentified antiviral potentials.

For example, when in 2002, the SARS pandemics took place in China, many efforts were devoted to discover therapeutic agents to fight the coronavirus producing the disease. To this aim the two principal protein targets in drug discovery were the SARS-CoV S protein and its protease Mpro. Molecules able to block the activity of SARS-CoV Mpro were identified and optimized with the support of VS [112]. The virus mutability generally represents a big issue as even if a therapeutic agent has been identified it could result inactive in a diverse virus variant.

Lately, VS has been mainly employed at the lead-discovery phase with docking as the main screening methodology. Docking is particularly useful at the early stages of lead discovery when only a relatively poor amount of information is available. Instead, similarity search strategies can be implemented only if at least one compound interactor is available. As an alternative, pharmacophore models require a larger amount of information to be implemented, including the knowledge of several ligands or the experimental structure of target/ligand complexes, and consequently, they can rarely be employed at the early stages of a drug discovery program. On the contrary, at advanced drug discovery phases, when a large amount of experimental data is available, 3D pharmacophore models can be particularly supportive of VS bringing to identify molecules provided with a large structural variability against specific targets. Similarity searches are advantageous as concerning computational time, with respect to docking that is rather time-consuming when applied to large-scale VS campaigns [112].

In the case of SARS-CoV-2, VS of large databases of compounds has been mainly applied to find inhibitors of viral entry in the host cells. At this regard, VS campaigns have been focused on discovering ligands of host ACE2 receptor and/or SARS-CoV-2 spike protein to block their interactions [117]. An active research area concerns as well with the identification of inhibitors of SARS-CoV-2 related proteases (like Mpro) [118, 119] and other enzymes [120-122] crucial for virus life cycle. Virtual screening is also crucial to speed up drug repurposing and within this context it has been applied to SARS-CoV-2 drug discovery research [123].

Applications of virtual screening to discovery inhibitors of diverse SARS-CoV-2 related proteins/enzymes acting during different phases of the SARS-CoV-2 life cycle will be in depth treated in the following paragraphs.

4.1. Inhibitors of viral entry

As described above, viral entry is the first step of viral infection and is based on the interaction between Spike (S) protein of SARS-CoV-2 virus and ACE2 receptor located on the surface of epithelial cells of the lungs and small intestine along with heart, kidney, and additional tissues [28]. More in detail, the RBD region in the S1 subunit of the S protein interacts with ACE2 receptor. The extent of SARS-CoV-2 outbreak and the key role of the S protein in viral infection attracted many efforts to get the structural details characterizing this viral protein and its interaction with the host cell receptor. Indeed, from the beginning of this pandemic, a considerable number of structures have been deposited in the PDB. More in detail, ~870 structures are available for the Spike protein alone or in complex with the ACE2 receptor (see Protein Data Bank, https://www.rcsb.org/, accession date 08/04/2022 [106], keywords search: "Spike glycoprotein" and "Severe acute respiratory syndrome coronavirus 2").

4.1.1. Structural features of S protein, ACE2 receptor and their interaction

The Spike protein is a class I TransMembrane (TM) glycoprotein with a trimeric organization (Fig. **2A**) in which each monomeric unit is formed by 1273 residues (referring to the Wuhan-Hu-1 strain of the initial pandemic) [32, 124].

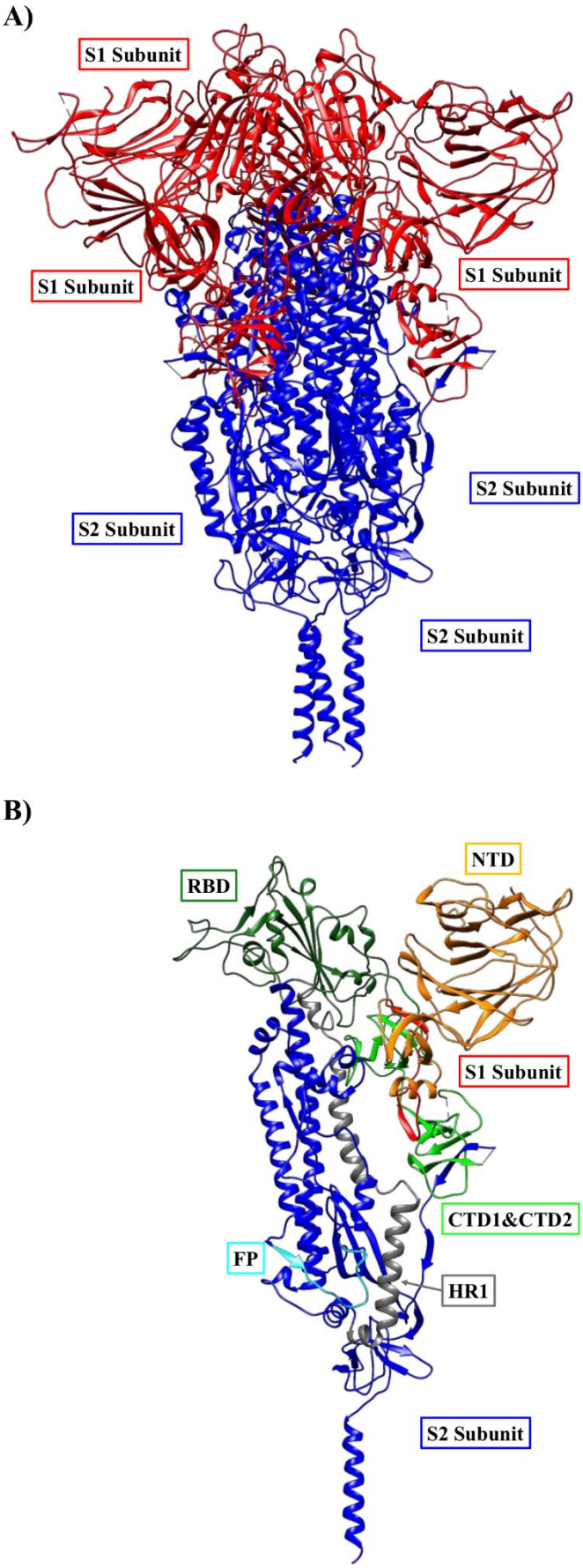

Fig. (2). Structure of SARS-CoV-2 spike protein in the prefusion state in the "close" configuration of RBD domains (cryo-EM structure, PDB code: 6XR8 [125]). **A)** Trimeric arrangement. S1 subunits (a.a. 14-685) are colored in red and S2 subunits (a.a. 686-1273) are colored in blue. **B)** Monomeric arrangement. S1 subunit: NTD (a.a. 14-305, orange), RBD (a.a. 331-527, dark green), CTD1 (a.a. 528-590, light green) and CTD2 (a.a. 591-685, light green). S2 subunit: FP (a.a. 788-806, cyan), HR1 (a.a. 912-984, mid gray). HR2 (a.a. 1163-1213), TM domain (a.a. 1213-1237), and CT (a.a. 1237-1273) are not shown.

The first N-terminal ~15-20 residues represent the signal peptide whereas, the following regions constitute the S1 subunit (a.a. 14-685), representing the key element for the interaction of Spike protein with ACE2, and the S2 subunit (a.a. 686-1273), which is fundamental for membrane fusion (Fig. **2B**) [32, 124, 125].

S1 is characterized by an N-terminal domain (NTD), a receptor-binding domain (RBD) and C-terminal domains (CTD1 and CTD2) (Fig. **2B**) [28, 124, 125]. In addition, RBD comprises the receptor-binding motif (RBM) which represents the protein region responsible for direct contacts with ACE2 (Fig. **2B**) [28, 124]. From a structural point of view, the NTD is characterized by a top region with two antiparallel β-strands linked by a short loop, a core region possessing a galectin-like antiparallel β-sandwich fold, that is composed by one six-stranded β-sheet and one seven-stranded β-sheet, and a bottom region characterized by two short β-sheets and a helix [124]. The RBD region possesses two subdomains, the first one made up of a five-stranded antiparallel β sheet with some short helices and loops making links and another one including the extended loop of RBM [124]. The RBM is responsible for the primary contacts with the carboxypeptidase domain of ACE2 receptor [124, 126]. The following two CTD domains mostly include β-structures made up by segments from S1 and the N-terminal portion of S2 close to the S1/S2 furin cleavage site. More in detail, two antiparallel β-sheets (consisting of two- and four-strands, respectively) are included in CTD1 whereas, CTD2 contains two four stranded β-sheets one of which includes a β-strand from the S2 subunit [124] (Fig **2B**).

The S2 domain encompasses the fusion peptide (FP), heptapeptide repeat sequence 1 (HR1), CH (Central Helix Region), Connector Domain (CD), HR2 (Heptad Repeat 2), TM (Trans Membrane) domain, and Cytoplasmic Tail (CT) domain (Fig **2B**) [28, 32, 124]. Interestingly, the TM domain is the region of the S protein responsible for the anchoring to the viral membrane whereas, other S proteins portions compose the extensive ectodomain which adorns the virion surface [124].

The FP region of S2 subunit consists of 15-20 residues which are conserved within viral family and are mostly hydrophobic (e.g., glycine or alanine) [32]. The two HR1 and HR2 domains are both formed by the repetitive "HPPHCPC" heptapeptide motif ("H" stands for a hydrophobic or traditionally bulky residue, P for polar or hydrophilic residue and C indicates additionally charged residue); HR1 is positioned at the C-terminal end of FP whereas, the second one is located at the N-terminal end of the TM domain (Fig. **2B**) [32].

ACE2 includes 805 residues, is a type-I transmembrane glycoprotein and has a catalytic zinc metallopeptidase domain at the N-terminus and a collectrin-like domain (CLD) at the C-terminus that terminates with one transmembrane helix and an intracellular segment made up of ~40 residues [127-129]. The peptidase domain represents the protein module recognized by RBD of Spike protein [127]. ACE2 catalytic activity is responsible for the maturation of angiotensin I (Ang

I, also named Ang1-10), a peptide hormone that controls vasoconstriction and blood pressure [127, 128]. More in detail, ACE2 exploits its single active site, with a zinc metallopeptidase activity, to remove the C-terminal leucine from Ang I and consequently produces Ang-(1-9), which in turn is further converted by other enzymes to the shorter vasodilator peptide hormone Ang-(1-7) [128, 129]. ACE2 can also directly process Ang I to Ang-(1-7) [128, 129].

The structure of a truncated ACE2 version containing the extracellular domains in the unbound and inhibitor-bound forms is available. The structure is characterized by the presence of 20 α-helices and nine 3_{10} helices, and contains as well six short β-structural segments (Fig. **3**). The electron density map is weak for the C-terminal part corresponding to the collectrin homology domain (residues 612-740) [130].

The structural elements in the metallopeptidase ACE2 domain form two subdomains which compose the two sides of a long and deep cleft whose floor is partly made up by an α-helix (helix 17) which seems to connect the two subdomains to each other (Fig. **3**) [130].

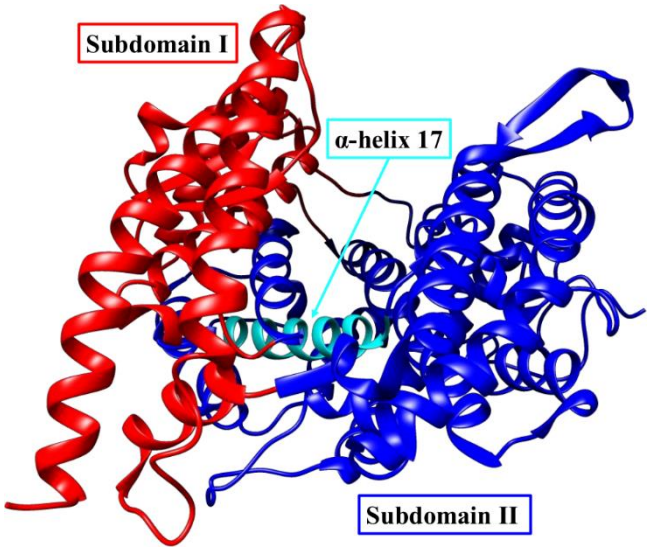

Fig. (3). X-ray structure of the truncated extracellular form of ACE2 receptor (residues 1–740, PDB code: 1R42 [130]). Subdomain I of ACE2 receptor (a.a. 19-102, 290-397, and 417-430) is colored in red and Subdomain II (a.a. 103-289, 398-416, and 431-615) is colored in blue. The α-helix n.17 (a.a. 511-531) on the floor of the deep cleft formed by Subdomain I and Subdomain II is colored in cyan.

In the prefusion state, the S trimer of SARS-CoV-2 shows the structural organization already found in other coronavirus spike proteins (Fig. **4**) [32, 124]. The prefusion structure is characterized by the S1 region assuming a "V-like" shape where NTD is on one side forming a kind of arm and the RBD, CTD1 and CTD2 are on the other side making the other "arm". This S1 structural organization wrap all around the S2 fragment that forms a central helical bundle protruding towards the viral membrane, the N-terminal extremity of HR1 [124]. Three RBD domains are located on the top of the trimer and can assume two different conformations [32, 124, 126, 131, 132] (Fig. **4**). The so called "up" organization is characterized by a specific "up" rotation of one of RBD domains that makes the RBM sequence accessible for ACE2 receptor (Fig. **4A**) [32, 124, 126, 131, 132]. As concerning the "down" conformation, each RBD is involved in contacts with the NTD from the adjacent monomer and is not available to ACE2 receptor [124]. In the prefusion complex, CTD1 and CTD2 are generally positioned below RBD and between two neighboring NTDs and are projected toward S2, thus suggesting their involvement in the structural rearrangements behind membrane fusion [124].

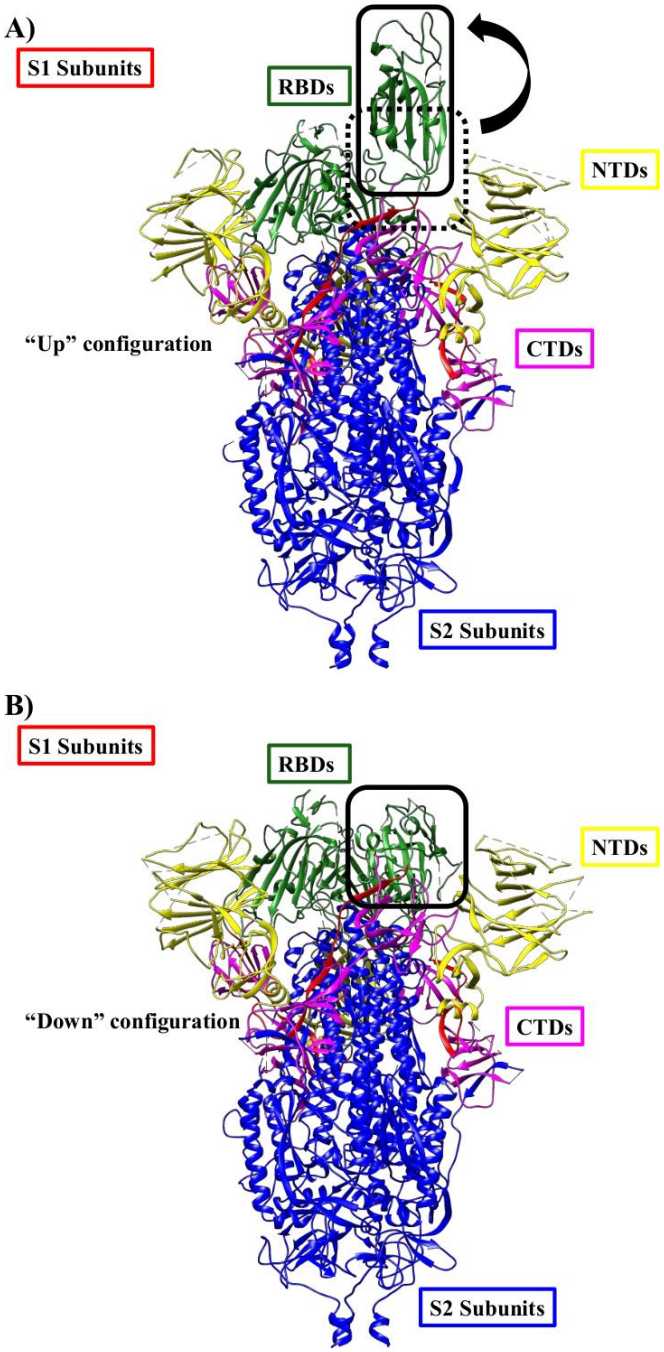

Fig. (4). Comparison between the structures of SARS-CoV-2 spike protein in prefusion state with "up" configuration of RBD domains (cryo-EM structure, PDB code: 6VYB [133]) and, with "down" configuration of RBD domains (cryo-EM structure, PDB code: 6VXX [133]). The NTD domains (a.a. 14-305) are colored in yellow. The RBD domains (a.a. 331-527) are colored green. The CTD domains (a.a. 528-590 and 591-685) are colored in magenta, other regions of S1 domains are in red [125]. **A)** Structure with "up" configuration. A black solid rectangle indicates the position of one RBD in the "up" configuration whereas, a black rectangle with dotted border indicates the position of the same RBD in the closed state. **B)** Structure with "down"

configuration. A black rectangle indicates the position of one RBD in the closed configuration.

The attachment of S protein to the host cell seems to largely depend on the combination of strong aromatic-aromatic interactions between S protein (in the "up" conformation) and ACE2 along with ionic intermolecular interactions. Indeed, the outer surface of RBM in S protein makes interactions with the N-terminal helix from the peptidase domain of ACE2. Residues from S protein RBD (i.e., K417, E484, N487 and N501) are involved into hydrogen bonds and salt bridges with residues from ACE2 (D30, K31, H34, Y41 and K353) (Fig. **5**) [125]. The binding is further strengthened by the hydrophobic interactions involving a single residue in the RBD domain of S protein (i.e., F486) and a set of three residues in ACE2 (i.e., L79, M82 and Y83) (Fig. **5**) [124].

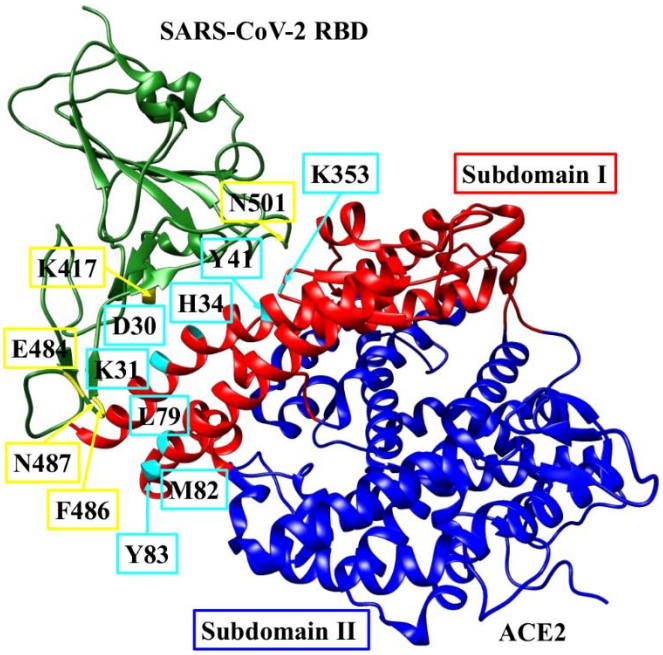

Fig. (5). Cryo-EM structure of the SARS-CoV-2 RBD-ACE2 complex (PDB code: 7DQA). SARS-CoV-2: the residues of RBD (i.e., a.a. 333-526) are reported in green [125]. ACE2 receptor: Subdomain I (a.a. 19-102, 290-397, and 417-430) is colored in red and Subdomain II (a.a. 103-289, 398-416, and 431-615) is colored in blue [130]. The residues involved in hydrogen bonds, salt bridges and hydrophobic interactions (i.e., K417, E484, F486, N487 and N501 from SARS-CoV-2 RBD and D30, K31, H34, Y41, L79, M82, Y83 and K353 from ACE2) are colored in yellow (SARS-CoV-2 RBD) and cyan (ACE2) [124].

Once the S protein has bound the host receptor, its S1/S2 cleavage site (a polybasic sequence -PRRAR- that can be recognized by furin) and the S2' cleavage site become accessible to host cells proteases and the protein undergoes structural rearrangements that bring to its fusion to the host cell membrane [126, 134]. The host cells proteases involved in the cleavage event are transmembrane protease serine 2 (TMPRSS2) and human airway trypsin- like protease (HAT) [1]. Interestingly, the position of S1/S2 cleavage site is different in each monomer of the S trimer whereas, that of S2' cleavage site is similar in each monomer [126]. The structural changes induced by RBD binding to ACE2 lead to the insertion of the FP region of S2 subunit into the host cell membrane [124]. In addition, the prehairpin coiled-coil of the S2 HR1 domain becomes accessible and thus the binding of HR1 trimer to the S2 HR2 domain can occur [124]. The result is the formation of the six-helical bundle, a fundamental structural element by which S2 can keep viral envelope and host cell membrane close together and thus favor viral fusion and entry [32, 124, 135].

4.1.2 Mutations in the S-protein and SARS-CoV-2 variants: a brief overview

Since the beginning of this pandemic, different variants of SARS-CoV-2 were identified, the variants represent mutant forms of the spike protein (https://www.who.int/en/activities/tracking-SARS-CoV-2-variants/ [136]). WHO, in collaboration with partners, created a classification to give the proper attention in the global monitoring and research on the variant discovered each time ([136], accession date 08/04/2022). Indeed, there are Variants of concern (VOC) which are associated with a) an increase in transmissibility or negative variation in COVID-19 epidemiology otherwise b) an enlargement in virulence or modification in clinical disease appearance or c) a lower efficiency of public health and social measures or accessible therapeutics, diagnostics and vaccines [136].

Instead, the Variants of interest (VOI) include those characterized by genetic variations that can or potentially could influence several viral features (e.g., transmissibility, disease severity, immune and diagnostic or therapeutic escape) ([136], accession date 08/04/2022). In addition, these variants have epidemiological effects with an evolving risk to global public health ([136], accession date 08/04/2022). This classification of variants is in a continuous updating process which depends on the evolution of their impact on humankind.

To date, the VOC group includes Alpha, Beta, Gamma, Delta variants and the most recently discovered Omicron variants; whereas, the VOI group includes diverse variants like Lambda and Mu ([136], accession date 08/04/2022). In addition, there is a group of formerly monitored variants including lineages which are no longer circulating and/or circulating for a long time without any impact on the overall epidemiological situation and/or no more characterized by concerning features. The Epsilon variant is a member of this group representing a former VOI while the alpha variant is also a member of this subset ([136], accession date 08/04/2022).

The variants are generally characterized by mutations which lead to an increased COVID-19 transmission by favoring different mechanisms exploited by SARS-CoV-2, such as the Spike protein binding to ACE2 and the Spike protein escaping from the binding of human antibodies [137]. Interestingly, most of the mutations consist in the substitution of a residue with another, but there are also deletion mutations in which residues are removed. These latter mutations are usually identified as responsible for substantial escape tendency of Spike protein from human immune system [138].

The Sanford University created the Coronavirus Antiviral & Resistance Database (CoVDB) in which the mutations identified for the variants are collected.

For example, the Alpha variant was firstly discovered in UK and has been associated with different deletion mutations (i.e., △69-70, △144-145) and missense mutations (i.e., N501Y, A570D, D614G, P681H, T716I, S982A, D1118H) (https://www.ecdc.europa.eu/en/covid-19/variants-concern

[139], https://covdb.stanford.edu/page/mutation-viewer [140] accession date 08/04/2022). The result is a normal level of transmission and a higher binding affinity of the Spike protein to ACE2 [138].

The beta variant was firstly discovered in South Africa and has been associated with deletion mutations (i.e., △241-243) and missense mutations (i.e., D80A, D215G, K417N, E484K, N501Y, D614G, A701V) ([139, 140] accession date 08/04/2022). The result is a large transmission potentiality and a higher binding affinity of Spike protein for ACE2 [138].

The gamma variant was firstly discovered in Brazil and has been associated with a different set of missense mutations (i.e., L18F, T20N, P26S, D138Y, R190S, K417T, E484K, N501Y, D614G, H655Y, T1027I, V1176F) ([139, 140] accession date 08/04/2022). The result is an increased level of transmission [138].

Delta variant was firstly discovered in India and has been associated with different deletion mutations (i.e., △E157-F158) and missense mutations (i.e., T19R, G142D, E156G, L452R, T478K, D614G, P681R, D950N) ([139, 140] accession date 08/04/2022). The result is a large level of transmission [138].

Epsilon variant was firstly discovered in USA and has been associated with different missense mutations (i.e., S13I, W152C, L452R, D614G) ([139, 140] accession date 08/04/2022). Interestingly, the result is a normal level of transmission [138].

Omicron variant was firstly discovered in South Africa and Botswana and has been associated with different deletion mutations (i.e., Δ69-70, Δ143-145, Δ212), missense mutations (i.e., A67V, T95I, G142D, N211I, G339D, S371L, S373P, S375F, K417N, N440K, G446S, S477N, T478K, E484A, Q493R, G496S, Q498R, N501Y, Y505H, T547K, D614G, H655Y, N679K, P681H, N764K, D796Y, N856K, Q954H, N969K, L981F) and an insertion mutation (i.e., 214EPEins) ([139, 140], accession date 08/04/2022). Interestingly, the most recent Omicron subvariant has been associated with a similar set of missense mutations but with some exceptions (i.e., T19I, L24S, G142D, V213G, G339D, S371F, S373P, S375F, T376A, D405N, R408S, K417N, N440K, S477N, T478K, E484A, Q493R, Q498R, N501Y, Y505H, D614G, H655Y, N679K, P681H, N764K, D796Y, Q954H, N969K) and deletion mutations not associated with the first subvariant (i.e., △25-27) ([139, 140] accession date 08/04/2022).

In this case, the data are still not sufficient to define a clear profile on genomics, transmissibility, efficacy of vaccines, treatment, and management [137].

Different structural studies were conducted on the variants found for SARS-CoV-2 Spike protein, and a considerable number of structures is already available in the PDB website [106] (338 structures, keywords search: “Spike glycoprotein”, “variant” and “Severe acute respiratory syndrome coronavirus 2”, accession date 08/04/2022). Virtual screening studies could be performed by employing these mutant S structures to either find out compounds able to hamper the interactions with host cell receptors or being able to destabilize the S mutant fold and eventually possess a therapeutic potential.

4.1.3 SARS-CoV-2 S-protein interactors other than ACE2

Remarkably, ACE2 is not the only receptor exploited by the Spike protein of SARS-CoV-2 to favor viral entry.

Computational studies speculated that SARS-CoV-2 S protein might also interact with nicotinic ACetylcholine Receptors (nAChRs), thus pointing out a great and diverse binding potential that could explain the multi-organ pathogenesis [28, 31].

Nevertheless, the cellular proteins ASialoGlycoprotein Receptor-1 (ASGR1) and Kringle Containing Transmembrane Protein 1 (KREMEN1) seem to be involved, together with ACE2, in the entry process [141]. KREMEN1 recognizes the entire extracellular region of spike protein presenting larger affinity for the RBD, whereas, ASGR1 recognizes both NTD and RBD modules [142] also exhibiting the highest affinity for the RBD [143].

A further example of receptor interacting with spike protein is provided by Ezrin (also known as cytovillin or villin-2), which is a protein involved in the regulation of inflammation [142]. Ezrin has an amino-terminal FERM ((Four point one, ERM (Ezrin, Radixin, Moesin)) domain, an α domain (i.e., protein module rich in α-helices) and a C-terminal domain containing the F-actin binding site. Previous studies showed that Ezrin employed its FERM domain to interact with the SARS-CoV spike protein thus decreasing viral entry. This finding let speculate that apart from blocking the main receptors linked to COVID-19, like ACE2, a molecule able to enlarge Ezrin activity or working as Ezrin agonist could provide therapeutic potential by decreasing SARS-CoV-2 viral entry [142]. Interestingly, the synthetic Ezrin-peptide HEP1 (TEKKRRETVEREKE) representing a part of the α domain of Ezrin, is able to counteract the dysregulation of innate immune responses to SARS-CoV-2 [142, 144, 145].

As introduced above, the Spike protein is characterized by 22 N-linked glycosylation sequons by which the protein evades the surveillance of the host immune system [146]. These 22 N-linked glycosylation sequons also include 8 sequences representing the sites for the attachment of oligomannose-type glycans [146]. These chains seem to be recognized by the carbohydrate recognition domain (CRD, also called Ca^{2+}-type lectin domain) of Mannose-Binding Lectin (MBL) which is a protein belonging to the collectin family possessing as well, a collagen-like domain [146]. Indeed, solution-based competition assays were conducted to evaluate the interaction of MBL to the spike protein, alone or in the presence of two specific ligands of the lectin (i.e., D-mannose, and N-acetyl-glucosamine) or a non-specific ligand of MBL (i.e., D-glucose). The results highlighted the ability of D-mannose, and N-acetyl-glucosamine to hamper the interaction between MBL and SARS-CoV-2 Spike protein, and thus suggesting Ca^{2+}-dependent binding of MBL to the Spike protein. The same studies revealed also that interactions may occur on a binding site formed by N603, N801 and N1074 from only one chain S protein or at an interaction point made up by N603, N1074 and N709, with N709 from an adjacent chain from two chains S protein [146]. Interestingly, the mutations characterizing the Spike protein of SARS-CoV-2 variants do not affect the glycosylation sites, thus suggesting a retention of ability to bind MBL. Inhibition of Spike protein binding to MBL has been described as a valuable target for therapeutic treatment against the hyperinflammation associated with SARS-CoV-2 infection in advanced disease stage [146].

Nevertheless, in literature, toll-like receptors (TLR) and neuropilin-1 (NRP1) were described as modulators of cellular entry and infectivity of SARS-CoV-2 [142]. Computational investigations let speculate that cell surface TLRs, in particular TLR4, could potentially recognize molecular patterns, possibly the SARS-CoV-2 S spike protein, to generate inflammatory answers [147].

The glucose regulated protein 78 (GRP78) is another interactor of S protein from SARS-CoV-2 and, as it will be better described in paragraph 4.1.4., it could provide an additional way that the virus could employ to enter host cells [148].

4.1.4 Examples of computational approaches to identify SARS-CoV-2 entry inhibitors

In a recent work, the biological activity-based modelling (BABM) approach was exploited to identify antiviral compounds able to modulate SARS-CoV-2 viral entry [149]. Canonical VS approaches search for molecules provided with structures comparable to those that are already considered active towards a specific target or disease. It is assumed that such structural similarity will be accompanied by analogue biological action. Differently from VS, BABM does not rely on the chemical structure but employs profiles of compounds activity including data on how a particular molecule behaves at diverse concentrations when acting on specific targets to formulate predictions about potential activity against a novel target or in a new kind of assay (https://ncats.nih.gov/news/releases/2021/assessing-a-compounds-activity-not-just-its-structure-could-deepen-the-pool-of-promising-drug-therapies [150], accession date 25/02/2022). A crucial advantage of BABM is represented by its speed. Practically BABM only needs to run a computational algorithm to discover several original drug leads, that could be even provided with novel chemical structures ([150], accession date 08/04/2022).

To verify the BABM method, the large amount of data produced by hundreds of qHTS (quantitative High-Throughput Screening) studies, that employed more than 500,000 compounds and drugs constituting the NCATS' (National Center for Advancing Translational Sciences) in-house library, was recruited. First, the capacity of BABM to employ activity profiles to recognize molecules already known to be active against the Zika and Ebola viruses was checked. Next, BABM was used to discover compounds efficacious against SARS-CoV-2 through analyses of the NCATS compounds library.

BABM let speculate that the activity profiles of 311 compounds could be related to some effect against the coronavirus [149]. These predicted molecules were further analyzed by two consecutive sets of live virus cytopathic effect assays and 85 of them were confirmed as active. More in detail, SARS-CoV-2 pseudotyped particle (PP) entry assays led to the identification of 53 viral entry inhibitors and GFP-LC3 (Green Fluorescence Protein - Light Chain 3B) assays led to identification of 35 autophagy modulators. Among these molecules, MLS000699212 showed a considerable inhibitory activity for SARS-CoV-2 entry (IC_{50} = 592 nM) and resulted efficacious in the authophagy assay, thus suggesting its double mechanism of action against the virus (Fig. **6**) [149].

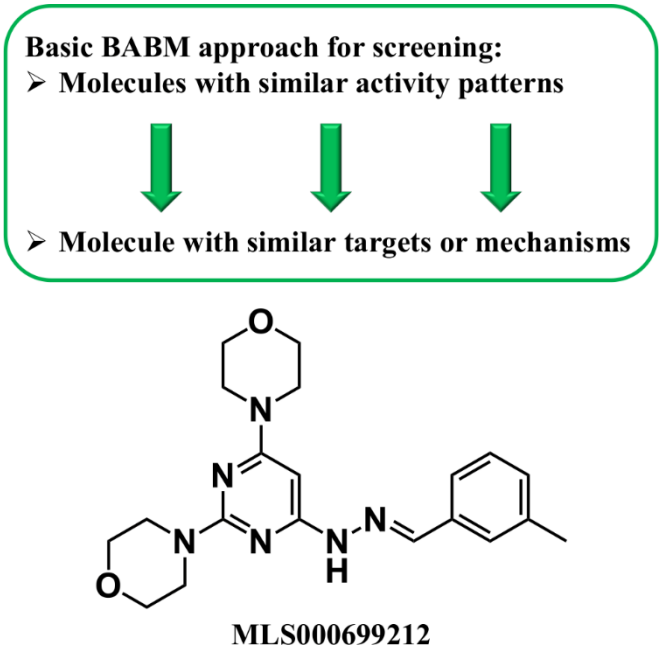

Fig. (6). Chemical structure of the best molecule found by the BABM approach against SARS-CoV- 2 [149] .

The glucose regulated protein 78 (GRP78) was shown to bind SARS-CoV-2 [148]. This protein represents a host surface receptor which under normal conditions localizes in the lumen of ER and is responsible for interacting and inactivating three enzymes linked to cell death or differentiation (i.e., Activating Transcription Factor 6 (ATF6), Protein kinase RNA-like Endoplasmic Reticulum Kinase (PERK), and Inositol-requiring Enzyme 1 (IRE1)) [148]. Following accumulation of a specific amount of unfolded proteins, GRP78 frees these enzymes and consequently favor their activation. This event leads to the inhibition of protein synthesis and enhancement of the refolding [151]. Interestingly, cell stress favors GRP78 evasion from ER and its translocation to the cell membrane, where GRP78 behaves as mediator of viral entry [151]. This protein was first identified as a binding-partner of the MERS-CoV Spike protein thus, the same interaction was proposed also for SARS-CoV-2 S protein. Indeed, *in silico* protein-protein docking studies established the possible binding site revealing favorable interactions between SARS-CoV-2 Spike protein and specific residues of GRP78. Therefore, GRP78 was validated *in silico* as potential alternative "route" that SARS-CoV-2 might exploit to enter host cells when they were in specific conditions characterized by low levels of ACE2 receptor [148, 151]. A virtual screening approach was next carried out starting from a library of 57 phytochemicals derived from different plants in Western Ghats (India). The attention was focused on phytochemicals with the aim to identify potential antiviral compounds with lower chance of presenting side effects with respect to already available drugs [148]. The key points of this work were the structure of SARS-CoV-2 spike protein, its binding site for GRP78 and the library of 57 phytochemical compounds. A group of five molecules (i.e., Tanshinone I, Ellipticine, Anabsinthin, Camptothecin and Piperolactam A) exhibited *in silico* a predicted binding energy which was lower than that characterizing the chosen reference compound (i.e., hydroxychloroquinone (HCQ)) (Fig. **7**). The best hit (i.e.,

Tanshinone I) formed a hydrogen bond with N343, which is a residue found also in the putative S protein binding site for GRP78 [148]. In addition, the molecule makes good hydrophobic contacts with F338, F342, V367, L368, and F374 residues of S protein, many of which are again located in the putative binding site for GRP78. Another good hit resulted the compound Piperolactam A (Fig. **7**), an aristolactam from Piper betle Linn abundant in Western Ghats. Piperolactam A has a good pharmacokinetics profile and, in addition, it makes a certain number of hydrophobic contacts with F338, F342, and V367, which are residues belonging to the predicted interaction area of SARS-CoV-2 spike protein for GRP78. Therefore, the computational approach let speculate that Piperolactam A could represent a potential antiviral agent against SARS-CoV-2 [148]. A similar study reported on additional small molecules and peptides that could hamper binding between SARS-CoV-2 S protein and the GRP78 cellular receptor. Such inhibitors were identified by means of computational screening of accessible databases of bioactive peptides and polyphenolic molecules and the investigation of their interaction topology by a docking approach [152]. In a recent work, 527,209 natural compounds from 5 diverse libraries (including among others the Human Metabolome Database, the Marine Natural Products and the well-known ZINC Database) were used as input for a virtual screening approach against the receptor binding domain of SARS-CoV-2 S protein [153]. The best *in silico* hits (i.e., those with docking scores lower or equal to -4.6 corresponding to 12,291 molecules) were further subjected to a second round of molecular docking and then filtered considering their ADMET (Absorption, Distribution, Metabolism, Excretion, and Toxicity) features. The resulting best compounds, that also were commercially available (i.e., 10 molecules), were analyzed by a virus neutralization assay looking at the enhancement of viral entry through the plasma membrane path under physiologically relevant conditions. In the end four compounds (i.e., ZINC04090608, SN00074072, ZINC02122196 and ZINC02111387) showed 18-40% viral inhibition (Fig. **8**). Although these compounds show an antiviral activity lower than that of neutralizing antibodies, that are instead able to block 100% of viral particles in the nM range, they represent promising starting molecules whose antiviral properties could be increased by chemical modifications [153].

Similarly, a different research team started from a library of natural products, deriving from Taiwan Database of Extracts and Compounds, to identify molecules able to hamper the interaction between the SARS-CoV-2 S protein and the ACE2 receptor [154]. This time, a structure-based virtual screening study led to identification of 39 natural products as *in silico* hits. These compounds were tested experimentally by ITC (Isothermal Titration Calorimetry) to check binding to the S protein. ITC revealed micromolar binding affinities for six molecules (i.e., Dioscin, dissociation constant (K_d)= 0.468 μM; Celastrol, K_d=1.712 μM; Saikosaponin C, K_d=6.650 μM; Epimedin C, K_d=2.86 μM; Torvoside K, K_d=3.761 μM; Amentoflavone, K_d=4.27 μM; Fig. **9**).

Lentivirus particles pseudotyped (Vpp) infection assays showed for these hits 50-90% inhibition of viral infection efficacy [154]. To further observe the toxicity of these antiviral potential compounds in normal cells, cytotoxicity assessment of these compounds was carried out. Among the six molecules, Dioscin and Celastrol appeared the most toxic ones since their IC_{50} values by MTT assays (1.5625 μM for Dioscin and 0.9866 μM for Celastrol) resulted markedly lower than those of the other four molecules (i.e., IC50 > 100 μM) (Fig. **9**) [154].

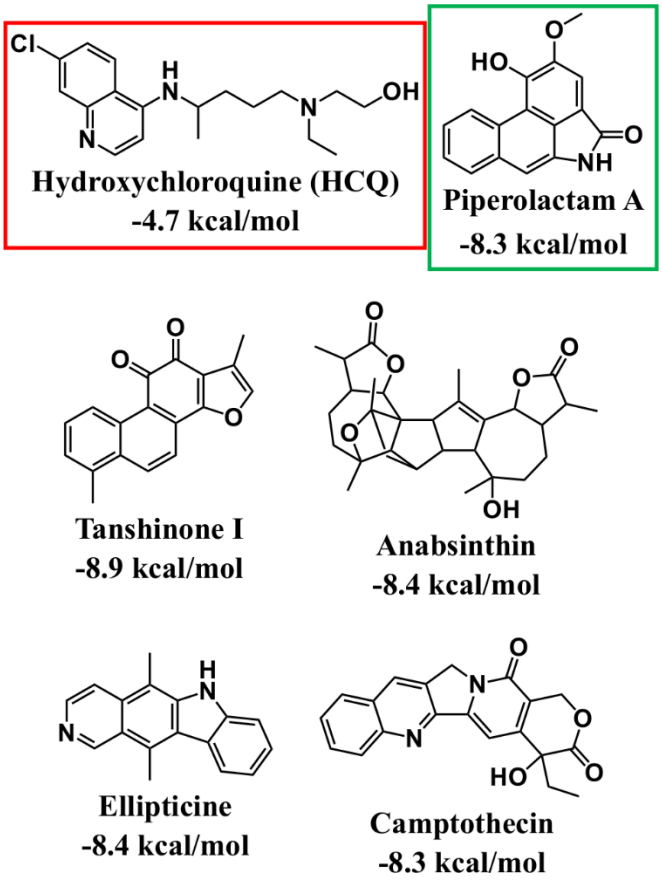

Fig. (7). Chemical structures of best hits deriving from a virtual screening study based on the structure of SARS-CoV-2 spike protein, its binding site for GRP78 and a library of phytochemicals. The red rectangle highlights the reference compound used as comparison term. The green rectangle highlights the molecule possessing a better docking score respect to HCQ reference compound along with a promising pharmacokinetics profile [148].

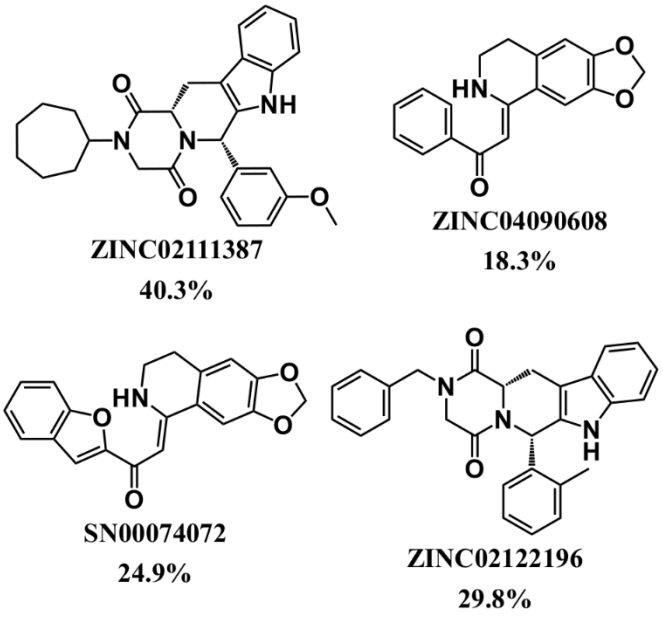

Fig. (8). Chemical structures of molecules identified by a virtual screening approach by employing the SARS-CoV-2 RBD as receptor and 3D structures of 527,209 natural compounds as ligands [153]. The shown compounds present favorable ADMET properties and their antiviral activities were confirmed experimentally by *in vitro* assays. The % of viral inhibition at the highest tested concentration is also reported.

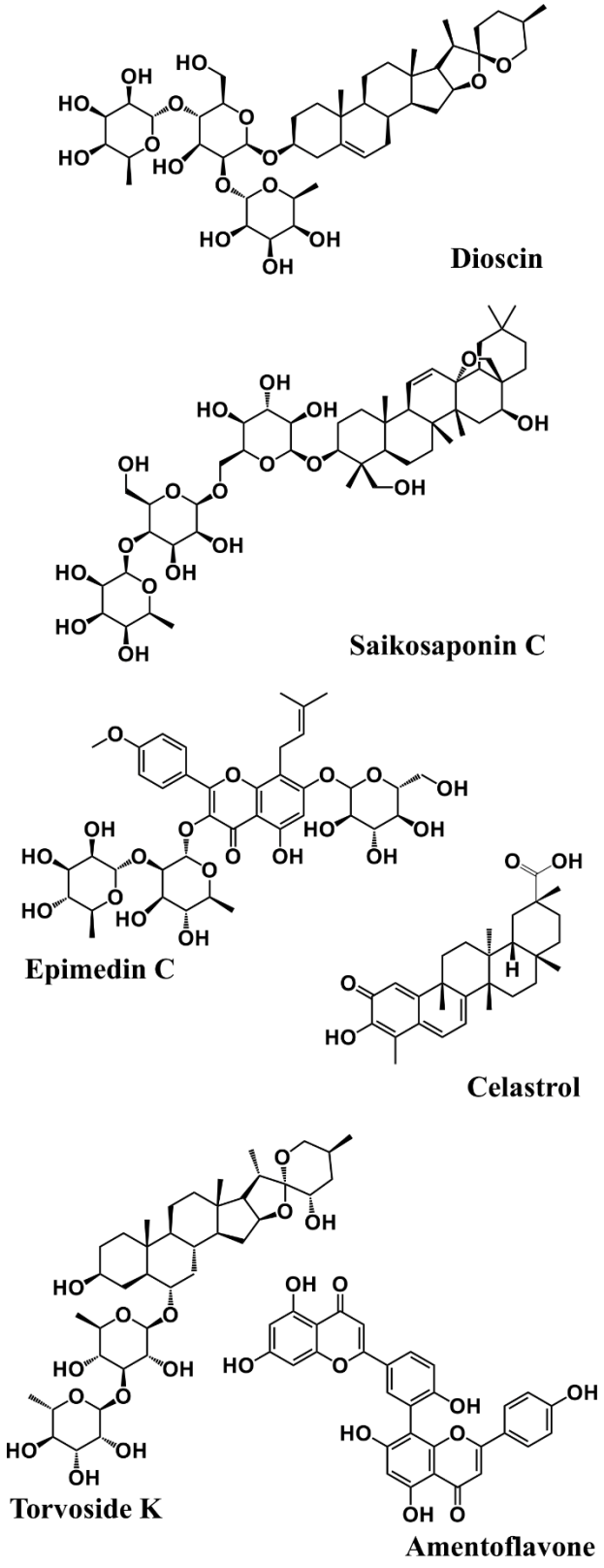

Fig. (9). Chemical structures of potential inhibitors of SARS-CoV-2 entry discovered by a multidisciplinary approach characterized by different consecutive steps: 1) structure-based virtual screening, 2) ITC binding assays, 3) Vpp infection assay, 4) MTT assay in normal cells [154].

4.2. Targeting SARS-CoV-2 Proteases

The role of proteases in the SARS-CoV-2 virus infection has been largely investigated. Firstly, proteases are needed to allow the entry of SARS-CoV-2 into host cell, an event requiring priming (i.e., activation) of the S protein by host proteases. The group of host proteases includes endosomal cathepsin, TMPRSS2, furin, and trypsin [155, 156]. Indeed, the serine proteases TMPRSS2 and furin through priming of the S glycoprotein promote viral invasion along with consequent loss of a proper equilibrium between immune response and disease severity [155, 156]. The S2' cleavage site of SARS-CoV-2 S protein (See paragraph 4.1.1) has been linked to TMPRSS2 whereas, S1/S2 cleavage site has been associated to furin [156]. The host cell surface expresses TMPRSS2 that, through S proteolysis, allows fusion of viral and host cell membranes. Cathepsins B and L are instead two cysteine proteases that support viral entry of SARS-CoV-2 through a route different from the one followed by TMPRSS2. In fact, these cathepsins are located in endosomes, and intervene after SARS-CoV-2 endocytosis favoring the fusion between viral and endosomal membranes [157]. Instead, TMPRSS11D is another example of host protease which, like TMPRSS2 follows a non-endosomal pathway to favor viral entry [158].

A key point of the viral life cycle is viral replication that requires formation of the replication-transcription complex (RTC). The viral cysteine proteases PLpro and 3CLpro (also known as Mpro) play a crucial role in the generation of replication complex by operating maturation of the two large polyproteins pp1a and pp1ab in 16 NSPs (named NSP1 through NSP16) [33, 159] (See also paragraph 2.1.1).

Given their connection with viral entry/fusion and replication, proteases are appealing targets for the development of antiviral agents. In this section we will mainly focus on viral proteases and briefly discuss their structural features and the computational screening approaches employed to find out molecule inhibitors of their activities.

Mpro is a protein of 33.8 kDa that functions as a dimeric enzyme [160] (Fig. **10A**). The single monomer possesses a N-terminal domain I, a domain II and a C-terminal domain III (Fig. **10B**) [160]. The first two domains form six antiparallel β-barrels; a catalytic site is located at the interface between domain I and domain II and includes a catalytic dyad made up by H41 (from domain I) and C145 (from the N-terminal domain II) (Fig. **10B**) [160-163]. The active site is surface exposed and interacts with the position from P1' to P5 of a substrate with its subpockets S1' to S5. Substrate-binding subsites S1, S2 and S4 present a well-defined shape whereas, substrate-binding subsites S1', S3, and S5 are devoid of a definite shape [163]. The S1 subsite in which a Gln residue in the P1 position of a substrate is generally located, includes protease residues H163, M165, E166, H172 on one side and F140, L141, N142, G143, S144 on the other side creating the oxyanion hole [163]. The S2 subsite is bordered by the aromatic ring of H41, the main chains joining D187, R188, Q189 and the residues M49, Y54 and M165 contribute as well. M49 due to a conformational flexibility, when the enzyme is

free from any ligand, can vacate its position thus permitting to different P2 groups to access this subpocket in the case of inhibitor binding [163]. The S3 subsite is positioned in between E166 and Q189; the S5 subsite is located between P168 in the fragment M165-H172 and residues from T190 to A194. Finally, S4 is formed around the long loop made up between F185 and A194 [163]. Instead, the C-terminal domain III is characterized by a globular ensemble of five antiparallel α-helices and comprises two residues (i.e., R298 and Q299) that are important for dimerization (Fig. **10B**) [96, 163].

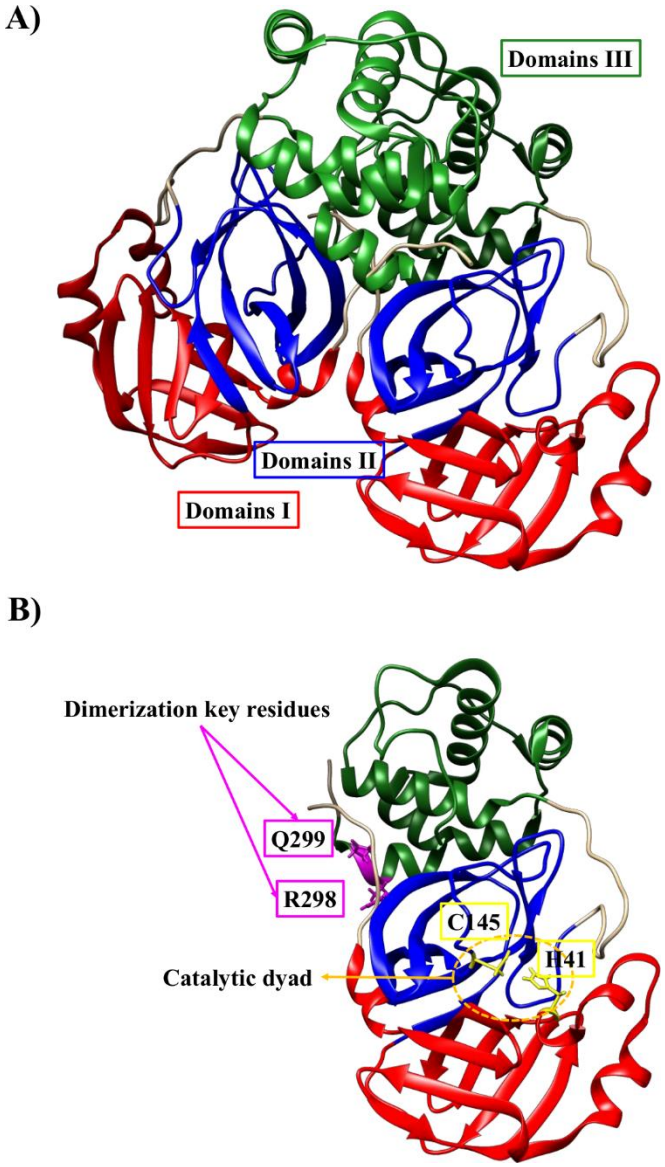

Fig. (10). X-ray structure of Mpro from SARS-CoV-2 (PDB code: 7BB2 [160]). **A)** Dimeric state. **B)** Monomeric state. Red, blue, and green are used for the N-terminal domain I (a.a. 10–99), domain II (a.a. 100–182) and C-terminal domain III (a.a. 198–303), respectively. In panel **B)** residues important for dimerization (i.e., R298 and Q299) and those of the catalytic dyad (i.e., H41 and C145) [96] are colored magenta and yellow, respectively.

Computational studies were conducted to reveal structural features characterizing the interaction between Mpro active site and a substrate-like peptide and to better understand the enzymatic proteolysis reaction [164]. Thus, a 3D structure model of Mpro in complex with the substrate-like sequence Ac-SAVLQ↓SGF-NMe (Ac=N-terminal acetylation, N-Me=N-Methylated C-terminal end, the arrow indicates the cleavage site, with Q in P1) was first generated starting from the structure of the SARS-CoV-2 free protease and by alignment with a co-crystal structure of SARS-CoV protease in complex with a peptide aldehyde inhibitor. Through multiscale simulation methods, binding between SARS-CoV-2 Mpro and Ac-SAVLQSGF-NMe was studied in detail together with analysis of the free energy scenery linked to the two steps of the proteolysis reaction (i.e., acylation and diacylation) and the related transition states. The computational study pointed out crucial interactions that could enhance the acylation process and could be kept into account for the development of potent and selective "blockers" of Mpro proteolytic activity. The work suggested that the residue in P1' should play the pivotal role to positively modulate, both thermodynamically and kinetically, Mpro inhibition [164].

One of the strategies proposed to find out inhibitors of Mpro consisted in the screening of libraries of compounds to identify covalent-inhibitors attacking the C145 cysteine residue positioned at the catalytic site [165]. In fact, Mpro enzymatic activity largely depends on the nucleophilic attack of C145 to an electrophilic ligand. To set up reliable docking runs, first computational studies were conducted to predict the right positions of known covalent inhibitors in the active site of Mpro. Docking paraments were set in such a way to produce poses for the protein/ligand complexes similar to those in corresponding available crystal structures deposited in the PDB [165]. Once the computational parameters were established, virtual screening was started by employing a collection of 41,757 electrophilic inhibitors, deriving from different libraries (PubcChem, Enamine and Asinex): 17 potential covalent inhibitors of Mpro were identified by looking for compounds with their electrophilic groups positioned in the docking poses close to C145 [165]. Among these molecules, compound 1658938 attracted attention as it showed a good docking score and was characterized by a low cytotoxicity (Fig. **11A**). A second screening was instead carried oud using 32 FDA approved covalent drugs: four compounds provided good outcomes (i.e., Dimethylfumarate, Fosfomycin, Ibrutinib, Saxagliptin) [165].

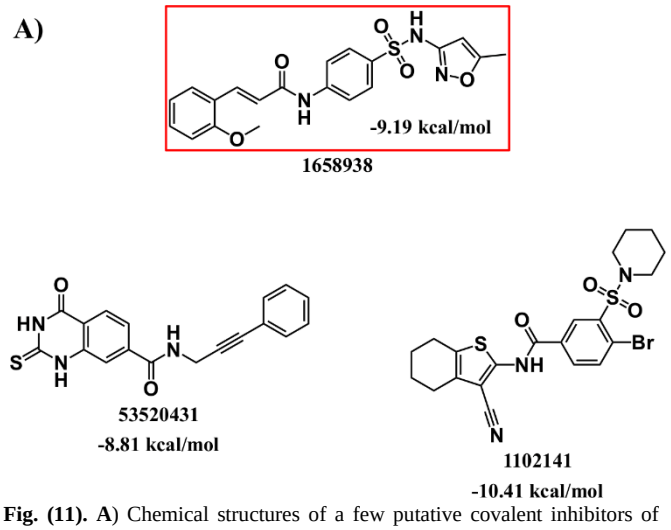

Fig. (11). A) Chemical structures of a few putative covalent inhibitors of Mpro predicted by a virtual screening approach starting from three different libraries (PubChem, Enamine and Asinex). The red rectangle highlights the molecule 1658938 with a low cytotoxicity [165].

A large number of compound databases has been thus far implemented for virtual screening approaches against Mpro. It is worth noting that the Mpro active site flexibility is a feature to be considered when dealing with such computational docking studies [166]. One of such studies interestingly, reported on the virtual screening of a library composed by 4,384 molecules, that have already been approved for human use, against Mpro into three diverse conformational states. Among the best ten *in silico* hits identified for each conformer, only those able to make contacts with one of the two catalytic residues (i.e., H41 or C145) were selected for further validation by MD simulations. These latter analyses revealed that binding free energies of most of the selected molecules were lower than those associated for the model complex avidin/biotin (i.e., -20.4 kcal/mol) thus pointing out a potential good and stable interactions between compounds and Mpro (Fig. **11B**). Finally this work suggested 9 compounds as possible Mpro inhibitors [166].

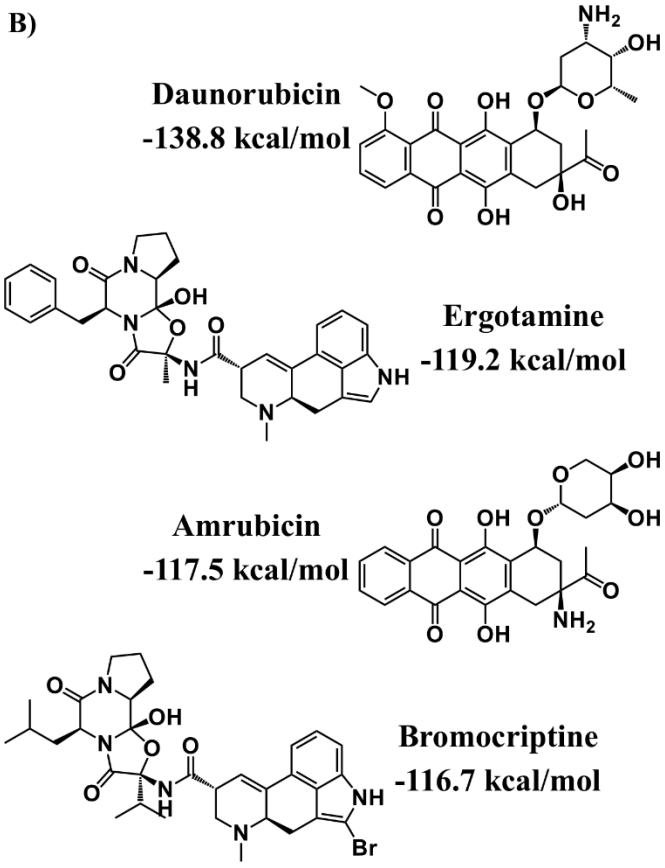

Fig. (11). B) Chemical structures of a few Mpro inhibitors identified through a virtual screening strategy starting from different Mpro conformers and a library of molecules, that have already been approved for human use, the binding free energies of the related complexes with Mpro are indicated as well [166].

Another virtual screening route employed a database of 300 compounds that was assembled by choosing 211 phenols and 13 fatty acids from the OliveNet™ library, diverse antibiotics for comparison, available protease inhibitors, the α-ketoamide inhibitor as a control [167]. In details, the α-ketoamide 13b ligand was considered as the reference molecule for the virtual screening protocol since it was reported to inhibit Mpro with an IC_{50} equal to 0.67 ± 0.18 μM [167]. The docking poses obtained for the complex between Mpro active site and this inhibitor were employed as comparison term in the virtual screening approach to select the best hits based on similar intermolecular interaction patterns. The virtual screening against Mpro and the following MD studies revealed stable interactions between a few molecules (like Hypericin and Cyanidin-3-O-glucoside) and the protease (Fig. **11C**) [167]. Next, the best *in silico* hits were tested *in vitro* by enzyme-linked immunosorbent assay. The experimental tests showed lower potency of the selected compounds in comparison with the known covalent protease inhibitor GC376, that was used as positive control (Fig. **11C**). However, the weak activities - in the micromolar range- of the newly identified compounds let speculate they could represent just starting points for further investigations against SARS-CoV-2 Mpro [167].

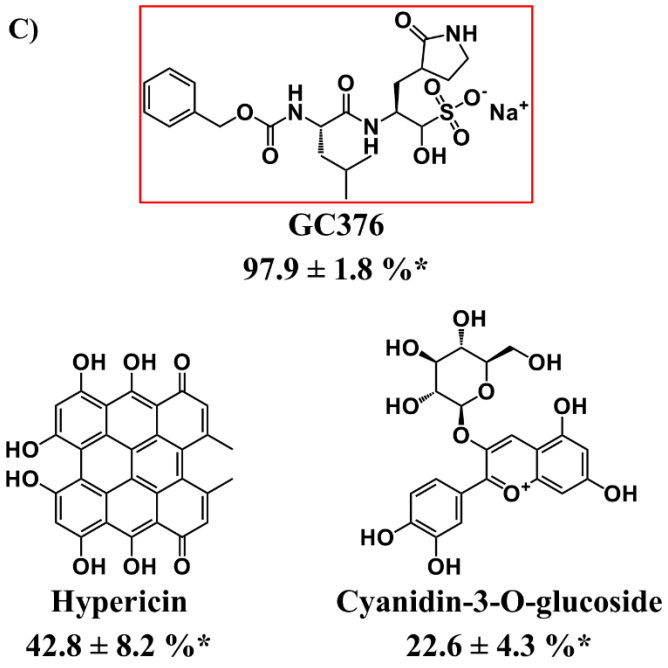

Fig. (11). C) Chemical structures of a few Mpro inhibitors found by virtual screening employing a database composed by phenolic compounds and fatty acids from OliveNet™ library as well as by curated pharmacological and dietary compounds [167]. A red rectangle is used to highlight the covalent inhibitor (positive control -GC376-) employed in the enzyme-linked immunosorbent assay. * = values of the percentage protease inhibition at 50 μM compound concentration.

In a different work, starting from the knowledge that both SARS-CoV-2 and HIV-1 are single-stranded RNA viruses (+ ssRNA) and that a few inhibitors of HIV (like Indinavir and Darunavir) are supposed to be potential excellent binders of SARS-CoV-2 Mpro protease or possess antiviral activity against many viruses including SARS-CoV, a complex multi-step computational screening approach was set up [168]. Briefly, a library of 1528 anti-HIV1 compounds was considered in the first cycle of screening protocol which selected first 356 compounds with strong antiviral properties towards Mpro. Next 41/356 compounds were filtered as potential good interactors of Mpro. These compounds in turn were screened by a deep learning model based on the IC_{50} values of known inhibitors [168]. The resulting 22 hits were further filtered by a structure activity relationship (SAR) mapping and functional group analysis and 2 molecules (i.e.,

4-([5-(2-Nitrophenyl)-2-furyl] methylene)-3-phenyl-5(4H)-isoxazolone (also named hit-9) and 4-Chloro-N-(1-methyl-1H-benzimidazole-5-yl) benzamide (also named hit-10) (Fig. **11D**) were retrieved [168]. Interestingly, all screened compounds were already described as active against Mpro of the avian coronavirus Infectious Bronchitis Virus (IBV), and this suggested their potential activities also against Mpro of SARS-CoV-2 [168].

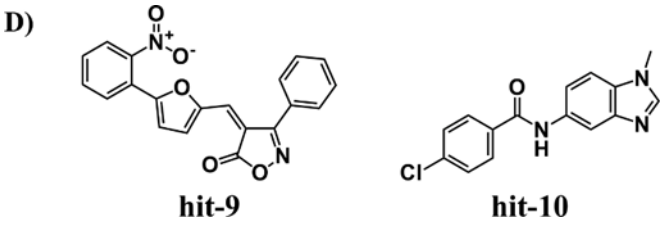

Fig. (11). D) A multi-step screening approach starting from a library of 1528 anti-HIV1 compounds led to the SARS-CoV-2 Mpro inhibitors hit9 and hit-10 [168].

Remdesivir and Ritonavir have already been identified as effective drugs against COVID-19 [169]. A compound library was assembled by looking for molecules with some structure similarity to the two drugs. Next, virtual screening was conducted to find out the best compounds targeting SARS-CoV-2 Mpro [169]. The best 20 molecules identified by this structure-based virtual screening (SBVS) approach were further analyzed to evaluate the strength and stability of their interaction with the binding pocket residues of SARS-CoV-2 Mpro. This analysis allowed the identification of 3 compounds that could be possibly efficacious against COVID-19 (Fig. **11E**).

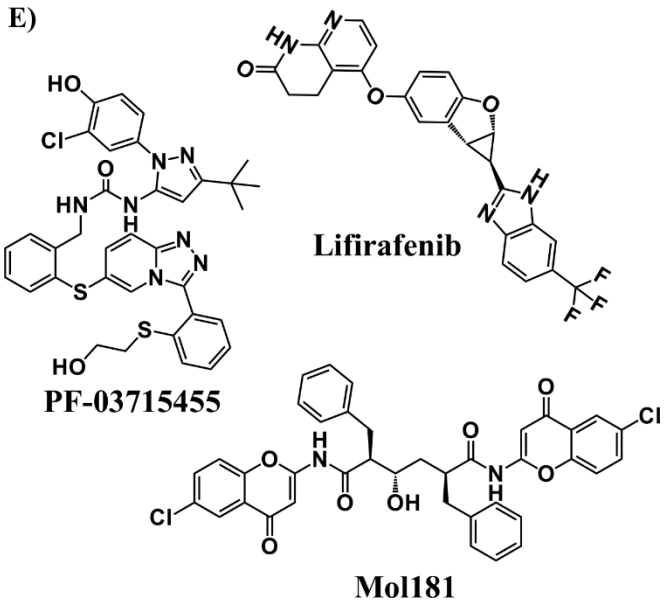

Fig. (11). E) Chemical structures of inhibitors found for Mpro by SBVS after assembling a library of compounds with structure similarity to Remdesivir and Ritonavir [169].

Similarly, SBVS combined with MM-BGSA (Molecular Mechanics/Generalized Born Surface Area) studies, were carried out for the analysis of three different compound collections (i.e., natural products, coronaviruses main protease inhibitors, and FDA approved drugs) in order to evaluate their ability to target Mpro [170]. The study led to hits belonging to different scaffold classes like oligopeptides, one and two tetrahydropyran rings, cyclic peptides, dipeptides tripepetides (Fig. **12A**) [170].

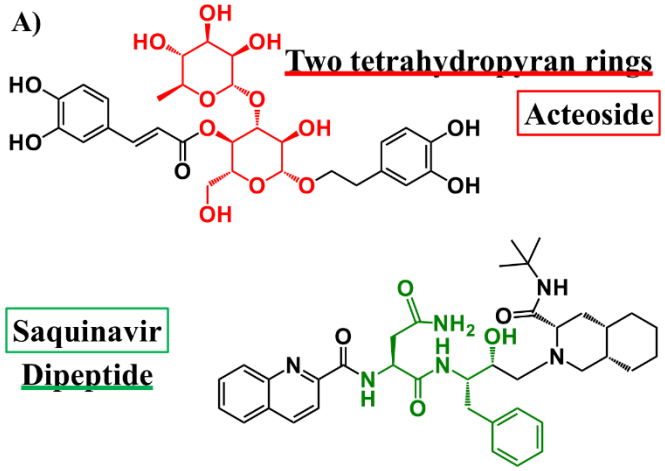

Fig. (12). A) Chemical structures of the Mpro inhibitors acteoside and saquinavir. Red is employed to color the two tetrahydropyran rings in the acteoside and green is used for the dipeptide scaffold in saquinavir [170].

Starting from FDA-approved drug/diagnostic agents and Asinex BioDesign libraries and the 3D structure of Mpro, virtual screening was performed to find out protease inhibitors [171]. The VS strategy included the HTVS (High-Throughput Virtual Screening) that represents a low precision protocol, followed by the SP (Standard Precision) and XP (eXtra Precision) methods. The docking software package creates multiple diverse ligand conformations depending on the chosen precision. The receptor region used for docking was set by starting from the co-crystal structure of SARS-CoV-2 Mpro in complex with the known N3 inhibitor [161] after extracting the ligand. A filtering strategy relying on a pharmacophore model was adopted to select the best virtual hits from the chosen compound collections [171]. The pharmacophore model was generated by considering the pattern of both steric and electronic characteristics that are needed to obtain the likely best interactions with Mpro active site. The procedure identified as potential Mpro inhibitors, 6 molecules belonging to FDA approved drugs library and 20 molecules from Asinex library. Interestingly, in line with a few of the previously described study, the screening showed a few HIV protease inhibitor as possible anti-COVID19 compounds. In particular, one of the FDA molecules (i.e., Ritonavir) was already in phase II/III and IV clinical trials for the treatment of COVID-19 (Fig. **12B**) [171].

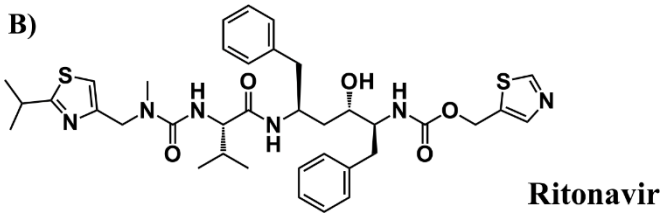

Fig. (12). B) Chemical structure of ritonavir, the inhibitor identified by parallel multi steps virtual screenings of FDA approved drugs and Asinex libraries and already in clinical trial [171].

The computational strategy proposed in another work employed LASSBio Chemical Library and a docking protocol with a Fragment-Based Pharmacophore Model (FBPM) [118]. The FBPM was built by analysis of the intermolecular interactions found between previously identified fragments and the Mpro catalytic site. Briefly the pharmacophore model considered His41, His163 and Glu166, in the Mpro active site as key points for molecular recognition and was exploited to select and rank docking poses for Mpro/ligand complexes [118]. The inhibition of Mpro enzymatic activity by the best selected *in silico* hits was proved by RapidFire High-Throughput Mass Spectrometry assay. This protocol led to the identification of LASSBio-1945, an 1,3-benzodioxolyl sulfonamide which presented an IC_{50} value equal to 15.97 μM and a percentage of SARS-CoV-2 inhibition equal to 68.26% at 50 μM compound concentration (Fig. **12C**). LASSBio-1945 was thus suggested as a promising starting point for subsequent hit-to-lead optimization steps [118].

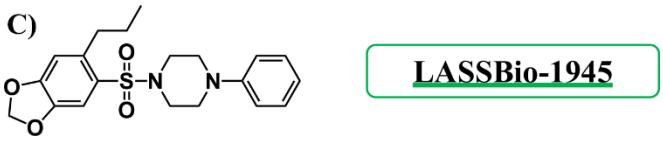

Fig. (12). C) Chemical structure of the Mpro inhibitor LASSBio-1945 identified by combination of virtual screening with FBPM, and RapidFire High-Throughput Mass Spectrometry assay. [118].

The protease inhibitor database MEROPS was also exploited for the identification of potential inhibitors against Mpro through an ensemble of computational methods [172]. More in detail, 2700 molecules were selected from this library and virtually screened against Mpro. The resulting 32 molecules were further analyzed by molecular docking to acquire the best initial structural data for the following MD validation [172]. Results obtained for the novel compounds were compared to those associated with the known SARS-CoV-2 inhibitors N3 and α-ketoamide 13b. N3 and α-ketoamide 13b were used as reference compounds for comparison purposes also in the following step in which binding energies were evaluated. In the end 15 molecules with favorable binding affinities were selected with this strategy [172].

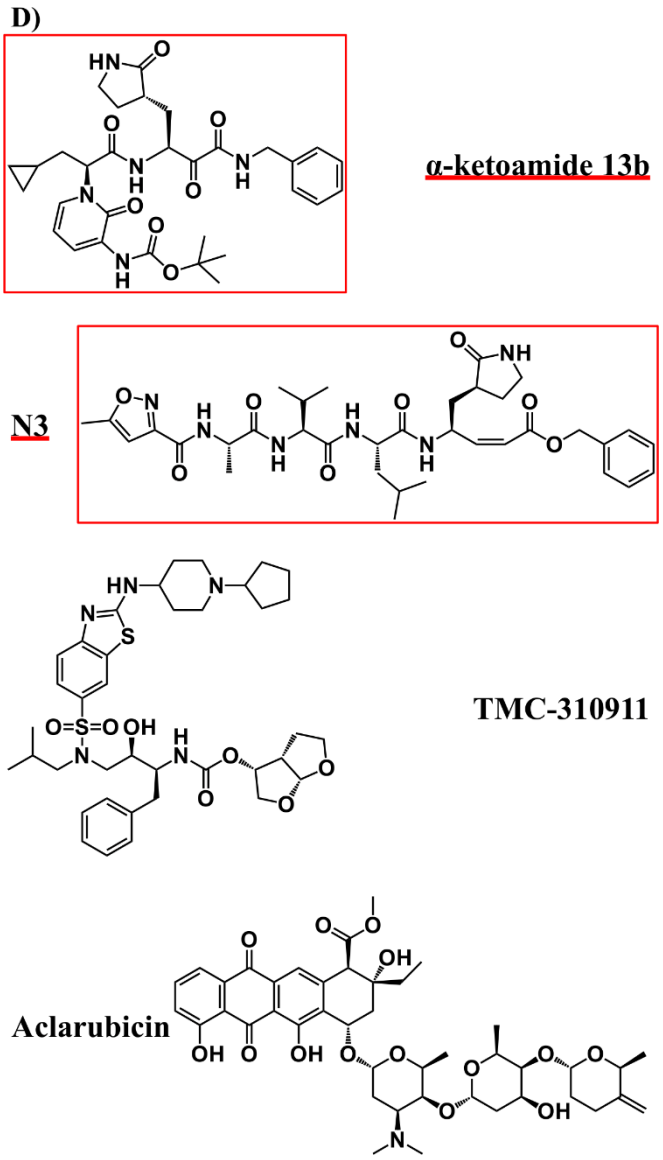

Fig. (12). D) Chemical structure of two Mpro inhibitors (TMC-310911 and Aclarubicin) obtained through a virtual screening strategy employing the protease inhibitor database MEROPS. Red rectangles are used to highlight the chemical structures of the reference known inhibitors [172].

Another interesting route to identify non covalent Mpro protease inhibitors relies on the multimodal structure-based ligand design strategy called Ligand Generative Adversarial Network (LIGANN) [173]. To implement LIGANN, the X-ray structure of Mpro (PDB code 6LU7 [161]) was initially submitted to the PlayMolecule web application [174]. Ligands were next created to match both the shape and chemical features of the binding site and translated into SMILES sequences to allow straight the *de novo* structure-based drug design. The procedure created 93 compounds, optimally encompassing a large portion of chemical space, that were employed in docking studies [173]. The best docked compounds (i.e., n. 19, 27, 30, 39 and 77) were characterized by a similar binding network with aromatic side chains linked by rotatable bonds in a sort of linear organization (Fig. **12E**) [173].

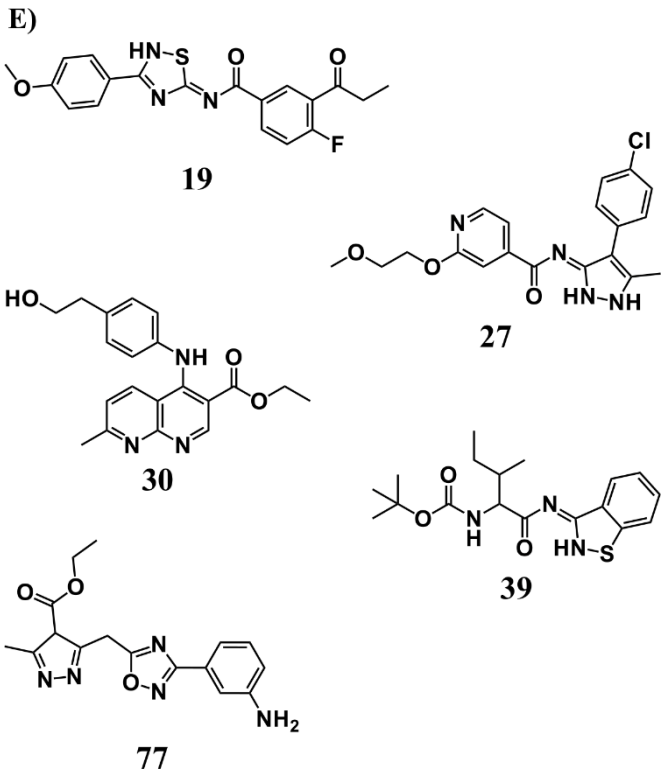

Fig. (12). E) LIGANN approach to find Mpro inhibitors: chemical structures of a few good docking hits [173].

A large library of food chemicals (named FooDB), including 22,880 molecules, along with a second wide database of compounds belonging to the dark chemical matter (named DCM), comprising 139,329 members, were as well employed in the search of active compounds against SARS-CoV-2 Mpro with the goal to analyze a wide portion of chemical space and compounds collections not yet investigated against SARS-CoV-2 [175]. The implemented computational approach included similarity searching, diverse docking strategies and analysis of ADMETox parameters. The first step of selection consisted on the comparison of different fingerprints of the compound libraries with those of reference molecules. The chosen molecules were further screened by molecular docking using two softwares and then selected considering a combination of criteria (i.e., consensus scoring, information of protein-ligand contacts, and the ADMET profile). Most of the 105 identified molecules (some of which are reported in Fig. **13A**) are also commercially available [175].

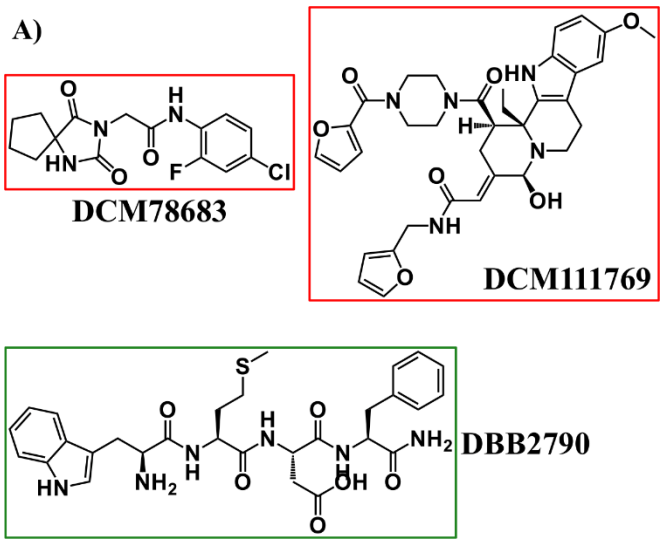

Fig. (13). A) Chemical structures of potential inhibitors found for Mpro starting from FooDB and DCM databases [175]. Red rectangles enclose the molecules from DCM database whereas, the green rectangle highlights a hit deriving from the FooDB database.

Nature is a promising source of compounds for virtual screening studies and inhibitors search and this is also true for SARS-CoV-2. Indeed, different studies, employing libraries of natural products, have been reported in literature to discover original Mpro inhibitors [176-178]. For example, two different databases of natural products (i.e., Super Natural II and Traditional Chinese Medicine (TCM)) were implemented in a virtual screening protocol through ligand-based approaches (i.e., by looking for the similarity between compounds in the databases and known Mpro inhibitors like the N3 and α-ketoamide 13b) and structure-based canonical docking routes. The resulting molecules were further analyzed by MD simulations and their ADMET profiles were determined to get the final list of potential Mpro inhibitor candidates (Fig. **13B**) [176].

In another work a database composed by 3063 compounds derived from more than 200 plants from Asia was exploited for the identification of Mpro ligands by a protocol based on a first step of docking run which selected, based on binding energies, 19 compounds [177]. Further computational filtering by MM-GBSA (Molecular Mechanics/Generalized Boltzman Surface Area**)** selected 3 best compounds whose ADMET profiles were evaluated to prove the drug-like character. Subsequently, MD simulations were conducted as well to further validate the molecules as promising inhibitors of Mpro by looking at the stability of their complexes with the protease. The molecules that better survived at each step of this screening protocol were Curcumin, Gartanin and Robinetin (Fig **13B**) [177].

Momordica charantia L. and *Azadirachta indica* are two antiviral plants that are employed in Nigeria and tropical countries for the cure of viral and parasitic infections being an extraordinary source of phytochemicals that are usually linked to antiviral properties [178]. A library of 86 compounds derived from the two different plants was assembled. To investigate their potential ability to target and inhibit SARS-CoV-2 Mpro, structure-based virtual screening and MD simulations were performed. Such studies were also conducted for 3 FDA approved drugs (i.e., Remdesivir, Hydroxychloroquine and Ribavirin) that were considered as

reference compounds (i.e., comparison terms) for new ligands validation [178]. The combination of MD simulations and pharmacokinetic studies led to the identification of Momordicine and Momordicoside F2 with good inhibition potentials if compared with the reference molecules (Fig. **13B**). In addition, MD simulations confirmed the interaction of these molecules with key residues at the Mpro active site and indicated a good stability of their complexes with the enzyme [178].

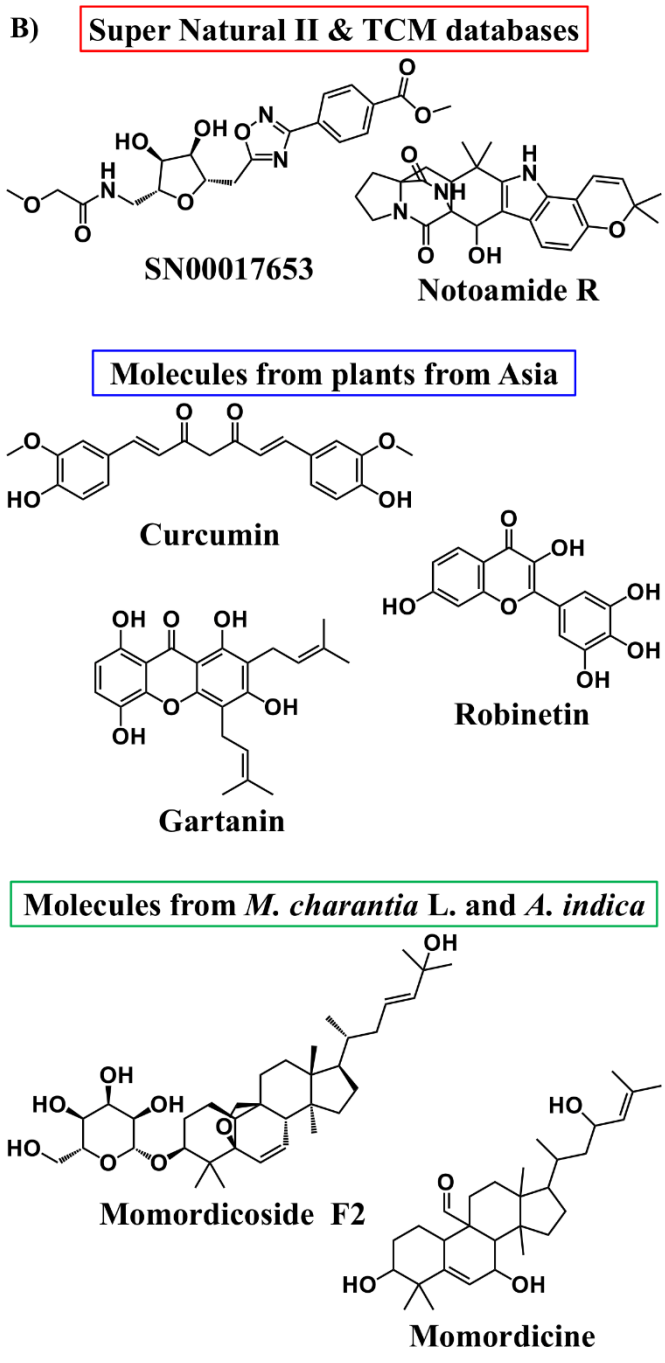

Fig. (13). B) Chemical structures of some of the best inhibitors found for Mpro starting from different databases of natural products [176-178].

As evident through the paragraph many virtual screening strategies were centered around SARS-CoV-2 Mpro, PLpro was also targeted in a reduced number of works as will be described below.

PLpro is another SARS-CoV-2 cysteine protease, an enzyme which cleaves pp1a and pp1ab polyproteins at three sites with the "LXGG↓XX" consensus sequence (where X=any amino acid and the cleavage occurs C-terminally with respect to the second glycine) [179, 180]. The effect of the cleavage by PLpro is the release of NSP1, NSP2, and NSP3 proteins, which are essential for viral replication [180]. From a structural point of view, this enzyme presents a small N-terminal ubiquitin-like (Ubl) domain and the "thumb-palm-fingers" catalytic domain (Fig. **14A**) [179].

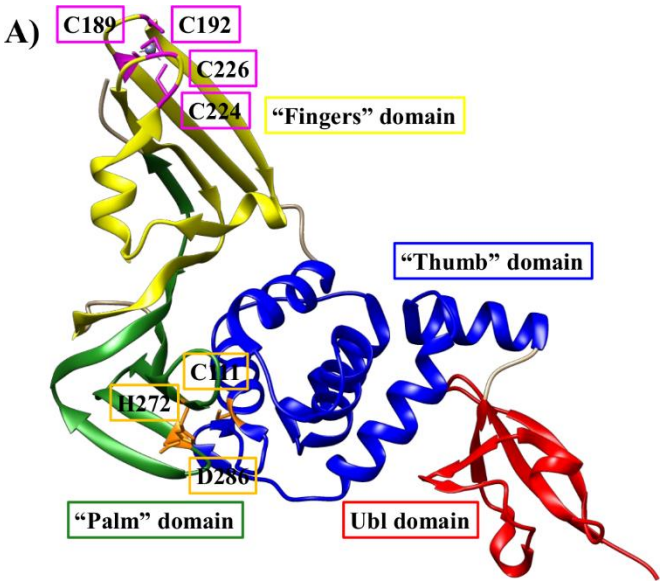

Fig. (14). A) X-ray structure of PLpro from SARS-CoV-2 (PDB code: 6WZU [179]). The Ubl domain is shown in red whereas, blue, green and yellow are used for "thumb", "palm" and "fingers" subdomains respectively. The catalytic residues (i.e., C111, H272, and D286) are colored in orange whereas, cysteine residues coordinating zin ion and fundamental for structural integrity (i.e., C189, C192, C224, and C226) are colored in magenta.

The first domain (Ubl) encompasses residues 1-60 and is characterized by five β-strands, one α-helix, and one 3_{10} helix whereas, the second domain possesses the "thumb-palm-fingers" architecture and is the catalytic domain (Fig. **14A**) [179]. More in detail, the "thumb" subdomain contains six α-helices and a small β-hairpin; the "palm" subdomain possesses six β-strands; the catalytic residues (i.e., C111, H272, and D286) are positioned at the interface between the "thumb" and "palm" subdomains (Fig. **14A**) [179].

The last subdomain "fingers" is composed by six β-strands and two α-helices and contains a zinc ion that is essential for the structural integrity of this enzyme (Fig. **14A**). Four cysteines (i.e., C189, C192, C224, and C226) positioned within two loops inside two β-hairpins coordinate the zinc ion (Fig. **14A**). Within the large "thumb-palm-fingers" domain, a mobile β-turn/loop, encompassing residues G266-G271, is present adjacent to the active site and by acting as a lid, it modulates the access to the active site and closes the site upon substrate and/or inhibitor binding (Fig. **14A**) [179].

A study suggested Ebselen as an inhibitor of PLpro; Ebselen is a selenoorganic drug characterized by well-known anti-inflammatory, anti-atherosclerotic, and cytoprotective properties and with a clean safety profile in human clinical trials [181]. This compound was shown able to covalently inhibit PLpro activity with an IC_{50} ~2 μM and thus was used as starting point to generate a library of 11 derivatives by

substitution/functionalization of the N-phenyl ring (Fig. **14B**) [181]. Eleven Ebselen analogue compounds were virtually screened against PLpro and among them, those with the phenyl ring orto-functionalized by hydroxy or methoxy groups (see compounds 1d and 1e in Fig. **14B**) showed additional interactions with PLpro active site and consequently exhibited an inhibitory potency which was an order of magnitude higher respect to Ebselen (Fig. **14B**) [181].

Interestingly structure-based virtual screening coupled to HTS demonstrated also that Ebselen is able to block SARS-CoV-2 Mpro activity with IC_{50}=0.67 μM and also possesses some antiviral properties in cell-based assays with EC_{50} = 4.67 μM [161].

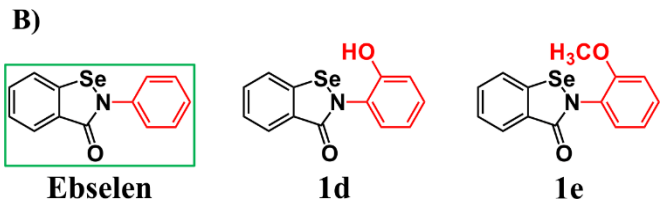

Fig. (14). B) Chemical structures of Ebselen and analogue compounds able to covalently inhibit SARS-CoV-2 PLpro activity [181]. The reference compound "Ebselen" is enclosed in the green rectangle whereas, chemical functionalizations in the N-phenyl ring are highlighted in red.

An alternative approach was based on the similarities of PLpro with Ubiquitin-specific protease 2 (USP2) as concerning structural fold and conserved catalytic triads C-H-D/N. Indeed, this study was first focused on the USP2 structure and led to the identification of a molecule named Z93 as USP2 inhibitor through a multidisciplinary approach relying on virtual screening and *in vitro* cell-based assays [182]. Next, the combination of molecular docking studies and MD simulations showed that Z93 inserted well also in the binding pocket of SARS-CoV-2 PLpro, thus suggesting its potential activity against it (Fig. **14C**, upper panel) [182].

Another work started from a library of 93 molecules, comprising 38 drugs and analogues with antiviral activity and 55 molecules from natural sources with protease inhibitory activity [183]. Screening by computational tools showed Amentoflavone and MK-3207 as potential SARS-CoV-2 PLpro ligands and potential inhibitors (Fig. **14C**, lower panel) [183].

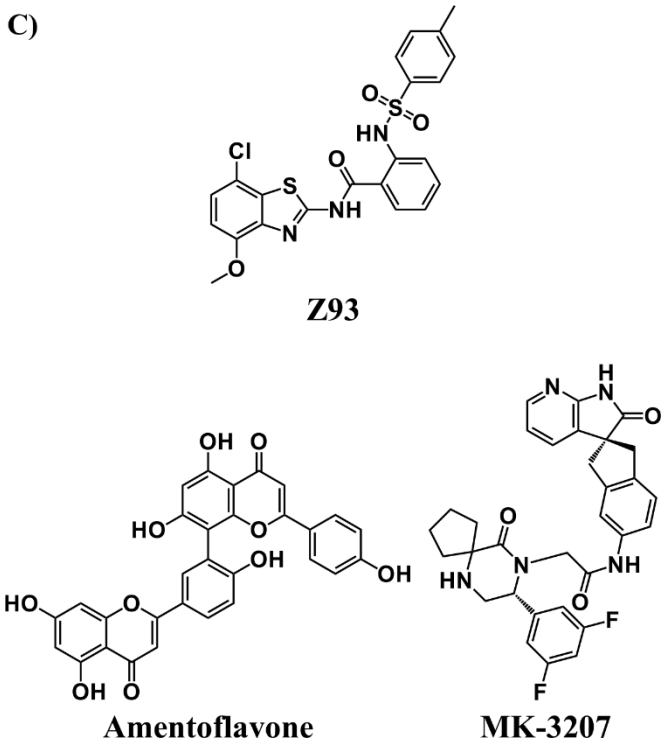

Fig. (14). C) Upper panel: Chemical structure of a potential PLpro inhibitor found starting from molecules targeting USP2 [182]. **Lower panel:** Chemical structure of potential PLpro inhibitors identified from a small library including drugs, molecules with antiviral activity and natural origin compounds with protease inhibitory activity [183].

4.3. Lead compounds against non-structural proteins (helicase, polymerase, endoribonuclease)

In the route to get a molecule able to block SARS-CoV-2 infection, different enzymes exploited by the virus (i.e., helicase, polymerase, and endoribonuclease) have been investigated as potential drug targets.

NSP12 (also known as RdRp, RNA-dependent RNA polymerase) is a protein involved in the replication and transcription of the viral RNA genome [184, 185]. This protein is characterized by a N-terminal β hairpin (residues V31-K50) followed by the N-terminal nidovirus RdRp-associated NucleotidyltRANsferase (NiRAN) domain (residues Q117-A250) including seven helices and three β strands (Fig. **15**) [185]. The Interface domain of NSP12 (residues L251-R365) possesses three helices and five β strands and foreruns the RdRp domain (residues L366 to F920) (Fig. **15**). This latter module assumes a cupped right-handed structural topology with a Finger subdomain (S397-A581 and K621-G679 residues), a Palm subdomain (T582-P620 and T680-Q815 residues) and a Thumb subdomain (L819-F920 residues). The Finger and Thumb subdomains adopt a closed circle shape (Fig. **15**), this closed structural configuration is favored by interaction with NSP7 and NSP8 [185]. In addition, two sets of residues (i.e., H295, C301, C306, C310 and C487, H642, C645, C646) form the conserved binding motifs which coordinate two zinc ions and are responsible for the structural integrity of the RdRp domain [185].

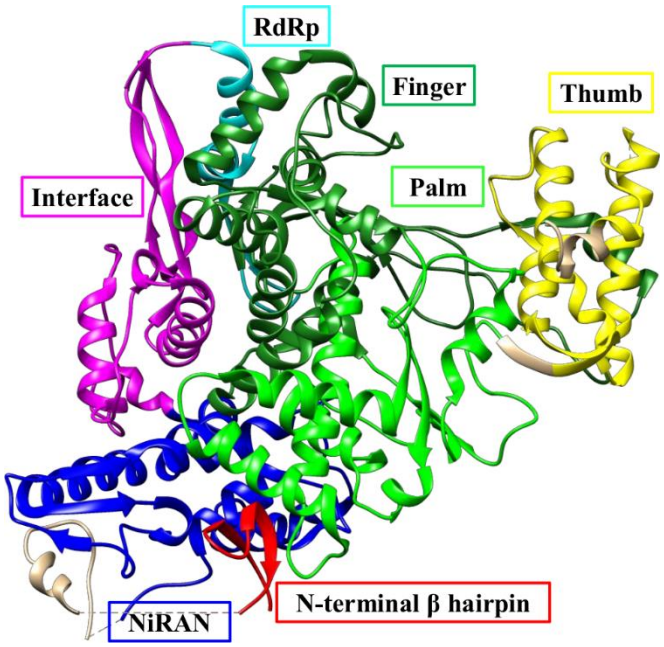

Fig. (15). Cryo-EM structure of SARS-CoV-2 NSP12 extrapolated from the NSP12-NSP7-NSP8 RdRp complex (PDB code: 7BV1 [185]). The N-terminal β hairpin is colored red whereas, the NiRAN domain is colored blue. Cyan is used to indicate additional residues in the RdRp domain (a.a. 366-396). The Interface domain is shown in magenta. The finger, palm and thumb subdomains are colored in green, light green and yellow, respectively. Residues linking NiRAN and the N-ter β hairpin domains are reported in ivory.

One of the strategies proposed to identify NSP12 inhibitors consisted in a multi-screening approach, made up of molecular vector-based, structure-based and force field-based methodologies, of an approved drugs library (1906 compounds) [121]. The protocol included two sequential molecular vector-based screening for estimation of protein-ligand interactions. The first one consisted in the DFCNN (Dense Fully Connected Neural Network), representing a deep learning-based model used to predict protein-drug binding probability whereas, the second one was the DeepBindBC (DeepBind Binary Classifier), consisting of a structure-based drug screening. In details, DFCNN does not employ the spatial data at interaction spot but molecular vector information linked to both ligand and protein pocket and evaluates the protein - ligand couple as non interaction or interaction assigning a probability score ranging from 0 to 1. DeepBindBC employs instead the 3D model of a protein-ligand complex to evaluate potential binding from data on atom contacts at interaction interface [121]. Structure-based canonical docking was also conducted with AutoDock Vina [186]. The stability of the generated drug/NSP12 complexes was tested by MD simulations. This screening strategy against the RdRp binding pocket in NSP12 led to the identification of four drug hits (i.e., Pralatrexate, Azithromycin, Sofosbuvir, Amoxicillin). Experimental validation highlighted the *in vitro* capacity of Pralatrexate and Azithromycin (Fig. **16**) to inhibit SARS-CoV-2 replication [121].

Antiviral drugs were virtually screened against SARS-CoV-2 RdRp active site [187]. One of these molecules (i.e., Galidesivir) was considered as reference compound for the next step of ligand-based virtual screening against the PubChem database to select 1061 drug-like compounds with more than 95% structural similarity with Galidesivir. The resulting molecules were further filtered by considering Lipinski's rules and the resulting 677 compounds were next employed in docking runs against RdRp from SARS-CoV-2. In the end the study led to the identification of two drug-like compounds as potential strong inhibitors of SARS-CoV-2 (i.e., CID123624208 and CID11687749) (Fig. **16**) [187].

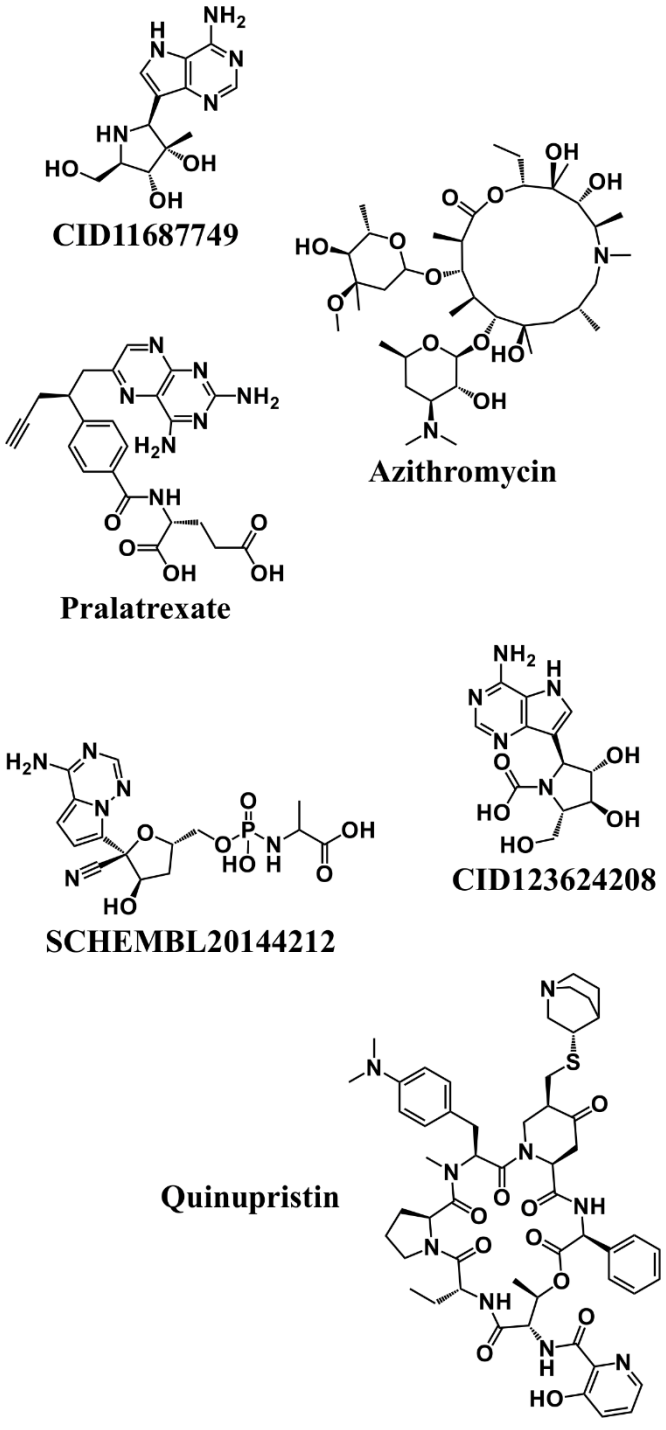

Fig. (16). Chemical structures of some of the best inhibitors found for NSP12 by different virtual screening approaches [121, 187-189].

A similar approach was adopted starting from another reference antiviral drug (i.e., Remdesivir) [188]. Remdesivir is active towards SARS-CoV-2 by blocking its RdRp. Interestingly, viral RdRps are strongly subjected to mutations that confer them drug resistance. A starting virtual screening selected 704 molecules provided with 90% similarity to the Remdesivir. Estimation of druggability and prediction of antiviral inhibition filtered 32/704 and 7/704 compounds, respectively. Analyses of intermolecular interactions revealed that the final seven molecules were able to bind the RdRp with better affinity compared to Remdesivir and also show higher predicted antiviral inhibition percentages. The compound named SCHEMBL20144212 was suggested as good SARS-CoV-2 inhibitor since it was predicted to possess the highest interaction affinity for both the native and mutant (P323L) RdRp (Fig. **16**) [188].

HTVS (High-Throughput Virtual Screening) on the active site of the SARS-CoV-2 RdRp using ensemble docking and a collection of commercially available small-molecules was described in literature [190]. The study showed better scores for compounds containing aromatic moieties at the two extremities, e.g., pyrimidine, triazol or benzene analogues on one side and benzene, pyrrole or indole on the other side. In addition, good *in silico* hits possessed a nitrogen-rich guanidine or thioether-amide linker connecting the two sides [190]. Another work was based on virtual screening of FDA approved drugs that were assayed against RdRp of SARS-CoV-2 using both an experimental structure and a homology model based on sequence similarity with SARS-CoV. Three different docking strategies (ensemble, rigid and flexible docking runs) were implemented. Ensemble docking is based on the concept that the protein structure used as input is an ensemble of conformers; instead, rigid docking exploits only one static conformation of the protein [189]. The first method can be considered the best route to describe the nature of a protein structure but requires a higher computational cost compared to the second method. Instead, the flexible docking is based on the freedom of movement of a few residues during docking and thus can be considered as a compromise between ensemble and rigid docking methods. However, all three approaches used within this work led to the identification of Quinupristin (an antibiotic known to cause relatively minor side effects) as potential inhibitor of NSP12 (Fig. 16) [189].

NSP13 is a 67 kDa protein that belongs to the helicase super family 1B and plays different functions [191]. The helicase activity is necessary in SARS-CoV-2 for the regulation of RNA metabolism. Indeed, the enzyme NSP13 exploits the energy of nucleotide triphosphate hydrolysis to induce unwinding of ds RNA or DNA in the direction from 5' to 3'. Nevertheless, NSP13 presents the RNA 5' triphosphatase activity by which it is involved in the formation of the 5' cap structure of viral mRNAs. NSP13 binds NSP12 and functions in coordination with the RTC (i.e., the NSP7/NSP8/NSP12 complex). The helicase activity is considerably stimulated by this interaction. NSP13 presents a N-terminal zinc binding domain (ZBD) which is responsible for the coordination of 3 zinc ions (two by a Really Interesting New Gene (RING)-like motif and one by a treble-clef Zinc-finger module) with structural functions [191-193]. In addition NSP13 contains a "stalk" domain made up of a three-helix bundle and a 1B domain with a 6-stranded RIFT-type anti-parallel β-barrel along with two "RecA(Recombinat protein A) like" helicase subdomains 1A and 2A, that also form a cleft containing the nucleotide binding site and where hydrolysis occurs (Fig. **17A**) [191]. The Rec-A core domains of 1A and 2A are connected to 1B domain by a long linker (i.e., 30 residues) devoid of secondary structure elements [191]. Cryo electron microscopy studies of the complex formed by NSP13 and the RTC have been conducted. The resulting structure includes two NSP13 and two NSP8 units: two NSP13 monomers exploit their ZBD domains to make contacts with NSP8 while interestingly, only one of the two NSP13 units is also involved in the interaction with NSP12 (Fig. **17B**) [194].

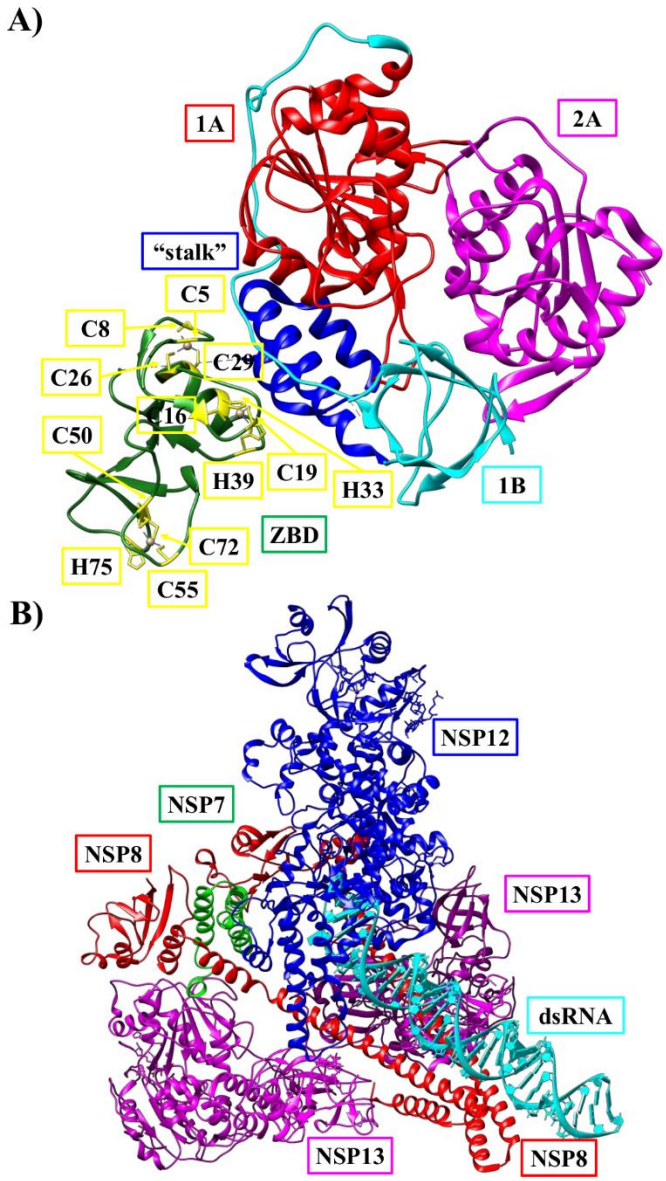

Fig. (17). A) X-ray structure of the NSP13 of SARS-CoV-2 (PDB code: 6ZSL [191], only chain A is reported). The ZBD domain (a.a. 1-99) is reported in green, and the residues involved in the coordination of zinc ions (C5, C8, C16, C19, C26, C29, H33, H39, C50, C55, C72, H75) are highlighted in yellow. The "stalk" (a.a. 100-149), 1B domain (a.a. 150-260), the "RecA like" helicase subdomains 1A and 2A (a.a. 261-441 and 442-596, respectively [195]) are colored blue, cyan, red and magenta, respectively. **B)** Electron Microscopy structure of the complex formed by NSP13 and the SARS-CoV-2 RTC (PDB code: 6XEZ [194]). The structure includes two NSP8 units (red), two NSP13 units (magenta), one NSP7 molecule (green) and one NSP12 molecule (blue) as well as a ds RNA fragment (cyan).

One of the strategies proposed for the identification of NSP13 inhibitors started from homology modelling and molecular dynamics to get unbound and ATP/RNA-bound conformations of the enzyme [196]. Then, a library of ~970,000 chemical compounds was used as input for the high-throughput virtual screening against the ATP binding cleft [196]. The resulting best molecules (i.e., drug approved compounds) were further analyzed to evaluate their activity in inhibiting purified recombinant SARS-CoV-2 helicase. In the end two drugs (i.e., Lumacaftor and Cepharanthine) were suggested as promising inhibitors and potential therapeutics against COVID-19 (Fig. 18) [196]. Interestingly, Lumacaftor in combination with other drugs is employed in the treatment of patients affected by cystic fibrosis [197] whereas, Cepharanthine is employed to treat snake bites and several chronic diseases like alopecia [198]. A screening of the Medicinal Plant Database for drug design through a combination of docking runs, MD simulations and free binding energy calculations led also to the identification of another compound (i.e., PubChem ID: 110143421) possibly able to target NSP13 ATP binding site (Fig. 18) [199].To further discover novel SARS-CoV-2 helicase inhibitors, a protein-ligand interaction fingerprint study was employed to get a 3D pharmacophore model starting from the critical contacts between co-crystallized fragments and the NSP13 helicase active site [200]. Then, the 3D pharmacophore model was employed to set up a virtual screening approach with the well-known ZINC [98] database that includes 250 million of compounds. The resulting molecules were further analyzed by consecutive steps of MD simulations and MM-PBSA (Molecular Mechanics Poisson-Boltzman Surface Area) based binding energy calculations and one compound (i.e., FWM-1) was suggested as potential potent NSP13 inhibitor (Fig. 18) [200]. Similarly, docking studies coupled to molecular dynamics simulations were employed to analyze a compound database composed of more than 14,000 phytochemicals [201]. This protocol led to the identification of different potential binders of NSP13 (e.g., Picrasidine M and (+)-Epiexcelsin) [201] (Fig. 18).

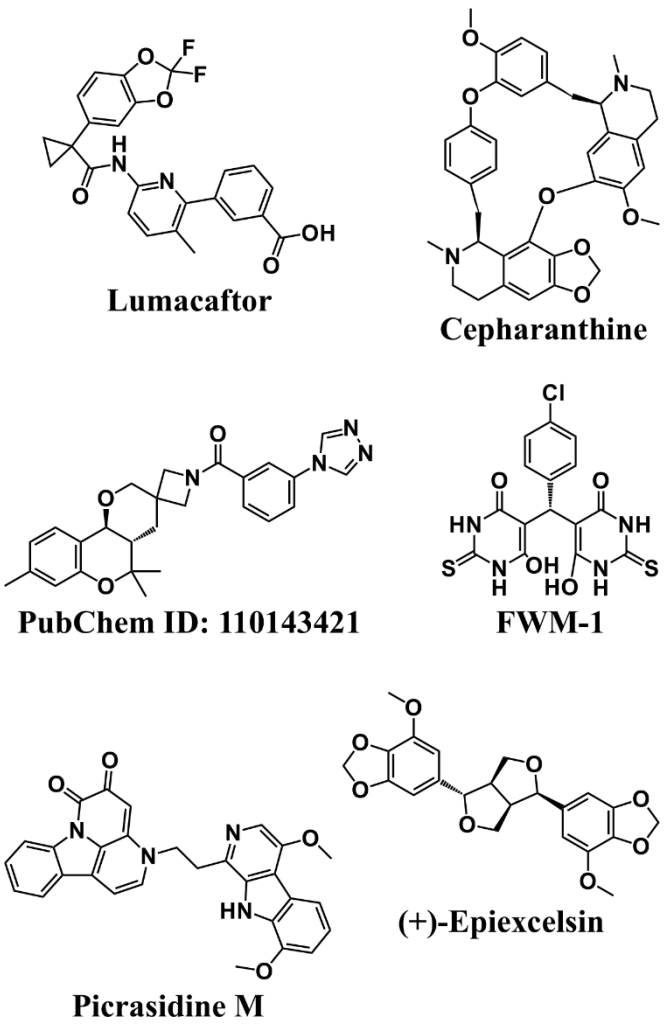

Fig. (18). Chemical structures of a few NSP13 inhibitors discovered by *in silico* approaches [196, 199-201] .

NSP14 of SARS-CoV-2 is another enzyme important for viral genome replication and transcription; it exerts two functions: one by its N-terminal ExoN domain (residues 1-287) and the other by its C-terminal N7-MTase domain (residues 288-526) (Fig. **19**) [202-204]. The ExoN domain ensures the accuracy in the RNA synthesis by eliminating the wrongly incorporated nucleotides or nucleotide analogs from the growing RNA strand thus avoiding the occurrence of lethal mutations. The N7-MTase domain is responsible for 5' capping of the viral RNA that is important for escaping the host defense and for assisting in translation. Interestingly, the ExoN activity of NSP14 is stimulated by NSP10 that interacts with the ExoN domain and favors structural stability of the ExoN active site [204]. The N7-MTase has as main substrate the Guanosine-P3-Adenosine-5',5'-Triphosphate (G3A) that is necessary for guanine activation. N7-MTase catalyzes a reaction completely dependent on G3A binding for achieving the 5' cap structure of viral genomic and sub-genomic RNAs [203]. Initially, in absence of an experimentally determined structure for NSP14, computational studies were centered on obtaining a homology model starting from atomic coordinates of the SARS-CoV NSP14/NSP10 complex [203]. The structural features characterizing the interaction of G3A with the N7-MTase domain of NSP14 from SARS-CoV-2 was next obtained with the support of docking and molecular dynamic

simulations. Virtual screening of the Traditional Chinese Medicine database was further conducted against the modelled structure of SARS-CoV-2 NSP14 [203]. The next consecutive steps of MM-GBSA calculations, MD simulations, and principal component analysis (PCA) calculations led to the identification of different potential inhibitors of NSP14 [203] able to interact with the G3A binding site of homology modeled N7-MTase domain. The best hits suggested by this computational approach, by blocking substrate-binding, could hamper the viral 5'-end RNA capping process [203].

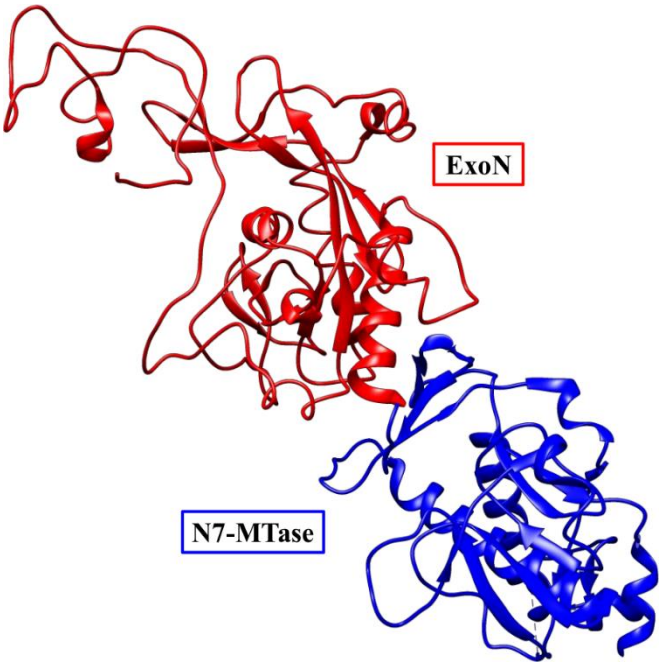

Fig. (19). Cryo-EM structure of SARS-CoV-2 NSP14-NSP10-RNA complex (PDB code: 7N0B [204]), only the NSP14 structure is shown). Red is used to highlight the ExoN domain (A1-V287) while blue is used to indicate the N7-MTase domain (K288-Q527).

A subset of compounds from the ZINC database (i.e., FDA, world-not-FDA and investigational-only subsets) was virtually screened against a SARS-CoV-2 NSP14 homology model, that was built again based on the similarity between SARS-CoV and SARS-CoV-2. Different drugs like Hypericin (Fig. **11C**) and Saquinavir (Fig. **12A**) were identified as binders of both the N- and C-terminal domains of NSP14 [202].

As concerning NSP15, the enzyme is a uridine specific endoribonuclease that is exploited for the cleavage of viral RNA and for the escaping from the host immune defense system [205]. NSP15 structure is characterized by the N-terminal domain (a.a. S2-R62) with two α-helices (i.e., α1 and α2) sided by an antiparallel β-sheet, including β1, β2, and β3 strands, the central domain (a.a. N63-Q188) composed by various secondary structural elements: three β-hairpins (β5-β6, β7-β8, and β12-β13), a mixed β-sheet (including β4, β9, β10, β11, β14, and β15), two α helices (α3 and α5) and one 3_{10} helix and by the C-terminal catalytic NendoU domain (a.a. E192-K345) with two antiparallel β-sheets (i.e., β16-β17-β18 and β19-β20-β21) whose edges delineate the catalytic site (Fig. **20**) [206]. In addition, five α-helices (i.e., α6, α7, α8, α9, and α10) are positioned on the sides of the concave surface formed by the β-sheets (Fig. **20**) [206]. The active site of NSP15 contains six crucial residues (H235, H250, K290, T341, Y343, and S294) that are conserved amongst SARS-CoV, MERS-CoV, and SARS-CoV-2.

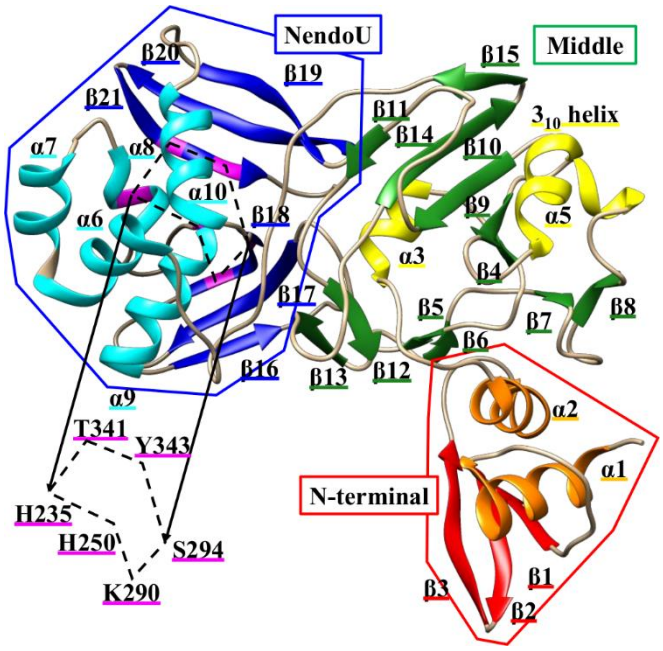

Fig. (20). X-ray structure of SARS-CoV-2 NSP15 (PDB code: 6VWW [206], only the chain A is reported). Red and orange are used to respectively indicate the β and α structures of the N-terminal domain. Green and yellow indicate respectively the β and α structures of the middle domain. The β and α structures of the C-terminal catalytic NendoU domain are colored blue and cyan, respectively. Conserved residues in the active site are highlighted in magenta.

As for the other targets, also in the case of NSP15 many computational efforts have been conducted to find inhibitors employing a variety of compound libraries. For example, the Asinex antiviral database and a library of 10,000 approved and experimental drugs were implemented for virtual screening by employing crystal structures of NSP15 [207, 208]. These studies suggested compounds N1, N2 and Olaparib (Fig. **21**) as promising NSP15 ligands and potential anti-COVID19 drugs [207, 208]. Different natural product databases were also employed for virtual screening approaches against NSP15 [209-211]. For example, a combination of a docking-based virtual screening and validation by MD simulations steps was conducted by implementing the Selleckchem Natural product database, that includes 2,863 FDA approved compounds, 3,176 FDA approved compounds, that also passed Phase I clinical trial, 2,973 pre-clinical/clinical compounds collection, other diverse bioactive and natural compounds. Results from the virtual approach, by screening in total 24,678 compounds showed Thymopentin and Oleuropein (Fig. **21**) as molecules able to form stable complexes with NSP15 and thus promising inhibitors of this protein [209]. The protocol described in another work considered the natural compound library of ~11,000 molecules from the ZINC database and combined different computational techniques, including virtual screening, modelling, drug-likeliness evaluation, molecular docking, molecular dynamics simulations [210]. The *in silico* study proposed compounds with dihydroxyphenyls (i.e., PubChem ID: 95372568 and 1776037) as ligands able to stably interact with NSP15, and suggested their potential usage as starting hits to build novel NSP15 inhibitors (Fig. **21**) [210]. Moreover, the Nuclei of Bioassays, Ecophysiology and

Biosynthesis of Natural Products (NuBBE) database was employed for a computation screening protocol against the active sites of NSP15. Sequential steps of HTVS, docking optimization, and binding energies calculations were conducted and revealed two molecules (i.e., NuBBE-1970 and NuBBE-242) that could strongly and stably bind NSP15 [211].

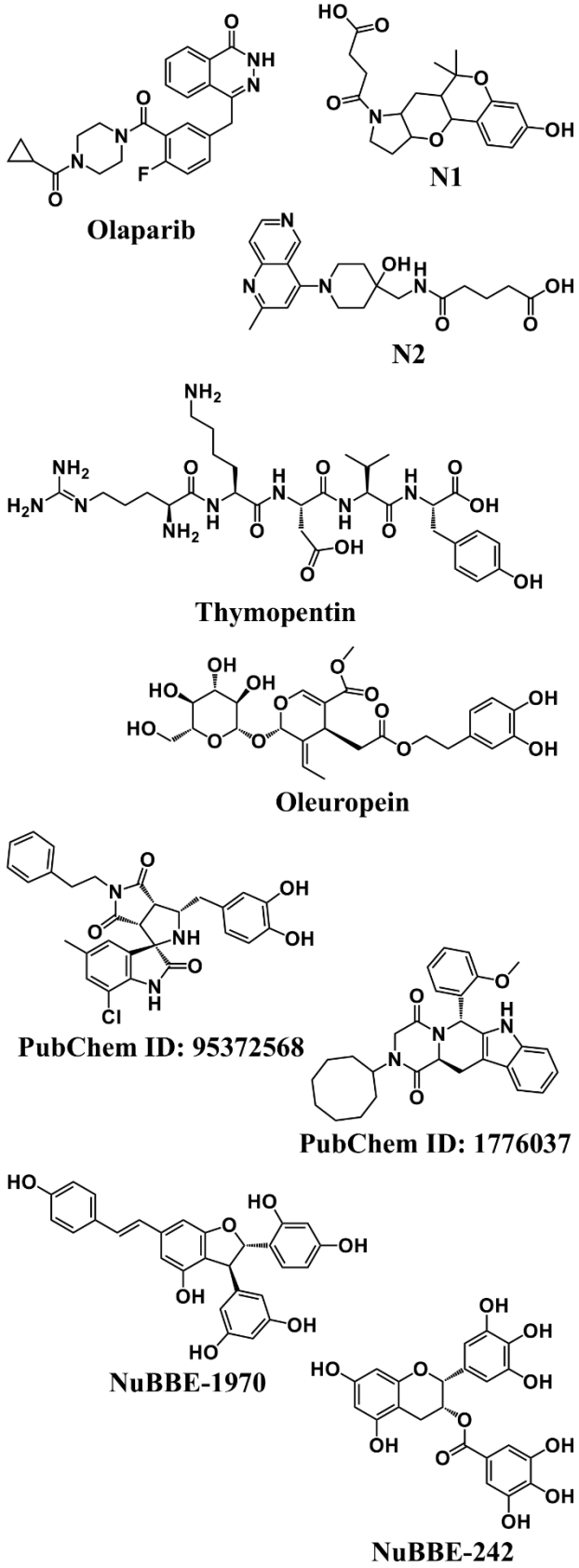

Fig. (21). Chemical structures of some of the best NSP15 inhibitors found by virtual screening [207-211].

The multiplicity of examples reported represents only part of the computational screening campaigns that were carried out to find antiviral agents attacking enzymes crucial during SARS-CoV-2 life cycle. More experimental validation and, in certain cases improvement of drug-likeness, is surely needed before starting employing the computational hits for COVID-19 prevention and treatment.

4.4 Multi-Target approaches

Discovering therapeutics that can target more than one viral enzyme represents an important strategy against SARS-COV-2 infection. In the last two years many *in silico* screening approaches have been devoted to discovering drugs targeting multiple viral proteins at the same time, or mixtures of drugs each having binding affinity towards a specific viral target. The choice of single or multiple protein targets to fight COVID-19 depends on the different stages of the viral infection under consideration. In fact, to inhibit the host cell recognition, it is convenient to target only the S protein of SARS-COV-2 in order to avoid formation the Spike RBD (Receptor Binding Domain)/ACE2 complex. However, after host cell recognition happens, several proteins related to viral transcription and replication processes play important roles in infection progression and it can be useful to inhibit them with a multi-target approach [212]. The multi-target approach presents also the advantage to overcome the issues related to the rapid mutation of viral proteins when mixtures of drugs are used as, if a specific target mutates, diverse drugs contained in the mixture can still target the other unmutated proteins making the treatment efficacious. Therapies including mixtures of drugs are already prescribed for HIV infection. An example is the FDA-approved drug Combivir, a mixture of AZT (Azidothymidine) and 3TC (Lamivudine) that targets enzymes involved in different steps of HIV replication [212].

In silico methods in drug discovery are considered simply applicable and time saving, especially when drug candidates are FDA approved compounds, already employed to treat other diseases, that might be repurposed against COVID-19. In fact, the drug repurposing approach is a less expensive and time consuming way to identify new therapies, because in most cases preclinical safety studies have already be done [213]. For this reason, many computational works implemented virtual screening of FDA approved drugs *versus* SARS-COV-2 proteins. In particular protein-ligand docking methods have been widely used since, as previously described in this review, they are supported by the availability in the PBD of several 3D structures of viral proteins and the possibility to obtain the structures of many approved drugs - in the proper format needed for virtual screenings- from numerous online databases.

Multi target docking studies have been frequently focused on drug repurposing of FDA approved antiviral drugs, that have already been used for other viral infections [214-217], or even prescribed for different diseases [212, 218-228].

For example, in a work by Nunes et al. [217] a virtual screening was performed using 22 antiviral drugs obtained from the DrugBank database, in addition to the antibiotic Azithromycin and the antinematode Ivermectin, against seven SARS-COV-2 non-structural proteins: NSP3 (PLpro), ADRP

(ADP Ribose Phosphatase region of NSP3), NSP5 (Mpro), NSP9 (RNA-replicase), NSP12 (RdRp), NSP15 (endoribonuclease), and NSP16 (2'O-methyltransferase) *via* molecular docking and molecular dynamics (MD) simulations [217]. Molecular docking simulations were performed using Autodock Vina v1.1.2 software [186], by setting the grid boxes at the active site of the proteins. The results of the virtual screening experiments were ordered on the basis of the binding affinity of the best scoring compounds, and to support the results of docking simulations, the complexes of the best three ligands, Paritaprevir (PAR), Simeprevir (SIM), and Glecaprevir (GLE), with all seven targets, were subjected to MD simulations. Based on the results of this study, PAR (Fig. **22**) was predicted as a possible drug targeting all tested NSPs, principally ADRP and Mpro. Moreover, the results suggested SIM (Fig. **22**) as a possible strong inhibitor of Mpro. In particular, MD simulations revealed a high stability of the PAR/ADRP complex, due to hydrophobic contacts engaged by phenanthridine and methylpyrazine rings of PAR with the binding site of the protein. Thus, the authors of this work proposed that a mixture of PAR and SIM could induce a cooperative response against COVID-19 [217].

In another study [220], 1,520 PCL (FDA approved Prestwick Chemical Library) compounds were used to perform multi-target virtual screening against non-structural proteins NSP3 (ADRP region of PLpro), NSP9 (RNA-replicase), NSP12 (RdRp) and NSP15 (endoribonuclease) of SARS-COV-2 [220]. The authors were inspired to select compounds from the PCL library because in previous works a few of these molecules were reported to have promising antiviral activity against SARS-COV, MERS-COV, and SARS-COV-2 viruses [220]. Virtual screening by molecular docking was performed with Schrödinger software (Glide module) [229] and MD simulations were done to validate docking results for the best scoring ligand-protein complexes. The results suggested four best compounds: Hesperidin (*vs* NSP3), Diosmin (*vs* NSP9), Catenulin (*vs* NSP12), and Acarbose (*vs* NSP15). In particular, Diosmin revealed the best multi-targeting ability as it showed interactions with all four proteins, followed by Hesperidin that interacted with three protein targets. Both drugs are known to be chemopreventive agents against cancer, viral infection and inflammatory related symptoms and are being explored in clinical trial phase 1 as treatment route against COVID-19 [220]. The best candidate Diosmin (Fig. **22**) showed important H bond interactions with all the proteins as evidenced by molecular docking results. Moreover, MD simulations revealed the conformational flexibility and stability of the Diosmin in complex with all four NSP targets, providing validation of the docking experiments and supporting the multi-target ability of Diosmin. Thus, this work suggests Diosmin as a possible multi-target drug that should be further validated as a therapeutic against COVID-19 [220].

Another example is the work by Thurakkal et al. [227] in which 76 organosulfur compounds were screened against 5 SARS-COV-2 proteins: NSP5 (Mpro), NSP3 (PLpro), S (spike protein), NSP12 (RdRp) and NSP13 (helicase) by molecular docking studies. During the virtual screening also known inhibitors of target proteins were implemented as reference compounds: Indinavir for Mpro, Darunavir for PLpro, Arbidol for Spro, Remdesivir for RdRp and Ivermectin for helicase [227]. The authors chose organosulfur compounds for virtual screening because they are a class of molecules characterized by sulfur-containing functional groups (for example sulfones, sulfonamides, disulfides, and others), that have important influence in the pharmaceutical area due to their antioxidant, anti-inflammatory and anti-microbial activities [227]. The library of organosulfur compounds included FDA approved drugs, drugs proposed for several diseases and also drugs implemented for SARS-CoV. Even in this case, the results of virtual screening, that was performed with AutoDock Vina [186], were further validated by MD simulations that were performed with the best hit compounds, as assessed by docking, bound to each target (i.e., Lurasidone, Lurasidone sulfoxide, Lurasidone endo, Fananserin, and Lurasidone exo) (Fig. **22**). MD simulations were also carried out for complexes made up with reference ligands and all the different protein targets. In addition, the ADME properties of the best scoring compounds were predicted to explore their pharmacokinetics and druggability properties by means of SwissADME (http://www.swissadme.ch/[230]) and pkCSM (http://biosig.unimelb.edu.au/pkcsm/prediction, [231]) tools. From the 5 selected ligands, Lurasidone and Lurasidone exo were found to be virtually effective on inhibiting all five SARS-COV-2 proteins targeted with significant binding affinities [227].

A large volume of literature regarding multi target virtual screenings by docking methods is centered on natural products as valuable source of drugs to be repurposed for COVID-19 treatment [232-240]. In fact, among natural products there are molecules from plants and mushrooms, such as flavonoids, polysaccharides, alkaloids and polyphenols, conventionally used in infectious diseases treatment due to their properties of immune-booster, antimicrobic, and anti-inflammatory agents [241]. Different herbal medicines are reported to be useful against respiratory viral infections, thus, they could be effective to treat COVID-19 [241]. In this contest, several Chinese groups have implemented computational studies by molecular docking multi target screenings and network pharmacology selecting ligands from databases of natural products belongings to Traditional Chinese medicine (TCM) [234, 240, 242-245], and proposed that TCM preparations could inhibit host-cell recognition and replication of the virus by binding to ACE2 and Mpro proteins, and play an anti-inflammatory role by acting on several signaling pathways [246]. TCM has been combined with Western medicine in fighting COVID-19, thus assuming a significant role in disease prevention and control [246].

An example of drug repurposing of compounds from natural sources is reported in a recent study by Alanazi et al. [247], in which a virtual screening of 150 nutraceuticals included in DrugBank against 14 SARS-CoV-2 proteins was performed. Nutraceuticals are bioactive phytochemicals relatively nontoxic prescribed for treatment of diseases including atherosclerosis, inflammation, cardiovascular diseases, hypertension, cancer, diabetes, and others. The group of viral targets selected for virtual screening included NSP1, NSP3 (PLpro), NSP5 (Mpro), NSP9 (RNA-replicase), NSP12 (RdRp), NSP13 (helicase), NSP15 (endoribonuclease), S (spike), E (envelope), M (membrane), N (nucleocapsid), the accessory proteins 3a, 6, and 7a. The structures of SARS-CoV-2 N, NSP3, NSP5, NSP9 and NSP15 proteins were retrieved from the PDB, and homology modelling was performed for the other proteins using the SWISS-MODEL server [248]. A first step of virtual screening was carried out

using Schrödinger Glide [229], then, top-scoring compounds were also subjected to docking studies using GOLD [249] and AutoDock Vina [186] software. Molecular docking identified several inhibitors; among them, Rutin, NADH, and Ginsenoside Rg1 (Fig. **22**) were ranked as the compounds with the highest binding affinity for most of the SARS-CoV-2 proteins.

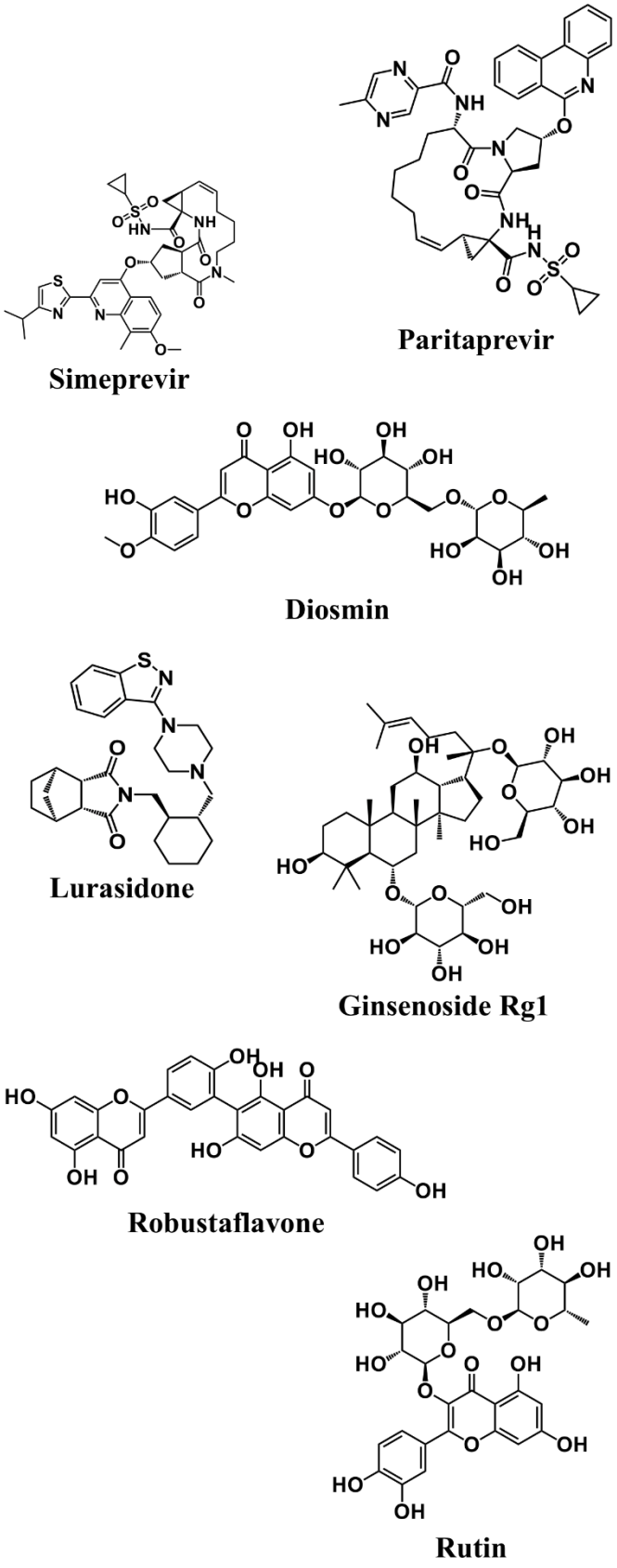

Fig. (22). Chemical structures of some of the inhibitors found by multi-Target approaches [217, 220, 227, 247, 250].

Rutin is a flavonol glycoside broadly found in plants with antioxidant properties and is a main component of nutritional supplements. Moreover, it is an FDA-approved drug prescribed for strengthening weakened capillaries. NADH is a coenzyme performing important metabolic activities that is being considered for its effectiveness in cardiovascular diseases, dementia related to Alzheimer and Parkinson diseases, and chronic fatigue syndrome. Ginsenoside Rg1 belongs to the class of ginsenosides compounds contained in ginseng plants, known to have functions in blood, cardiovascular, nervous, and immune systems. These nutraceutical compounds were proposed to further experimental verification as inhibitors of SARS-CoV-2 proteins and of viral-host recognition [247].

In another recent study [250] 104 anti-HIV phytochemicals have been investigated *in silico* as potential inhibitors of SARS-CoV-2 non-structural proteins. The repurposing of previously reported anti-HIV phytochemicals against SARS-CoV-2 was inspired by the fact that both HIV and SARS-CoV-2 represent single-stranded RNA viruses that employ Rdps and encode precursor polyproteins crucial for their corresponding infectivity. Thus, the anti-HIV phytochemicals were implemented in molecular docking with NSP3 (PLpro), NSP5 (Mpro), NSP10, NSP12 (RdRp), NSP13 (helicase), NSP15 (endoribonuclease), and NSP16 (2'O-methyltransferase) from SARS-CoV-2. The structures of all proteins were obtained from the PDB except NSP13 helicase, for which a model was built starting from the SARS-CoV protein. Molecular docking experiments were performed on UCSF Chimera 1.14 [251] software with AutoDock Vina as docking algorithm. Top compounds in complex with the NSPs were also further investigated through MD simulations. In addition, the drug-likeness and ADME properties were predicted using SwissADME for the top compounds against NSPs [230], together with toxicity profiles that were predicted using OSIRIS Property Explorer software (http://www.cheminfo.org/Chemistry/Cheminformatics/Property_explorer/index.html [252]). The results of this work indicated that polyhydroxylated aromatic substructures of polyphenols are important for binding to the catalytic sites of NSPs. It is well known that polyphenolic natural products such as flavonoids and tannins possess antiviral power and anti-inflammatory, immune, anti-cancer, prebiotic and antioxidants properties. The top-ranking polyphenolics Amentoflavone, Robustaflavone (Fig. **22**), Punicalin, Volkensiflavone, Rhusflavanone, Morelloflavone, Hinokiflavone, and Michellamine B were proposed to be further experimentally validated through *in vitro* and *in vivo* assays, or be considered as models for drug design of novel anti-COVID-19 agents [250].

Among compounds from natural sources, peptides libraries have also been explored in docking-based virtual screening approaches as possible viral proteins ligands [232, 239, 253]. An example is reported in the work by Wong et al. [239] in which the potential of peptides from quinoa seed proteins as multi-target inhibitors of SARS CoV-2 spike RBD domain, NSP5 (Mpro), and NSP3 (PLpro) was investigated by means of molecular docking and virtual screening. Peptides to be screened were obtained from 5 quinoa proteins (2S albumin-like, 11S seed storage globulin, 11S globulin seed storage

protein 2-like, 13S globulin seed storage protein 1-like, and 13S globulin seed storage protein2- like) hydrolyzed *in silico* by papain and subtilisin (1465 peptides generated) by using the BIOPEP-UWM web-server [254]. Quinoa peptides obtained by *in silico* hydrolysis were implemented as peptide inputs in the FASTA format. Reference peptides earlier reported to potentially bind SARS-CoV-2 viral proteins were also included in virtual screening. In addition, SwissADME [230] was used to investigate ADME properties and drug like nature of peptides, in addition, peptide potential toxicity was predicted through the ToxinPred server (http://crdd.osdd.net/raghava/toxinpred [255]). AllerTOP v.2.0 (http://www.ddg-pharm fac.net/Aller TOP [256]) was used for allergenicity prediction. Seven of the screened peptides were reported to interact with the key binding and catalytic residues of the viral proteins, by means of interactions mainly driven by hydrogen bonds and hydrophobic contacts. On the basis of docking results the best ranked peptides had scores comparable or better than formerly reported anti-SARS-CoV-2 peptides, moreover, they were assumed to be non-toxic and non-allergenic. Among them, the peptide sequence VEDKGMMHQQRMMEKAMNIPRMCGTMQRKCRMS was found to interact with the highest number of key residues on the protein targets. Thus, this peptide was proposed by the authors as a promising candidate for further development of peptide-based drugs against COVID-19 [239].

There are also in literature a few multi-target virtual screening-based studies not related to drug repurposing, as the screened ligands represent newly synthesized compounds [257], large libraries of small molecules from ZINC database [258], virtual analogues of particular chemical scaffolds such as the approved drug for influenza virus Arbidol [259] and benzene [260] and even carbon nano materials with therapeutic properties [261].

In detail, Skariyachan et al. [261] investigated the binding potential of carbon nanotube and nano fullerene towards different SARS-CoV-2 proteins by molecular docking and MD simulations. Carbon nanotubes (CNTs) represent nanomaterials with therapeutic properties due to their mechanical features, the presence of functionalizable groups, and structural stability. Nanomaterials can be also employed to project biocompatible delivery systems for drug or vaccine against COVID-19. In addition, nanoparticles possess inhibitory properties against several microorganisms. The SARS-CoV-2 proteins targeted during virtual screening were the Spike, NSP12 (RdRp), NSP5 (Mpro), NSP3 (PLpro), and the RNA binding domain of the nucleocapsid protein and their 3D structures were obtained from the PDB, instead, the 3D structures of carbon nanotubes and nano-fullerene were computationally modeled. Docking runs were performed with Autodock Vina [186]. PreADMET [262] and admetSAR [263] tools were used to predict the drug-likeness and pharmacokinetic features of the molecules. Molecular docking studies evidenced that both nanoparticles have significant binding affinity towards all SARS-CoV-2 targets, but carbon nanotubes showed better interaction when compared to carbon fullerene. MD simulation studies established that the dynamic interactions between viral targets and nanomaterials were stable. The PreADMET and admetSAR tools predicted some toxicity of the nanoparticles but despite this, the authors highlighted that the ADME properties obtained from the computational predictions were comparable to those reported for many of the prescribed drugs and that these nanoparticles could be employed as potential lead molecules against multiple targets of SARS-CoV-2 after further experimental validations [261].

All the computational studies based on the multi-target approach applied to COVID-19 identified a few compounds, often drugs to be repurposed, that would be worth testing into COVID-19 therapy. These computational data provide insightful indications for the development of new drugs, but the actual antiviral potency and therapeutic effects of these compounds must be tested in experimental models of SARS-CoV-2 infection.

CONCLUSION

Computational approaches provide a cheap and fast starting route to discover compound modulators of proteins playing key functions in different diseases. Consequently, during the last few years, such *in silico* tools have been largely employed to look for novel therapeutics against COVID-19. Computational studies are particularly useful to provide potential inhibitors of key SARS-CoV-2 proteins acting at different phases of viral life cycle but, of course they need proper experimental validation. It is unlikely that a virtual screening campaign will bring to a drug, but it is possible that the computational strategy will lead to a hit that will require medicinal chemistry efforts to improve potency and drug-likeness. In the case of SARS-CoV-2 to further accelerate the overall process, drug repurposing coupled to structure-based virtual screening surely constitutes an appealing option.

Indeed, one of the advantages of exploiting drug repurposing relies on the fact that the repurposed drug can reach the market at 10 times lower costs and in a short time period (about 0.5 shorter) if compared to a completely novel drug [73]. Drug repurposing strategies can be fully computational, relying on experimental biological methodology or combine experimental and computational routes. Computational drug repurposing includes Network-based, AI (Artificial Intelligence)-based and Structure-based approaches, examples of the last methodology have been given through the review [213]. To quickly discover repurposable drugs against SARS-CoV-2 a network-based system pharmacology approach can be for instance employed, by analyzing and quantifying the connections between the ensemble of coronavirus-human cell interactions and the drug targets identified within the human protein–protein interaction network [225]. Interestingly, CovMulNet19 represents a network medicine tool that can be used for drug repurposing against COVID-19. This approach relies on a wide-ranging COVID-19 grid including knowledge of all available identified interactions related to SARS-CoV-2 proteins, human proteins able to bind them, diseases and symptoms that are connected to these human proteins and molecules potentially capable of targeting them [264]. Another network-based drug repurposing platform for COVID-19 consists of DGDr-Net (Disease-Gene-Drug Network). DGDr-Net includes 592 diseases, 26,681 human genes and 2,173 drugs, and medical data for 18 canonical comorbidities [265]. Similarly, SAveRUNNER (Searching off-lAbel dRUg aNd NEtwoRk), is a network-based algorithm able to correlate drug and disease by evaluating the interplay between drug targets and the disease-specific proteins in the human interactome [266]. In this process, connections between drugs

and diseases belonging to the same network neighborhoods receive higher priority [266]. As concerning AI-based approaches, the ML (Machine Learning) technology is used to learn from examples and build predictive models even when there is a really poor knowledge of the fundamental biological processes or when computational simulations relying on crucial physical models cannot be performed as they result to be too expensive. [267]. Structure-based drug-repurposing employs instead largely molecular docking to predict if chemical compounds can interact with macromolecules, whose 3D structures are available or can be built by modelling methods [213, 225].

Despite the critical role of drug repurposing in the beginning of SARS-CoV-2 outbreak, a detailed description of drug repurposing strategies exploited against SARS-CoV-2 is beyond the main goal of the present review. Instead, this work intends to provide readers with a portray of the multiplicity of computational routes that could conduct in a fast and efficient way to novel anti-SARS-CoV-2 therapeutics. Particular attention is given to docking-based virtual screening approaches. The largest efforts have been thus far centered on targeting by computational tools viral entry through inhibition of the interaction between S-protein and ACE2 receptor [148, 153, 154]. Another large area investigated by computational tools is linked to the discovery of inhibitors of viral proteases -especially Mpro- thus avoiding maturation of viral proteins necessary for replication [159, 162, 166, 169, 170]. Other viral non-structural proteins provided with enzymatic activities like NSP13 (helicase), NSP12 (RdRp), NSP15 (endoribonuclease) and NSP14 enzymes are important for viral genome replication and transcription and for escaping the host defense machinery [121, 199, 202, 209] and their draggabilities have been also investigated quite a bit by virtual screening campaigns.

Such computational studies analyzed the most diverse databases of molecules to search a vast portion of chemical space and investigate molecules of natural origins (like plant extracts, dietary compounds) [167, 177, 199] as well as FDA approved drugs comprising already established antiviral agents efficacious against other viruses like HIV [168, 212, 250]. The need to urgently eradicate COVID-19 led to the flourish of computational approaches to find novel therapeutics and to the identification of many anti-SARS-CoV-2 potential active compounds. Unfortunately, most of the collected data still lacks proper in vitro and in vivo validation and the conclusions drawn from the vast virtual screening campaigns remain still rather speculative. More efforts need to be devoted in the close future to prove the therapeutic power of *in silico* identified compounds with the goal to catch, among the very large number of computational hits, novel therapeutic agents to prevent and/or treat COVID-19.

*Address correspondence to Marilisa Leone at the Institute of Biostructures and Bioimaging, National Research Council of Italy, Via De Amicis 95, 80145, Naples, Italy; E-mail: marilisa.leone@cnr.it

LIST OF ABBREVIATIONS

ASGR1: ASialo Glycoprotein Receptor-1

ACE2: Angiotensin-Converting Enzyme 2

ADRP: ADP Ribose Phosphatase

AI: Artificial Intelligence

ATF6: Activating Transcription Factor 6

BABM: Biological Activity-Based Modelling

CASP: Critical Assessment of Structure Prediction

CD: Connector Domain

CH: Central Helix Region

CLD: Collectrin-Like Domain

CORDITE: CORona Drug InTEractions

CT: Cytoplasmic Tail

CoVDB: Coronavirus Antiviral & Resistance Database

CoVex: CoronaVirus explorer

CoVs: CoronaViruses

DeepBindBC: DeepBind Binary Classifier

DFCNN: Dense Fully Connected Neural Network

DGDr-Net: Disease-Gene-Drug Network

ds RNA(DNA): double stranded RNA(DNA)

ER: Endoplasmatic Reticulum

ERGIC: ER-Golgi Intermediate Compartment

ExoN: ExoNuclease

FBPM: Fragment Based Pharmacophore Model

FDA: Food and Drug Administration

FERM: Four point one, ERM (Ezrin, Radixin, Moesin)

FP: Fusion Peptide

FPPR: Fusion Peptide Proximal Region

gRNA: genomic RNA

G3A: Guanosine-P3-Adenosine-5',5'-Triphosphate

GFP-LC3: Green Fluorescence Protein - Light Chain 3B

GRP78: Glucose Regulated Protein 78

HAT: Human Airway Trypsin- like protease

HCoVs: Human CoronaViruses

HIF-1: Hypoxia-Inducible Factor 1

HCQ: HydroxyChloroQuinone

HR1: Heptapeptide Repeat sequence 1

HR2: Heptad Repeat 2

HTS: High-Throughput Screening

HTVS: High-Throughput Virtual Screening

IBV: Infectious Bronchitis Virus

IL: InterLeukin

IRE1: Inositol-Requiring Enzyme 1

KREMEN1: KRinglE Containing TransMEmbraNe Protein 1

LIGANN: Ligand Generative Adversarial Network

MD: Molecular Dynamics

MERS: Middle East Respiratory Syndrome

ML: Machine Learning

MM-BGSA: Molecular Mechanics/Generalized Born Surface Area

MM/GBSA: Molecular Mechanics/Generalized Boltzman Surface Area

MM/PBSA: Molecular Mechanics Poisson-Boltzman Surface Area

MTase: MethylTransferase

N7-MTase: N7 MethylTransferase

NCATS: National Center for Advancing Translational Sciences

NHI: National Health Insurance

NiRAN: NucleotidyltRANsferase

NSP: Non-Structural Protein

NTD: N-Terminal Domain

NRP1: NeuRoPilin-1

ORF: Open Reading Frame

PDB: Protein Data Bank

PERK: Protein kinase RNA-like Endoplasmic Reticulum Kinase

Pfam: Protein families

PHB1: ProHiBitin 1

PHB2: ProHiBitin 2

PHIPSTer: Pathogen-Host Interactome Prediction using STructure similarity

PP: Pseudotyped Particle

PPI: Protein-Protein Interaction

qHTS: quantitative High-Throughput Screening

RBD: Receptor-Binding Domain

RBM: Receptor-Binding Motif

RecA: Recombinat protein A

RING: Really Interesting New Gene

SAM: S-Adenosyl Methionine

SARS: Severe Acute Respiratory Syndrome

SARS-CoV-2: Severe Acute Respiratory Syndrome Coronavirus 2

SAveRUNNER: Searching off-lAbel dRUg aNd NEtwoRk

SBVS: Structure-Based Virtual Screening

SP: Standard Precision

+ssRNA: positive-sense single-stranded RNA

TLR-3: Toll-Like Receptor 3

TM: TransMembrane

TMD: Trans Membrane Domain

TMPRSS2: TransMembrane PRoteaSe Serine 2

TMPRSS11D: TransMembrane ProteaSe Serine 11D

Ubl: Ubiquitin-like

USP2: Ubiquitin-Specific Protease 2

UniProt: Universal Protein Resource

VirHostNet: Virus Host Network

VS: Virtual Screening

WHO: World Health Organization

VOC: Variants Of Concern

VOI: Variants Of Interest

XP: eXtra Precision

CONSENT FOR PUBLICATION

Not applicable.

FUNDING

None.

CONFLICT OF INTEREST

The author has no conflict of interest to declare.

ACKNOWLEDGEMENTS

We apologize with colleagues that could not be cited due to space restrictions. M.V. is thankful to the GIDRM (Gruppo Italiano Discussione Risonanze Magnetiche) for the “Annalaura Segre-Donatella Capitani” fellowship.

REFERENCES

[1] Alsobaie, S. Understanding the Molecular Biology of SARS-CoV-2 and the COVID-19 Pandemic: A Review. *Infect. Drug. Resist.*, **2021**, *14*, 2259-2268.

[2] Kannan, S.; Shaik Syed Ali, P.; Sheeza, A.; Hemalatha, K. COVID-19 (Novel Coronavirus 2019) - recent trends. *Eur. Rev. Med. Pharmacol. Sci.*, **2020**, *24*(4), 2006-2011.

[3] Zhao, N.; Zhou, Z.L.; Wu, L.; Zhang, X.D.; Han, S.B.; Bao, H.J.; Shu, Y.; Shu, X.G. An update on the status of COVID-19: a comprehensive review. *Eur. Rev. Med. Pharmacol. Sci.*, **2020**, *24*(8), 4597-4606.

[4] Dhama, K.; Khan, S.; Tiwari, R.; Sircar, S.; Bhat, S.; Malik, Y.S.; Singh, K.P.; Chaicumpa, W.; Bonilla-Aldana, D.K.; Rodriguez-Morales, A.J. Coronavirus Disease 2019-COVID-19. *Clin. Microbiol. Rev.*, **2020**, *33*(4), e00028-00020.

[5] Zhu, Z.; Lian, X.; Su, X.; Wu, W.; Marraro, G.A.; Zeng, Y. From SARS and MERS to COVID-19: a brief summary and comparison of severe acute respiratory

infections caused by three highly pathogenic human coronaviruses. *Respir. Res.*, **2020**, *21*(1), 224.
[6] Fontanet, A.; Autran, B.; Lina, B.; Kieny, M.P.; Karim, S.S.A.; Sridhar, D. SARS-CoV-2 variants and ending the COVID-19 pandemic. *Lancet*, **2021**, *397*(10278), 952-954.
[7] Gralinski, L.E.; Menachery, V.D. Return of the Coronavirus: 2019-nCoV. *Viruses*, **2020**, *12*(2), 135.
[8] Xie, P.; Ma, W.; Tang, H.; Liu, D. Severe COVID-19: A Review of Recent Progress With a Look Toward the Future. *Front. Public Health*, **2020**, *8*, 189.
[9] Rabaan, A.A.; Al-Ahmed, S.H.; Haque, S.; Sah, R.; Tiwari, R.; Malik, Y.S.; Dhama, K.; Yatoo, M.I.; Bonilla-Aldana, D.K.; Rodriguez-Morales, A.J. SARS-CoV-2, SARS-CoV, and MERS-COV: A comparative overview. *Infez. Med.*, **2020**, *28*(2), 174-184.
[10] Cui, J.; Li, F.; Shi, Z.L. Origin and evolution of pathogenic coronaviruses. *Nat. Rev. Microbiol.*, **2019**, *17*(3), 181-192.
[11] Song, Z.Q.; Xu, Y.F.; Bao, L.L.; Zhang, L.; Yu, P.; Qu, Y.J.; Zhu, H.; Zhao, W.J.; Han, Y.L.; Qin, C. From SARS to MERS, Thrusting Coronaviruses into the Spotlight. *Viruses*, **2019**, *11*(1), 59.
[12] Lu, R.J.; Zhao, X.; Li, J.; Niu, P.H.; Yang, B.; Wu, H.L.; Wang, W.L.; Song, H.; Huang, B.Y.; Zhu, N.; Bi, Y.H.; Ma, X.J.; Zhan, F.X.; Wang, L.; Hu, T.; Zhou, H.; Hu, Z.H.; Zhou, W.M.; Zhao, L.; Chen, J.; Meng, Y.; Wang, J.; Lin, Y.; Yuan, J.Y.; Xie, Z.H.; Ma, J.M.; Liu, W.J.; Wang, D.Y.; Xu, W.B.; Holmes, E.C.; Gao, G.F.; Wu, G.Z.; Chen, W.J.; Shi, W.F.; Tan, W.J. Genomic characterisation and epidemiology of 2019 novel coronavirus: implications for virus origins and receptor binding. *Lancet*, **2020**, *395*(10224), 565-574.
[13] Hassan, S.S.; Ghosh, S.; Attrish, D.; Choudhury, P.P.; Aljabali, A.A.A.; Uhal, B.D.; Lundstrom, K.; Rezaei, N.; Uversky, V.N.; Seyran, M.; Pizzol, D.; Adadi, P.; Soares, A.; El-Aziz, T.M.A.; Kandimalla, R.; Tambuwala, M.M.; Azad, G.K.; Sherchan, S.P.; Baetas-da-Cruz, W.; Takayama, K.; Serrano-Aroca, A.; Chauhan, G.; Palu, G.; Brufsky, A.M. Possible Transmission Flow of SARS-CoV-2 Based on ACE2 Features. *Molecules*, **2020**, *25*(24), 5906.
[14] Li, Q.; Guan, X.; Wu, P.; Wang, X.; Zhou, L.; Tong, Y.; Ren, R.; Leung, K.S.M.; Lau, E.H.Y.; Wong, J.Y.; Xing, X.; Xiang, N.; Wu, Y.; Li, C.; Chen, Q.; Li, D.; Liu, T.; Zhao, J.; Liu, M.; Tu, W.; Chen, C.; Jin, L.; Yang, R.; Wang, Q.; Zhou, S.; Wang, R.; Liu, H.; Luo, Y.; Liu, Y.; Shao, G.; Li, H.; Tao, Z.; Yang, Y.; Deng, Z.; Liu, B.; Ma, Z.; Zhang, Y.; Shi, G.; Lam, T.T.Y.; Wu, J.T.; Gao, G.F.; Cowling, B.J.; Yang, B.; Leung, G.M.; Feng, Z. Early Transmission Dynamics in Wuhan, China, of Novel Coronavirus-Infected Pneumonia. *N. Engl. J. Med.*, **2020**, *382*(13), 1199-1207.
[15] Rothe, C.; Schunk, M.; Sothmann, P.; Bretzel, G.; Froeschl, G.; Wallrauch, C.; Zimmer, T.; Thiel, V.; Janke, C.; Guggemos, W.; Seilmaier, M.; Drosten, C.; Vollmar, P.; Zwirglmaier, K.; Zange, S.; Wolfel, R.; Hoelscher, M. Transmission of 2019-nCoV Infection from an Asymptomatic Contact in Germany. *N. Engl. J. Med.*, **2020**, *382*(10), 970-971.
[16] Trougakos, I.P.; Stamatelopoulos, K.; Terpos, E.; Tsitsilonis, O.E.; Aivalioti, E.; Paraskevis, D.; Kastritis, E.; Pavlakis, G.N.; Dimopoulos, M.A. Insights to SARS-CoV-2 life cycle, pathophysiology, and rationalized treatments that target COVID-19 clinical complications. *J. Biomed. Sci.*, **2021**, *28*(1), 9.
[17] Hoffmann, M.; Kleine-Weber, H.; Pohlmann, S. A Multibasic Cleavage Site in the Spike Protein of SARS-CoV-2 Is Essential for Infection of Human Lung Cells. *Molecular Cell*, **2020**, *78*(4), 779-784.
[18] Jiang, S.; Du, L.; Shi, Z. An emerging coronavirus causing pneumonia outbreak in Wuhan, China: calling for developing therapeutic and prophylactic strategies. *Emerg. Microbes Infect.*, **2020**, *9*(1), 275-277.
[19] Ren, L.L.; Wang, Y.M.; Wu, Z.Q.; Xiang, Z.C.; Guo, L.; Xu, T.; Jiang, Y.Z.; Xiong, Y.; Li, Y.J.; Li, X.W.; Li, H.; Fan, G.H.; Gu, X.Y.; Xiao, Y.; Gao, H.; Xu, J.Y.; Yang, F.; Wang, X.M.; Wu, C.; Chen, L.; Liu, Y.W.; Liu, B.; Yang, J.; Wang, X.R.; Dong, J.; Li, L.; Huang, C.L.; Zhao, J.P.; Hu, Y.; Cheng, Z.S.; Liu, L.L.; Qian, Z.H.; Qin, C.; Jin, Q.; Cao, B.; Wang, J.W. Identification of a novel coronavirus causing severe pneumonia in human: a descriptive study. *Chin. Med. J. (Engl.)*, **2020**, *133*(9), 1015-1024.
[20] Xu, Z.; Shi, L.; Wang, Y.; Zhang, J.; Huang, L.; Zhang, C.; Liu, S.; Zhao, P.; Liu, H.; Zhu, L.; Tai, Y.; Bai, C.; Gao, T.; Song, J.; Xia, P.; Dong, J.; Zhao, J.; Wang, F.S. Pathological findings of COVID-19 associated with acute respiratory distress syndrome. *Lancet Respir. Med.*, **2020**, *8*(4), 420-422.
[21] Huang, C.; Wang, Y.; Li, X.; Ren, L.; Zhao, J.; Hu, Y.; Zhang, L.; Fan, G.; Xu, J.; Gu, X.; Cheng, Z.; Yu, T.; Xia, J.; Wei, Y.; Wu, W.; Xie, X.; Yin, W.; Li, H.; Liu, M.; Xiao, Y.; Gao, H.; Guo, L.; Xie, J.; Wang, G.; Jiang, R.; Gao, Z.; Jin, Q.; Wang, J.; Cao, B. Clinical features of patients infected with 2019 novel coronavirus in Wuhan, China. *Lancet*, **2020**, *395*(10223), 497-506.
[22] Cheng, Z.K.J.; Shan, J. 2019 Novel coronavirus: where we are and what we know. *Infection*, **2020**, *48*(2), 155-163.
[23] Ali, M.A.M.; Spinler, S.A. COVID-19 and thrombosis: From bench to bedside. *Trends Cardiovasc. Med.*, **2021**, *31*(3), 143-160.
[24] Wiersinga, W.J.; Rhodes, A.; Cheng, A.C.; Peacock, S.J.; Prescott, H.C. Pathophysiology, Transmission, Diagnosis, and Treatment of Coronavirus Disease 2019 (COVID-19): A Review. *JAMA*, **2020**, *324*(8), 782-793.
[25] Chen, H.; Guo, J.; Wang, C.; Luo, F.; Yu, X.; Zhang, W.; Li, J.; Zhao, D.; Xu, D.; Gong, Q.; Liao, J.; Yang, H.; Hou, W.; Zhang, Y. Clinical characteristics and intrauterine vertical transmission potential of COVID-19 infection in nine pregnant women: a retrospective review of medical records. *Lancet*, **2020**, *395*(10226), 809-815.
[26] Coronavirus Death Toll. https://www.worldometers.info/coronavirus/coronavirus-death-toll/
[27] Burki, T. Understanding variants of SARS-CoV-2. *Lancet*, **2021**, *397*(10273), 462.
[28] Yadav, R.; Chaudhary, J.K.; Jain, N.; Chaudhary, P.K.; Khanra, S.; Dhamija, P.; Sharma, A.; Kumar, A.; Handu, S. Role of Structural and Non-Structural Proteins and Therapeutic Targets of SARS-CoV-2 for COVID-19. *Cells*, **2021**, *10*(4), 821.
[29] Brant, A.C.; Tian, W.; Majerciak, V.; Yang, W.; Zheng, Z.M. SARS-CoV-2: from its discovery to genome

structure, transcription, and replication. *Cell Biosci.*, **2021**, *11*(1), 136.
[30] Arya, R.; Kumari, S.; Pandey, B.; Mistry, H.; Bihani, S.C.; Das, A.; Prashar, V.; Gupta, G.D.; Panicker, L.; Kumar, M. Structural insights into SARS-CoV-2 proteins. *J. Mol. Biol.*, **2021**, *433*(2), 166725.
[31] Oliveira, A.S.F.; Ibarra, A.A.; Bermudez, I.; Casalino, L.; Gaieb, Z.; Shoemark, D.K.; Gallagher, T.; Sessions, R.B.; Amaro, R.E.; Mulholland, A.J. Simulations support the interaction of the SARS-CoV-2 spike protein with nicotinic acetylcholine receptors and suggest subtype specificity. *bioRxiv*, **2020**.
[32] Huang, Y.; Yang, C.; Xu, X.F.; Xu, W.; Liu, S.W. Structural and functional properties of SARS-CoV-2 spike protein: potential antivirus drug development for COVID-19. *Acta Pharmacol. Sin.*, **2020**, *41*(9), 1141-1149.
[33] Chen, Y.; Liu, Q.; Guo, D. Emerging coronaviruses: Genome structure, replication, and pathogenesis. *J. Med. Virol.*, **2020**, *92*(4), 418-423.
[34] Schubert, K.; Karousis, E.D.; Jomaa, A.; Scaiola, A.; Echeverria, B.; Gurzeler, L.A.; Leibundgut, M.; Thiel, V.; Muhlemann, O.; Ban, N. SARS-CoV-2 Nsp1 binds the ribosomal mRNA channel to inhibit translation. *Nat. Struct. Mol. Biol.*, **2020**, *27*(10), 959-966.
[35] Gupta, M.; Azumaya, C.M.; Moritz, M.; Pourmal, S.; Diallo, A.; Merz, G.E.; Jang, G.; Bouhaddou, M.; Fossati, A.; Brilot, A.F.; Diwanji, D.; Hernandez, E.; Herrera, N.; Kratochvil, H.T.; Lam, V.L.; Li, F.; Li, Y.; Nguyen, H.C.; Nowotny, C.; Owens, T.W.; Peters, J.K.; Rizo, A.N.; Schulze-Gahmen, U.; Smith, A.M.; Young, I.D.; Yu, Z.; Asarnow, D.; Billesbolle, C.; Campbell, M.G.; Chen, J.; Chen, K.H.; Chio, U.S.; Dickinson, M.S.; Doan, L.; Jin, M.; Kim, K.; Li, J.; Li, Y.L.; Linossi, E.; Liu, Y.; Lo, M.; Lopez, J.; Lopez, K.E.; Mancino, A.; Moss, F.R.; Paul, M.D.; Pawar, K.I.; Pelin, A.; Pospiech, T.H.; Puchades, C.; Remesh, S.G.; Safari, M.; Schaefer, K.; Sun, M.; Tabios, M.C.; Thwin, A.C.; Titus, E.W.; Trenker, R.; Tse, E.; Tsui, T.K.M.; Wang, F.; Zhang, K.; Zhang, Y.; Zhao, J.; Zhou, F.; Zhou, Y.; Zuliani-Alvarez, L.; Consortium, Q.S.B.; Agard, D.A.; Cheng, Y.; Fraser, J.S.; Jura, N.; Kortemme, T.; Manglik, A.; Southworth, D.R.; Stroud, R.M.; Swaney, D.L.; Krogan, N.J.; Frost, A.; Rosenberg, O.S.; Verba, K.A. CryoEM and AI reveal a structure of SARS-CoV-2 Nsp2, a multifunctional protein involved in key host processes. *bioRxiv*, **2021**.
[36] Cornillez-Ty, C.T.; Liao, L.; Yates, J.R., 3rd; Kuhn, P.; Buchmeier, M.J. Severe acute respiratory syndrome coronavirus nonstructural protein 2 interacts with a host protein complex involved in mitochondrial biogenesis and intracellular signaling. *J. Virol.*, **2009**, *83*(19), 10314-10318.
[37] Yoshimoto, F.K. The Proteins of Severe Acute Respiratory Syndrome Coronavirus-2 (SARS CoV-2 or n-COV19), the Cause of COVID-19. *Protein J.*, **2020**, *39*(3), 198-216.
[38] Armstrong, L.A.; Lange, S.M.; Dee Cesare, V.; Matthews, S.P.; Nirujogi, R.S.; Cole, I.; Hope, A.; Cunningham, F.; Toth, R.; Mukherjee, R.; Bojkova, D.; Gruber, F.; Gray, D.; Wyatt, P.G.; Cinatl, J.; Dikic, I.; Davies, P.; Kulathu, Y. Biochemical characterization of protease activity of Nsp3 from SARS-CoV-2 and its inhibition by nanobodies. *PLoS One*, **2021**, *16*(7), e0253364.
[39] Kim, Y.; Wower, J.; Maltseva, N.; Chang, C.; Jedrzejczak, R.; Wilamowski, M.; Kang, S.; Nicolaescu, V.; Randall, G.; Michalska, K.; Joachimiak, A. Tipiracil binds to uridine site and inhibits Nsp15 endoribonuclease NendoU from SARS-CoV-2. *Commun. Biol.*, **2021**, *4*(1), 193.
[40] Vithani, N.; Ward, M.D.; Zimmerman, M.I.; Novak, B.; Borowsky, J.H.; Singh, S.; Bowman, G.R. SARS-CoV-2 Nsp16 activation mechanism and a cryptic pocket with pan-coronavirus antiviral potential. *Biophys J.*, **2021**, *120*(14), 2880-2889.
[41] Redondo, N.; Zaldivar-Lopez, S.; Garrido, J.J.; Montoya, M. SARS-CoV-2 Accessory Proteins in Viral Pathogenesis: Knowns and Unknowns. *Front. Immunol.*, **2021**, *12*, 708264.
[42] Castano-Rodriguez, C.; Honrubia, J.M.; Gutierrez-Alvarez, J.; DeDiego, M.L.; Nieto-Torres, J.L.; Jimenez-Guardeno, J.M.; Regla-Nava, J.A.; Fernandez-Delgado, R.; Verdia-Baguena, C.; Queralt-Martin, M.; Kochan, G.; Perlman, S.; Aguilella, V.M.; Sola, I.; Enjuanes, L. Role of Severe Acute Respiratory Syndrome Coronavirus Viroporins E, 3a, and 8a in Replication and Pathogenesis. *Mbio*, **2018**, *9*(3), e02325--02317.
[43] Miorin, L.; Kehrer, T.; Sanchez-Aparicio, M.T.; Zhang, K.; Cohen, P.; Patel, R.S.; Cupic, A.; Makio, T.; Mei, M.; Moreno, E.; Danziger, O.; White, K.M.; Rathnasinghe, R.; Uccellini, M.; Gao, S.; Aydillo, T.; Mena, I.; Yin, X.; Martin-Sancho, L.; Krogan, N.J.; Chanda, S.K.; Schotsaert, M.; Wozniak, R.W.; Ren, Y.; Rosenberg, B.R.; Fontoura, B.M.A.; Garcia-Sastre, A. SARS-CoV-2 Orf6 hijacks Nup98 to block STAT nuclear import and antagonize interferon signaling. *Proc. Natl. Acad. Sci. U S A*, **2020**, *117*(45), 28344-28354.
[44] Zhao, X.; Chen, H.; Wang, H. Glycans of SARS-CoV-2 Spike Protein in Virus Infection and Antibody Production. *Front. Mol. Biosci.*, **2021**, *8*, 629873.
[45] Shajahan, A.; Pepi, L.E.; Rouhani, D.S.; Heiss, C.; Azadi, P. Glycosylation of SARS-CoV-2: structural and functional insights. *Anal. Bioanal. Chem.*, **2021**, *413*(29), 7179-7193.
[46] Ord, M.; Faustova, I.; Loog, M. The sequence at Spike S1/S2 site enables cleavage by furin and phospho-regulation in SARS-CoV2 but not in SARS-CoV1 or MERS-CoV. *Sci. Rep.*, **2020**, *10*(1), 16944.
[47] Johnson, B.A.; Xie, X.; Bailey, A.L.; Kalveram, B.; Lokugamage, K.G.; Muruato, A.; Zou, J.; Zhang, X.; Juelich, T.; Smith, J.K.; Zhang, L.; Bopp, N.; Schindewolf, C.; Vu, M.; Vanderheiden, A.; Winkler, E.S.; Swetnam, D.; Plante, J.A.; Aguilar, P.; Plante, K.S.; Popov, V.; Lee, B.; Weaver, S.C.; Suthar, M.S.; Routh, A.L.; Ren, P.; Ku, Z.; An, Z.; Debbink, K.; Diamond, M.S.; Shi, P.Y.; Freiberg, A.N.; Menachery, V.D. Loss of furin cleavage site attenuates SARS-CoV-2 pathogenesis. *Nature*, **2021**, *591*(7849), 293-299.
[48] Wrobel, A.G.; Benton, D.J.; Xu, P.; Roustan, C.; Martin, S.R.; Rosenthal, P.B.; Skehel, J.J.; Gamblin, S.J. SARS-CoV-2 and bat RaTG13 spike glycoprotein structures inform on virus evolution and furin-cleavage effects. *Nat. Struct. Mol. Biol.*, **2020**, *27*(8), 763-767.
[49] Gao, T.; Gao, Y.; Liu, X.; Nie, Z.; Sun, H.; Lin, K.; Peng, H.; Wang, S. Identification and functional analysis of the SARS-COV-2 nucleocapsid protein. *BMC Microbiol.*, **2021**, *21*(1), 58.

[50] Kang, S.; Yang, M.; Hong, Z.; Zhang, L.; Huang, Z.; Chen, X.; He, S.; Zhou, Z.; Zhou, Z.; Chen, Q.; Yan, Y.; Zhang, C.; Shan, H.; Chen, S. Crystal structure of SARS-CoV-2 nucleocapsid protein RNA binding domain reveals potential unique drug targeting sites. *Acta Pharm. Sin. B,* **2020**, *10*(7), 1228-1238.

[51] Ujike, M.; Taguchi, F. Incorporation of spike and membrane glycoproteins into coronavirus virions. *Viruses,* **2015**, *7*(4), 1700-1725.

[52] Gorkhali, R.; Koirala, P.; Rijal, S.; Mainali, A.; Baral, A.; Bhattarai, H.K. Structure and Function of Major SARS-CoV-2 and SARS-CoV Proteins. *Bioinform. Biol. Insights,* **2021**, *15*, 11779322211025876.

[53] Duart, G.; Garcia-Murria, M.J.; Grau, B.; Acosta-Caceres, J.M.; Martinez-Gil, L.; Mingarro, I. SARS-CoV-2 envelope protein topology in eukaryotic membranes. *Open Biol.,* **2020**, *10*(9), 200209.

[54] Sarkar, M.; Saha, S. Structural insight into the role of novel SARS-CoV-2 E protein: A potential target for vaccine development and other therapeutic strategies. *PLoS One,* **2020**, *15*(8), e0237300.

[55] Li, E.; Yan, F.; Huang, P.; Chi, H.; Xu, S.; Li, G.; Liu, C.; Feng, N.; Wang, H.; Zhao, Y.; Yang, S.; Xia, X. Characterization of the Immune Response of MERS-CoV Vaccine Candidates Derived from Two Different Vectors in Mice. *Viruses,* **2020**, *12*(1), 125.

[56] Brussow, H. Clinical trials with antiviral drugs against COVID-19: some progress and many shattered hopes. *Environ. Microbiol.,* **2021**, *23*(11), 6364-6376.

[57] Pomplun, S. Targeting the SARS-CoV-2-spike protein: from antibodies to miniproteins and peptides. *RSC Med Chem,* **2020**, *12*(2), 197-202.

[58] Creech, C.B.; Walker, S.C.; Samuels, R.J. SARS-CoV-2 Vaccines. *JAMA,* **2021**, *325*(13), 1318-1320.

[59] Mascellino, M.T.; Di Timoteo, F.; De Angelis, M.; Oliva, A. Overview of the Main Anti-SARS-CoV-2 Vaccines: Mechanism of Action, Efficacy and Safety. *Infect. Drug Resist.,* **2021**, *14*, 3459-3476.

[60] Alderson, J.; Batchelor, V.; O'Hanlon, M.; Cifuentes, L.; Richter, F.C.; Kopycinski, J.; Oxford-Cardiff, C.-L.C. Overview of approved and upcoming vaccines for SARS-CoV-2: a living review. *Oxf. Open Immunol.,* **2021**, *2*(1), iqab010.

[61] Krammer, F. SARS-CoV-2 vaccines in development. *Nature,* **2020**, *586*(7830), 516-527.

[62] Panchal, D.; Kataria, J.; Patel, K.; Crowe, K.; Pai, V.; Azizogli, A.R.; Kadian, N.; Sanyal, S.; Roy, A.; Dodd, O.J.; Acevedo-Jake, A.M.; Kumar, V.A. Peptide-Based Inhibitors for SARS-CoV-2 and SARS-CoV. *Adv. Ther. (Weinh),* **2021**, 2100104.

[63] Shahcheraghi, S.H.; Ayatollahi, J.; Aljabali, A.A.; Shastri, M.D.; Shukla, S.D.; Chellappan, D.K.; Jha, N.K.; Anand, K.; Katari, N.K.; Mehta, M.; Satija, S.; Dureja, H.; Mishra, V.; Almutary, A.G.; Alnuqaydan, A.M.; Charbe, N.; Prasher, P.; Gupta, G.; Dua, K.; Lotfi, M.; Bakshi, H.A.; Tambuwala, M.M. An overview of vaccine development for COVID-19. *Ther. Deliv.,* **2021**, *12*(3), 235-244.

[64] Sun, T.; Han, H.; Hudalla, G.A.; Wen, Y.; Pompano, R.R.; Collier, J.H. Thermal stability of self-assembled peptide vaccine materials. *Acta Biomater.,* **2016**, *30*, 62-71.

[65] Jaimes, J.A.; Andre, N.M.; Chappie, J.S.; Millet, J.K.; Whittaker, G.R. Phylogenetic Analysis and Structural Modeling of SARS-CoV-2 Spike Protein Reveals an Evolutionary Distinct and Proteolytically Sensitive Activation Loop. *J. Mol. Biol.,* **2020**, *432*(10), 3309-3325.

[66] Callaway, E. The race for coronavirus vaccines: a graphical guide. *Nature,* **2020**, *580*(7805), 576-577.

[67] Pollet, J.; Chen, W.H.; Strych, U. Recombinant protein vaccines, a proven approach against coronavirus pandemics. *Adv. Drug Deliv. Rev.,* **2021**, *170*, 71-82.

[68] Dong, Y.; Dai, T.; Wei, Y.; Zhang, L.; Zheng, M.; Zhou, F. A systematic review of SARS-CoV-2 vaccine candidates. *Signal Transduct. Target Ther.,* **2020**, *5*(1), 237.

[69] Biswas, P.; Hasan, M.M.; Dey, D.; Dos Santos Costa, A.C.; Polash, S.A.; Bibi, S.; Ferdous, N.; Kaium, M.A.; Rahman, M.D.H.; Jeet, F.K.; Papadakos, S.; Islam, K.; Uddin, M.S. Candidate antiviral drugs for COVID-19 and their environmental implications: a comprehensive analysis. *Environ. Sci. Pollut. Res. Int.,* **2021**, *28*(42), 59570-59593.

[70] Ebob, O.T.; Babiaka, S.B.; Ntie-Kang, F. Natural Products as Potential Lead Compounds for Drug Discovery Against SARS-CoV-2. *Nat. Prod. Bioprospect.,* **2021**, *11*(6), 611-628.

[71] Lau, J.L.; Dunn, M.K. Therapeutic peptides: Historical perspectives, current development trends, and future directions. *Bioorg. Med. Chem.,* **2018**, *26*(10), 2700-2707.

[72] Gorr, S.U.; Flory, C.M.; Schumacher, R.J. In vivo activity and low toxicity of the second-generation antimicrobial peptide DGL13K. *PLoS One,* **2019**, *14*(5), e0216669.

[73] Senger, M.R.; Evangelista, T.C.S.; Dantas, R.F.; Santana, M.; Goncalves, L.C.S.; de Souza Neto, L.R.; Ferreira, S.B.; Silva-Junior, F.P. COVID-19: molecular targets, drug repurposing and new avenues for drug discovery. *Mem. Inst. Oswaldo Cruz,* **2020**, *115*, e200254.

[74] Hufsky, F.; Lamkiewicz, K.; Almeida, A.; Aouacheria, A.; Arighi, C.; Bateman, A.; Baumbach, J.; Beerenwinkel, N.; Brandt, C.; Cacciabue, M.; Chuguransky, S.; Drechsel, O.; Finn, R.D.; Fritz, A.; Fuchs, S.; Hattab, G.; Hauschild, A.C.; Heider, D.; Hoffmann, M.; Holzer, M.; Hoops, S.; Kaderali, L.; Kalvari, I.; von Kleist, M.; Kmiecinski, R.; Kuhnert, D.; Lasso, G.; Libin, P.; List, M.; Lochel, H.F.; Martin, M.J.; Martin, R.; Matschinske, J.; McHardy, A.C.; Mendes, P.; Mistry, J.; Navratil, V.; Nawrocki, E.P.; O'Toole, A.N.; Ontiveros-Palacios, N.; Petrov, A.I.; Rangel-Pineros, G.; Redaschi, N.; Reimering, S.; Reinert, K.; Reyes, A.; Richardson, L.; Robertson, D.L.; Sadegh, S.; Singer, J.B.; Theys, K.; Upton, C.; Welzel, M.; Williams, L.; Marz, M. Computational strategies to combat COVID-19: useful tools to accelerate SARS-CoV-2 and coronavirus research. *Brief Bioinform.,* **2021**, *22*(2), 642-663.

[75] Bateman, A.; Martin, M.J.; Orchard, S.; Magrane, M.; Agivetova, R.; Ahmad, S.; Alpi, E.; Bowler-Barnett, E.H.; Britto, R.; Bursteinas, B.; Bye-A-Jee, H.; Coetzee, R.; Cukura, A.; Da Silva, A.; Denny, P.; Dogan, T.; Ebenezer, T.; Fan, J.; Castro, L.G.; Garmiri, P.; Georghiou, G.; Gonzales, L.; Hatton-Ellis, E.; Hussein, A.; Ignatchenko, A.; Insana, G.; Ishtiaq, R.; Jokinen, P.; Joshi, V.; Jyothi, D.; Lock, A.; Lopez, R.; Luciani, A.; Luo, J.; Lussi, Y.; Mac-Dougall, A.; Madeira, F.; Mahmoudy, M.; Menchi, M.; Mishra, A.; Moulang, K.;

Nightingale, A.; Oliveira, C.S.; Pundir, S.; Qi, G.Y.; Raj, S.; Rice, D.; Lopez, M.R.; Saidi, R.; Sampson, J.; Sawford, T.; Speretta, E.; Turner, E.; Tyagi, N.; Vasudev, P.; Volynkin, V.; Warner, K.; Watkins, X.; Zaru, R.; Zellner, H.; Bridge, A.; Poux, S.; Redaschi, N.; Aimo, L.; Argoud-Puy, G.; Auchincloss, A.; Axelsen, K.; Bansal, P.; Baratin, D.; Blatter, M.C.; Bolleman, J.; Boutet, E.; Breuza, L.; Casals-Casas, C.; de Castro, E.; Echioukh, K.C.; Coudert, E.; Cuche, B.; Doche, M.; Dornevil, D.; Estreicher, A.; Famiglietti, M.L.; Feuermann, M.; Gasteiger, E.; Gehant, S.; Gerritsen, V.; Gos, A.; Gruaz-Gumowski, N.; Hinz, U.; Hulo, C.; Hyka-Nouspikel, N.; Jungo, F.; Keller, G.; Kerhornou, A.; Lara, V.; Le Mercier, P.; Lieberherr, D.; Lombardot, T.; Martin, X.; Masson, P.; Morgat, A.; Neto, T.B.; Paesano, S.; Pedruzzi, I.; Pilbout, S.; Pourcel, L.; Pozzato, M.; Pruess, M.; Rivoire, C.; Sigrist, C.; Sonesson, K.; Stutz, A.; Sundaram, S.; Tognolli, M.; Verbregue, L.; Wu, C.H.; Arighi, C.N.; Arminski, L.; Chen, C.M.; Chen, Y.X.; Garavelli, J.S.; Huang, H.Z.; Laiho, K.; McGarvey, P.; Natale, D.A.; Ross, K.; Vinayaka, C.R.; Wang, Q.H.; Wang, Y.Q.; Yeh, L.S.; Zhang, J.; Consortium, U. UniProt: the universal protein knowledgebase in 2021. *Nucleic Acids Research*, **2021**, *49*(D1), D480-D489.

[76] Watkins, X.; Garcia, L.J.; Pundir, S.; Martin, M.J.; Consortium, U. ProtVista: visualization of protein sequence annotations. *Bioinformatics*, **2017**, *33*(13), 2040-2041.

[77] Mistry, J.; Chuguransky, S.; Williams, L.; Qureshi, M.; Salazar, G.A.; Sonnhammer, E.L.L.; Tosatto, S.C.E.; Paladin, L.; Raj, S.; Richardson, L.J.; Finn, R.D.; Bateman, A. Pfam: The protein families database in 2021. *Nucleic Acids Res.*, **2021**, *49*(D1), D412-D419.

[78] Singer, J.; Gifford, R.; Cotten , M.; Robertson, D. CoV-GLUE: A Web Application for Tracking SARS-CoV-2 Genomic Variation. *Preprints*, **2020**, 202006.200225.

[79] Guirimand, T.; Delmotte, S.; Navratil, V. VirHostNet 2.0: surfing on the web of virus/host molecular interactions data. *Nucleic Acids Res.*, **2015**, *43*(Database issue), D583-D587.

[80] Martin, R.; Lochel, H.F.; Welzel, M.; Hattab, G.; Hauschild, A.C.; Heider, D. CORDITE: The Curated CORona Drug InTERactions Database for SARS-CoV-2. *iScience*, **2020**, *23*(7), 101297.

[81] Sadegh, S.; Matschinske, J.; Blumenthal, D.B.; Galindez, G.; Kacprowski, T.; List, M.; Nasirigerdeh, R.; Oubounyt, M.; Pichlmair, A.; Rose, T.D.; Salgado-Albarran, M.; Spath, J.; Stukalov, A.; Wenke, N.K.; Yuan, K.; Pauling, J.K.; Baumbach, J. Exploring the SARS-CoV-2 virus-host-drug interactome for drug repurposing. *Nat. Commun.*, **2020**, *11*(1), 3518.

[82] Lasso, G.; Mayer, S.V.; Winkelmann, E.R.; Chu, T.; Elliot, O.; Patino-Galindo, J.A.; Park, K.; Rabadan, R.; Honig, B.; Shapira, S.D. A Structure-Informed Atlas of Human-Virus Interactions. *Cell*, **2019**, *178*(6), 1526-1541e1516.

[83] Chen, T.F.; Chang, Y.C.; Hsiao, Y.; Lee, K.H.; Hsiao, Y.C.; Lin, Y.H.; Tu, Y.C.E.; Huang, H.C.; Chen, C.Y.; Juan, H.F. DockCoV2: a drug database against SARS-CoV-2. *Nucleic Acids Res.*, **2021**, *49*(D1), D1152-D1159.

[84] Khan, M.A.; Islam, A. SARS-CoV-2 Proteins Exploit Host's Genetic and Epigenetic Mediators for the Annexation of Key Host Signaling Pathways. *Front. Mol. Biosci.*, **2020**, *7*, 598583.

[85] Sanami, S.; Alizadeh, M.; Nosrati, M.; Dehkordi, K.A.; Azadegan-Dehkordi, F.; Tahmasebian, S.; Nosrati, H.; Arjmand, M.H.; Ghasemi-Dehnoo, M.; Rafiei, A.; Bagheri, N. Exploring SARS-COV-2 structural proteins to design a multi-epitope vaccine using immunoinformatics approach: An in silico study. *Comput. Biol. Med.*, **2021**, *133*, 104390.

[86] Kumar, A.; Kumar, P.; Saumya, K.U.; Kapuganti, S.K.; Bhardwaj, T.; Giri, R. Exploring the SARS-CoV-2 structural proteins for multi-epitope vaccine development: an in-silico approach. *Expert Rev. Vaccines*, **2020**, *19*(9), 887-898.

[87] Li, Q.H.; Peng, W.; Ou, Y. Prediction and analysis of key protein structures of 2019-nCoV. *Future Virol.*, **2020**, *15*(6), 349-357.

[88] Dong, S.J.; Sun, J.C.; Mao, Z.; Wang, L.; Lu, Y.L.; Li, J.S. A guideline for homology modeling of the proteins from newly discovered betacoronavirus, 2019 novel coronavirus (2019-nCoV). *J. Med. Virol.*, **2020**, *92*(9), 1542-1548.

[89] Kryshtafovych, A.; Moult, J.; Billings, W.M.; Della Corte, D.; Fidelis, K.; Kwon, S.; Olechnovic, K.; Seok, C.; Venclovas, C.; Won, J.; participants, C.-C. Modeling SARS-CoV-2 proteins in the CASP-commons experiment. *Proteins*, **2021**, *89*(12), 1987-1996.

[90] O'Donoghue, S.I.; Schafferhans, A.; Sikta, N.; Stolte, C.; Kaur, S.; Ho, B.K.; Anderson, S.; Procter, J.; Dallago, C.; Bordin, N.; Adcock, M.; Rost, B. SARS-CoV-2 structural coverage map reveals state changes that disrupt host immunity. *bioRxiv*, **2020**.

[91] AQUARIA-COVID RESOURCE. https://aquaria.ws/covid19

[92] Kim, D.E.; Chivian, D.; Baker, D. Protein structure prediction and analysis using the Robetta server. *Nucleic Acids Res.*, **2004**, *32*, W526-W531.

[93] Du, Z.; Su, H.; Wang, W.; Ye, L.; Wei, H.; Peng, Z.; Anishchenko, I.; Baker, D.; Yang, J. The trRosetta server for fast and accurate protein structure prediction. *Nat. Protoc.*, **2021**, *16*(12), 5634-5651.

[94] Mahtarin, R.; Islam, S.; Islam, M.J.; Ullah, M.O.; Ali, M.A.; Halim, M.A. Structure and dynamics of membrane protein in SARS-CoV-2. *J. Biomol. Struct. Dyn.*, **2020**, 1-14.

[95] Somboon, T.; Mahalapbutr, P.; Sanachai, K.; Maitarad, P.; Lee, V.S.; Hannongbua, S.; Rungrotmongkol, T. Computational study on peptidomimetic inhibitors against SARS-CoV-2 main protease. *J. Mol. Liq.*, **2021**, *322*, 114999.

[96] Suarez, D.; Diaz, N. SARS-CoV-2 Main Protease: A Molecular Dynamics Study. *J. Chem. Inf. Model*, **2020**, *60*(12), 5815-5831.

[97] Mohamed, N.M.; Ali, E.M.H.; AboulMagd, A.M. Ligand-based design, molecular dynamics and ADMET studies of suggested SARS-CoV-2 M-pro inhibitors. *RSC Adv.*, **2021**, *11*(8), 4523-4538.

[98] Irwin, J.J.; Shoichet, B.K. ZINC--a free database of commercially available compounds for virtual screening. *J. Chem. Inf. Model*, **2005**, *45*(1), 177-182.

[99] Razzaghi-Asl, N.; Ebadi, A.; Shahabipour, S.; Gholamin, D. Identification of a potential SARS-CoV2 inhibitor via molecular dynamics simulations and amino acid decomposition analysis. *J. Biomol. Struct. Dyn.*, **2021**, *39*(17), 6633-6648.

[100] Bzowka, M.; Mitusinska, K.; Raczynska, A.; Samol, A.; Tuszynski, J.A.; Gora, A. Structural and Evolutionary Analysis Indicate That the SARS-CoV-2 Mpro Is a Challenging Target for Small-Molecule Inhibitor Design. *Int. J. Mol. Sci.*, **2020**, *21*(9), 3099.
[101] Arantes, P.R.; Saha, A.; Palermo, G. Fighting COVID-19 Using Molecular Dynamics Simulations. *ACS Cent. Sci*, **2020**, *6*(10), 1654-1656.
[102] Casalino, L.; Gaieb, Z.; Goldsmith, J.A.; Hjorth, C.K.; Dommer, A.C.; Harbison, A.M.; Fogarty, C.A.; Barros, E.P.; Taylor, B.C.; McLellan, J.S.; Fadda, E.; Amaro, R.E. Beyond Shielding: The Roles of Glycans in the SARS-CoV-2 Spike Protein. *ACS Cent. Sci.*, **2020**, *6*(10), 1722-1734.
[103] Raghuvamsi, P.V.; Tulsian, N.K.; Samsudin, F.; Qian, X.; Purushotorman, K.; Yue, G.; Kozma, M.M.; Hwa, W.Y.; Lescar, J.; Bond, P.J.; MacAry, P.A.; Anand, G.S. SARS-CoV-2 S protein:ACE2 interaction reveals novel allosteric targets. *Elife*, **2021**, *10*, e63646.
[104] Rath, S.L.; Kumar, K. Investigation of the Effect of Temperature on the Structure of SARS-CoV-2 Spike Protein by Molecular Dynamics Simulations. *Front. Mol. Biosci.*, **2020**, *7*, 583523.
[105] Sk, M.F.; Jonniya, N.A.; Roy, R.; Poddar, S.; Kar, P. Computational Investigation of Structural Dynamics of SARS-CoV-2 Methyltransferase-Stimulatory Factor Heterodimer nsp16/nsp10 Bound to the Cofactor SAM. *Front. Mol. Biosci.*, **2020**, *7*, 590165.
[106] The Protein Data Bank. https://www.rcsb.org/
[107] Vincenzi, M.; Leone, M. The Fight against Human Viruses: How NMR Can Help? *Curr. Med. Chem.*, **2021**, *28*(22), 4380-4453.
[108] Naik, B.; Gupta, N.; Ojha, R.; Singh, S.; Prajapati, V.K.; Prusty, D. High throughput virtual screening reveals SARS-CoV-2 multi-target binding natural compounds to lead instant therapy for COVID-19 treatment. *Int. J. Biol. Macromol.*, **2020**, *160*, 1-17.
[109] Pinzi, L.; Rastelli, G. Molecular Docking: Shifting Paradigms in Drug Discovery. *Int. J. Mol. Sci.*, **2019**, *20*(18), 4331.
[110] Chen, Z.; Li, H.L.; Zhang, Q.J.; Bao, X.G.; Yu, K.Q.; Luo, X.M.; Zhu, W.L.; Jiang, H.L. Pharmacophore-based virtual screening versus docking-based virtual screening: a benchmark comparison against eight targets. *Acta Pharmacol. Sin.*, **2009**, *30*(12), 1694-1708.
[111] Berenger, F.; Vu, O.; Meiler, J. Consensus queries in ligand-based virtual screening experiments. *J. Cheminform.*, **2017**, *9*(1), 60.
[112] Murgueitio, M.S.; Bermudez, M.; Mortier, J.; Wolber, G. In silico virtual screening approaches for anti-viral drug discovery. *Drug Discov. Today Technol.*, **2012**, *9*(3), e219-225.
[113] Tomori, T.; Hajdu, I.; Barna, L.; Lorincz, Z.; Cseh, S.; Dorman, G. Combining 2D and 3D in silico methods for rapid selection of potential PDE5 inhibitors from multimillion compounds' repositories: biological evaluation. *Mol. Divers.*, **2012**, *16*(1), 59-72.
[114] Meng, X.Y.; Zhang, H.X.; Mezei, M.; Cui, M. Molecular docking: a powerful approach for structure-based drug discovery. *Curr. Comput. Aided Drug Des.*, **2011**, *7*(2), 146-157.
[115] Schaller, D.; Sribar, D.; Noonan, T.; Deng, L.H.; Nguyen, T.N.; Pach, S.; Machalz, D.; Bermudez, M.; Wolber, G. Next generation 3D pharmacophore modeling. *Wiley Interdiscip. Rev. WIREs Comput. Mol. Sci.*, **2020**, *10*(4), e1468.
[116] Koes, D.R.; Camacho, C.J. Shape-based virtual screening with volumetric aligned molecular shapes. *J. Comput. Chem.*, **2014**, *35*(25), 1824-1834.
[117] Egieyeh, S.; Egieyeh, E.; Malan, S.; Christofells, A.; Fielding, B. Computational drug repurposing strategy predicted peptide-based drugs that can potentially inhibit the interaction of SARS-CoV-2 spike protein with its target (humanACE2). *PLoS One*, **2021**, *16*(1), e0245258.
[118] Franco, L.S.; Maia, R.C.; Barreiro, E.J. Identification of LASSBio-1945 as an inhibitor of SARS-CoV-2 main protease (M(PRO)) through in silico screening supported by molecular docking and a fragment-based pharmacophore model. *RSC Med. Chem.*, **2021**, *12*(1), 110-119.
[119] Chen, Y.W.; Yiu, C.B.; Wong, K.Y. Prediction of the SARS-CoV-2 (2019-nCoV) 3C-like protease (3CL (pro)) structure: virtual screening reveals velpatasvir, ledipasvir, and other drug repurposing candidates. *F1000Res.*, **2020**, *9*, 129.
[120] White, M.A.; Lin, W.; Cheng, X. Discovery of COVID-19 Inhibitors Targeting the SARS-CoV-2 Nsp13 Helicase. *J. Phys. Chem. Lett.*, **2020**, *11*(21), 9144-9151.
[121] Zhang, H.; Yang, Y.; Li, J.; Wang, M.; Saravanan, K.M.; Wei, J.; Tze-Yang Ng, J.; Tofazzal Hossain, M.; Liu, M.; Zhang, H.; Ren, X.; Pan, Y.; Peng, Y.; Shi, Y.; Wan, X.; Liu, Y.; Wei, Y. A novel virtual screening procedure identifies Pralatrexate as inhibitor of SARS-CoV-2 RdRp and it reduces viral replication in vitro. *PLoS Comput. Biol.*, **2020**, *16*(12), e1008489.
[122] Azeez, S.A.; Alhashim, Z.G.; Al Otaibi, W.M.; Alsuwat, H.S.; Ibrahim, A.M.; Almandil, N.B.; Borgio, J.F. State-of-the-art tools to identify druggable protein ligand of SARS-CoV-2. *Arch. Med. Sci.*, **2020**, *16*(3), 497-507.
[123] Maffucci, I.; Contini, A. In Silico Drug Repurposing for SARS-CoV-2 Main Proteinase and Spike Proteins. *J. Proteome Res.*, **2020**, *19*(11), 4637-4648.
[124] Zhang, J.; Xiao, T.; Cai, Y.; Chen, B. Structure of SARS-CoV-2 spike protein. *Curr. Opin. Virol.*, **2021**, *50*, 173-182.
[125] Cai, Y.; Zhang, J.; Xiao, T.; Peng, H.; Sterling, S.M.; Walsh, R.M., Jr.; Rawson, S.; Rits-Volloch, S.; Chen, B. Distinct conformational states of SARS-CoV-2 spike protein. *Science*, **2020**, *369*(6511), 1586-1592.
[126] Xue, Q.; Liu, X.; Pan, W.X.; Zhang, A.Q.; Fu, J.J.; Jiang, G.B. Computational Insights into the Allosteric Effect and Dynamic Structural Features of the SARS-COV-2 Spike Protein. *Chem. Eur. J.*, **2022**, *28*(6), e202200158.
[127] Yan, R.; Zhang, Y.; Li, Y.; Xia, L.; Guo, Y.; Zhou, Q. Structural basis for the recognition of SARS-CoV-2 by full-length human ACE2. *Science*, **2020**, *367*(6485), 1444-1448.
[128] Donoghue, M.; Hsieh, F.; Baronas, E.; Godbout, K.; Gosselin, M.; Stagliano, N.; Donovan, M.; Woolf, B.; Robison, K.; Jeyaseelan, R.; Breitbart, R.E.; Acton, S. A novel angiotensin-converting enzyme-related carboxypeptidase (ACE2) converts angiotensin I to angiotensin 1-9. *Circ. Res.*, **2000**, *87*(5), E1-E9.

[129] Kuba, K.; Imai, Y.; Ohto-Nakanishi, T.; Penninger, J.M. Trilogy of ACE2: a peptidase in the renin-angiotensin system, a SARS receptor, and a partner for amino acid transporters. *Pharmacol. Ther.*, **2010**, *128*(1), 119-128.
[130] Towler, P.; Staker, B.; Prasad, S.G.; Menon, S.; Tang, J.; Parsons, T.; Ryan, D.; Fisher, M.; Williams, D.; Dales, N.A.; Patane, M.A.; Pantoliano, M.W. ACE2 X-ray structures reveal a large hinge-bending motion important for inhibitor binding and catalysis. *J. Biol. Chem.*, **2004**, *279*(17), 17996-18007.
[131] Chen, G.-Y.; Yao, T.-Y.; Ahmed, A.; Pan, Y.-C.; Yang, J.-C.; Wu, Y.-C. The discovery of potential natural products for targeting SARS-CoV-2 spike protein by virtual screening. *bioRxiv*, **2020**.
[132] Carino, A.; Moraca, F.; Fiorillo, B.; Marchiano, S.; Sepe, V.; Biagioli, M.; Finamore, C.; Bozza, S.; Francisci, D.; Distrutti, E.; Catalanotti, B.; Zampella, A.; Fiorucci, S. Hijacking SARS-CoV-2/ACE2 Receptor Interaction by Natural and Semi-synthetic Steroidal Agents Acting on Functional Pockets on the Receptor Binding Domain. *Front. Chem.*, **2020**, *8*, 572885.
[133] Walls, A.C.; Park, Y.J.; Tortorici, M.A.; Wall, A.; McGuire, A.T.; Veesler, D. Structure, Function, and Antigenicity of the SARS-CoV-2 Spike Glycoprotein. *Cell*, **2020**, *181*(2), 281-292.e286.
[134] Peacock, T.P.; Goldhill, D.H.; Zhou, J.; Baillon, L.; Frise, R.; Swann, O.C.; Kugathasan, R.; Penn, R.; Brown, J.C.; Sanchez-David, R.Y.; Braga, L.; Williamson, M.K.; Hassard, J.A.; Staller, E.; Hanley, B.; Osborn, M.; Giacca, M.; Davidson, A.D.; Matthews, D.A.; Barclay, W.S. The furin cleavage site in the SARS-CoV-2 spike protein is required for transmission in ferrets. *Nat. Microbiol.*, **2021**, *6*(7), 899-909.
[135] Xia, S.; Zhu, Y.; Liu, M.Q.; Lan, Q.H.; Xu, W.; Wu, Y.L.; Ying, T.L.; Liu, S.W.; Shi, Z.L.; Jiang, S.B.; Lu, L. Fusion mechanism of 2019-nCoV and fusion inhibitors targeting HR1 domain in spike protein. *Cell. Mol. Immunol.*, **2020**, *17*(7), 765-767.
[136] Tracking SARS-CoV-2 variants. https://www.who.int/en/activities/tracking-SARS-CoV-2-variants/
[137] Araf, Y.; Akter, F.; Tang, Y.D.; Fatemi, R.; Parvez, M.S.A.; Zheng, C.F.; Hossain, M.G. Omicron variant of SARS-CoV-2: Genomics, transmissibility, and responses to current COVID-19 vaccines. *J. Med. Virol.*, **2022**, *94*(5), 1825-1832.
[138] Mehra, R.; Kepp, K.P. Structure and Mutations of SARS-CoV-2 Spike Protein: A Focused Overview. *ACS Infect. Dis.*, **2022**, *8*(1), 29-58.
[139] SARS-CoV-2 variants of concern as of 8 April 2022. https://www.ecdc.europa.eu/en/covid-19/variants-concern
[140] CORONAVIRUS ANTIVIRAL & RESISTANCE DATABASE. https://covdb.stanford.edu/page/mutation-viewer
[141] Hoffmann, M.; Pohlmann, S. Novel SARS-CoV-2 receptors: ASGR1 and KREMEN1. *Cell Res.*, **2022**, *32*(1), 1-2.
[142] Gadanec, L.K.; McSweeney, K.R.; Qaradakhi, T.; Ali, B.; Zulli, A.; Apostolopoulos, V. Can SARS-CoV-2 Virus Use Multiple Receptors to Enter Host Cells? *Int. J. Mol. Sci.*, **2021**, *22*(3), 992.
[143] Gu, Y.; Cao, J.; Zhang, X.; Gao, H.; Wang, Y.; Wang, J.; He, J.; Jiang, X.; Zhang, J.; Shen, G.; Yang, J.; Zheng, X.; Hu, G.; Zhu, Y.; Du, S.; Zhu, Y.; Zhang, R.; Xu, J.; Lan, F.; Qu, D.; Xu, G.; Zhao, Y.; Gao, D.; Xie, Y.; Luo, M.; Lu, Z. Receptome profiling identifies KREMEN1 and ASGR1 as alternative functional receptors of SARS-CoV-2. *Cell Res.*, **2022**, *32*(1), 24-37.
[144] Holms, R.D.; Ataullakhanov, R.I. Ezrin Peptide Therapy from HIV to COVID: Inhibition of Inflammation and Amplification of Adaptive Anti-Viral Immunity. *Int. J. Mol. Sci.*, **2021**, *22*(21), 11688.
[145] Arpin, M.; Chirivino, D.; Naba, A.; Zwaenepoel, I. Emerging role for ERM proteins in cell adhesion and migration. *Cell Adh. Migr.*, **2011**, *5*(2), 199-206.
[146] Stravalaci, M.; Pagani, I.; Paraboschi, E.M.; Pedotti, M.; Doni, A.; Scavello, F.; Mapelli, S.N.; Sironi, M.; Perucchini, C.; Varani, L.; Matkovic, M.; Cavalli, A.; Cesana, D.; Gallina, P.; Pedemonte, N.; Capurro, V.; Clementi, N.; Mancini, N.; Invernizzi, P.; Bayarri-Olmos, R.; Garred, P.; Rappuoli, R.; Duga, S.; Bottazzi, B.; Uguccioni, M.; Asselta, R.; Vicenzi, E.; Mantovani, A.; Garlanda, C. Recognition and inhibition of SARS-CoV-2 by humoral innate immunity pattern recognition molecules. *Nat. Immunol.*, **2022**, *23*(2), 275-286.
[147] Zhao, Y.; Kuang, M.; Li, J.; Zhu, L.; Jia, Z.; Guo, X.; Hu, Y.; Kong, J.; Yin, H.; Wang, X.; You, F. SARS-CoV-2 spike protein interacts with and activates TLR41. *Cell Res.*, **2021**, *31*(7), 818-820.
[148] Kothandan, R.; Rajan, C.; Arjun, J.; Raj, R.R.M.; Syed, S. Virtual screening of phytochemical compounds as potential inhibitors against SARS-CoV-2 infection. *Beni Suef Univ. J. Basic Appl. Sci.*, **2021**, *10*(1), 9.
[149] Huang, R.; Xu, M.; Zhu, H.; Chen, C.Z.; Zhu, W.; Lee, E.M.; He, S.; Zhang, L.; Zhao, J.; Shamim, K.; Bougie, D.; Huang, W.; Xia, M.; Hall, M.D.; Lo, D.; Simeonov, A.; Austin, C.P.; Qiu, X.; Tang, H.; Zheng, W. Biological activity-based modeling identifies antiviral leads against SARS-CoV-2. *Nat. Biotechnol.*, **2021**, *39*(6), 747-753.
[150] Assessing a Compound's Activity, Not Just Its Structure, Could Deepen the Pool of Promising Drug Therapies. https://ncats.nih.gov/news/releases/2021/assessing-a-compounds-activity-not-just-its-structure-could-deepen-the-pool-of-promising-drug-therapies
[151] Ibrahim, I.M.; Abdelmalek, D.H.; Elshahat, M.E.; Elfiky, A.A. COVID-19 spike-host cell receptor GRP78 binding site prediction. *J. Infect.*, **2020**, *80*(5), 554-562.
[152] Allam, L.; Ghrifi, F.; Mohammed, H.; El Hafidi, N.; El Jaoudi, R.; El Harti, J.; Lmimouni, B.; Belyamani, L.; Ibrahimi, A. Targeting the GRP78-Dependant SARS-CoV-2 Cell Entry by Peptides and Small Molecules. *Bioinform. Biol. Insights*, **2020**, *14*, 1177932220965505.
[153] Power, H.; Wu, J.; Turville, S.; Aggarwal, A.; Valtchev, P.; Schindeler, A.; Dehghani, F. Virtual screening and in vitro validation of natural compound inhibitors against SARS-CoV-2 spike protein. *Bioorg. Chem.*, **2022**, *119*, 105574.
[154] Chen, G.Y.; Pan, Y.C.; Wu, T.Y.; Yao, T.Y.; Wang, W.J.; Shen, W.J.; Ahmed, A.; Chan, S.T.; Tang, C.H.; Huang, W.C.; Hung, M.C.; Yang, J.C.; Wu, Y.C. Potential natural products that target the SARS-CoV-2 spike protein identified

by structure-based virtual screening, isothermal titration calorimetry and lentivirus particles pseudotyped (Vpp) infection assay. *J. Tradit. Complement. Med.*, **2021**, *12*(1), 73-89.
[155] Seth, S.; Batra, J.; Srinivasan, S. COVID-19: Targeting Proteases in Viral Invasion and Host Immune Response. *Front Mol Biosci*, **2020**, *7*, 215.
[156] Cheng, Y.W.; Chao, T.L.; Li, C.L.; Chiu, M.F.; Kao, H.C.; Wang, S.H.; Pang, Y.H.; Lin, C.H.; Tsai, Y.M.; Lee, W.H.; Tao, M.H.; Ho, T.C.; Wu, P.Y.; Jang, L.T.; Chen, P.J.; Chang, S.Y.; Yeh, S.H. Furin Inhibitors Block SARS-CoV-2 Spike Protein Cleavage to Suppress Virus Production and Cytopathic Effects. *Cell Rep.*, **2020**, *33*(2), 108254.
[157] Padmanabhan, P.; Desikan, R.; Dixit, N.M. Targeting TMPRSS2 and Cathepsin B/L together may be synergistic against SARS-CoV-2 infection. *PLoS Comput. Biol.*, **2020**, *16*(12), e1008461.
[158] Haque, S.K.M.; Ashwaq , O.; Sarief, A.; Mohamed, A.K.A.J. A comprehensive review about SARS-CoV-2. *Future Virol.*, **2020**, *15*(9), 625-648.
[159] Anirudhan, V.; Lee, H.; Cheng, H.; Cooper, L.; Rong, L. Targeting SARS-CoV-2 viral proteases as a therapeutic strategy to treat COVID-19. *J. Med. Virol.*, **2021**, *93*(5), 2722-2734.
[160] Costanzi, E.; Kuzikov, M.; Esposito, F.; Albani, S.; Demitri, N.; Giabbai, B.; Camasta, M.; Tramontano, E.; Rossetti, G.; Zaliani, A.; Storici, P. Structural and Biochemical Analysis of the Dual Inhibition of MG-132 against SARS-CoV-2 Main Protease (Mpro/3CLpro) and Human Cathepsin-L. *Int. J. Mol. Sci.*, **2021**, *22*(21), 11779.
[161] Jin, Z.; Du, X.; Xu, Y.; Deng, Y.; Liu, M.; Zhao, Y.; Zhang, B.; Li, X.; Zhang, L.; Peng, C.; Duan, Y.; Yu, J.; Wang, L.; Yang, K.; Liu, F.; Jiang, R.; Yang, X.; You, T.; Liu, X.; Yang, X.; Bai, F.; Liu, H.; Liu, X.; Guddat, L.W.; Xu, W.; Xiao, G.; Qin, C.; Shi, Z.; Jiang, H.; Rao, Z.; Yang, H. Structure of M(pro) from SARS-CoV-2 and discovery of its inhibitors. *Nature*, **2020**, *582*(7811), 289-293.
[162] Amporndanai, K.; Meng, X.; Shang, W.; Jin, Z.; Rogers, M.; Zhao, Y.; Rao, Z.; Liu, Z.J.; Yang, H.; Zhang, L.; O'Neill, P.M.; Samar Hasnain, S. Inhibition mechanism of SARS-CoV-2 main protease by ebselen and its derivatives. *Nat. Commun.*, **2021**, *12*(1), 3061.
[163] Kneller, D.W.; Phillips, G.; Weiss, K.L.; Pant, S.; Zhang, Q.; O'Neill, H.M.; Coates, L.; Kovalevsky, A. Unusual zwitterionic catalytic site of SARS-CoV-2 main protease revealed by neutron crystallography. *J. Biol. Chem.*, **2020**, *295*(50), 17365-17373.
[164] Ramos-Guzman, C.A.; Ruiz-Pernia, J.J.; Tunon, I. Unraveling the SARS-CoV-2 Main Protease Mechanism Using Multiscale Methods. *ACS Catal.*, **2020**, *10*, 12544-12554.
[165] Soulere, L.; Barbier, T.; Queneau, Y. Docking-based virtual screening studies aiming at the covalent inhibition of SARS-CoV-2 M(Pro) by targeting the cysteine 145. *Comput. Biol. Chem.*, **2021**, *92*, 107463.
[166] Jimenez-Alberto, A.; Ribas-Aparicio, R.M.; Aparicio-Ozores, G.; Castelan-Vega, J.A. Virtual screening of approved drugs as potential SARS-CoV-2 main protease inhibitors. *Comput. Biol. Chem.*, **2020**, *88*, 107325.
[167] Pitsillou, E.; Liang, J.; Karagiannis, C.; Ververis, K.; Darmawan, K.K.; Ng, K.; Hung, A.; Karagiannis, T.C. Interaction of small molecules with the SARS-CoV-2 main protease in silico and in vitro validation of potential lead compounds using an enzyme-linked immunosorbent assay. *Comput. Biol. Chem.*, **2020**, *89*, 107408.
[168] Nand, M.; Maiti, P.; Joshi, T.; Chandra, S.; Pande, V.; Kuniyal, J.C.; Ramakrishnan, M.A. Virtual screening of anti-HIV1 compounds against SARS-CoV-2: machine learning modeling, chemoinformatics and molecular dynamics simulation based analysis. *Sci. Rep.*, **2020**, *10*(1), 20397.
[169] El Aissouq, A.; Chedadi, O.; Bouachrine, M.; Ouammou, A. Identification of Novel SARS-CoV-2 Inhibitors: A Structure-Based Virtual Screening Approach. *J. Chem.*, **2021**, *2021*, 1-7.
[170] Gahlawat, A.; Kumar, N.; Kumar, R.; Sandhu, H.; Singh, I.P.; Singh, S.; Sjostedt, A.; Garg, P. Structure-Based Virtual Screening to Discover Potential Lead Molecules for the SARS-CoV-2 Main Protease. *J. Chem. Inf. Model*, **2020**, *60*(12), 5781-5793.
[171] Kanhed, A.M.; Patel, D.V.; Teli, D.M.; Patel, N.R.; Chhabria, M.T.; Yadav, M.R. Identification of potential Mpro inhibitors for the treatment of COVID-19 by using systematic virtual screening approach. *Mol. Divers.*, **2021**, *25*(1), 383-401.
[172] Keretsu, S.; Bhujbal, S.P.; Cho, S.J. Rational approach toward COVID-19 main protease inhibitors via molecular docking, molecular dynamics simulation and free energy calculation. *Sci. Rep.*, **2020**, *10*(1), 17716.
[173] Macchiagodena, M.; Pagliai, M.; Procacci, P. Identification of potential binders of the main protease 3CLpro of the COVID-19 via structure-based ligand design and molecular modeling. *Chem. Phys. Lett.*, **2020**, *750*, 137489.
[174] Computable drug discovery - Developing the algorithms to automate drug discovery. https://www.acellera.com/
[175] Santibanez-Moran, M.G.; Lopez-Lopez, E.; Prieto-Martinez, F.D.; Sanchez-Cruz, N.; Medina-Franco, J.L. Consensus virtual screening of dark chemical matter and food chemicals uncover potential inhibitors of SARS-CoV-2 main protease. *RSC Adv.*, **2020**, *10*(42), 25089-25099.
[176] Abel, R.; Paredes Ramos, M.; Chen, Q.; Perez-Sanchez, H.; Coluzzi, F.; Rocco, M.; Marchetti, P.; Mura, C.; Simmaco, M.; Bourne, P.E.; Preissner, R.; Banerjee, P. Computational Prediction of Potential Inhibitors of the Main Protease of SARS-CoV-2. *Front. Chem.*, **2020**, *8*, 590263.
[177] Mahmud, S.; Uddin, M.A.R.; Paul, G.K.; Shimu, M.S.S.; Islam, S.; Rahman, E.; Islam, A.; Islam, M.S.; Promi, M.M.; Emran, T.B.; Saleh, M.A. Virtual screening and molecular dynamics simulation study of plant-derived compounds to identify potential inhibitors of main protease from SARS-CoV-2. *Brief Bioinform.*, **2021**, *22*(2), 1402-1414.
[178] Ogidigo, J.O.; Iwuchukwu, E.A.; Ibeji, C.U.; Okpalefe, O.; Soliman, M.E.S. Natural phyto, compounds as possible noncovalent inhibitors against SARS-CoV2 protease: computational approach. *J. Biomol. Struct. Dyn.*, **2022**, *40*(5), 2284-2301.
[179] Osipiuk, J.; Azizi, S.A.; Dvorkin, S.; Endres, M.; Jedrzejczak, R.; Jones, K.A.; Kang, S.; Kathayat, R.S.; Kim, Y.; Lisnyak, V.G.; Maki, S.L.; Nicolaescu, V.; Taylor, C.A.;

Tesar, C.; Zhang, Y.A.; Zhou, Z.; Randall, G.; Michalska, K.; Snyder, S.A.; Dickinson, B.C.; Joachimiak, A. Structure of papain-like protease from SARS-CoV-2 and its complexes with non-covalent inhibitors. *Nat. Commun.*, **2021**, *12*(1), 743.

[180] Rut, W.; Lv, Z.; Zmudzinski, M.; Patchett, S.; Nayak, D.; Snipas, S.J.; El Oualid, F.; Huang, T.T.; Bekes, M.; Drag, M.; Olsen, S.K. Activity profiling and crystal structures of inhibitor-bound SARS-CoV-2 papain-like protease: A framework for anti-COVID-19 drug design. *Sci. Adv.*, **2020**, *6*(42), eabd4596.

[181] Weglarz-Tomczak, E.; Tomczak, J.M.; Talma, M.; Burda-Grabowska, M.; Giurg, M.; Brul, S. Identification of ebselen and its analogues as potent covalent inhibitors of papain-like protease from SARS-CoV-2. *Sci. Rep.*, **2021**, *11*(1), 3640.

[182] Mirza, M.U.; Ahmad, S.; Abdullah, I.; Froeyen, M. Identification of novel human USP2 inhibitor and its putative role in treatment of COVID-19 by inhibiting SARS-CoV-2 papain-like (PLpro) protease. *Comput. Biol. Chem.*, **2020**, *89*, 107376.

[183] Contreras-Puentes, N.; Alvíz-Amador, A. Virtual Screening of Natural Metabolites and Antiviral Drugs with Potential Inhibitory Activity against 3CL-PRO and PL-PRO. *Biomed. Pharmacol. J.*, **2020**, *13*(2), 933-941.

[184] Jochheim, F.A.; Tegunov, D.; Hillen, H.S.; Schmitzova, J.; Kokic, G.; Dienemann, C.; Cramer, P. The structure of a dimeric form of SARS-CoV-2 polymerase. *Commun. Biol.*, **2021**, *4*(1), 999.

[185] Yin, W.; Mao, C.; Luan, X.; Shen, D.D.; Shen, Q.; Su, H.; Wang, X.; Zhou, F.; Zhao, W.; Gao, M.; Chang, S.; Xie, Y.C.; Tian, G.; Jiang, H.W.; Tao, S.C.; Shen, J.; Jiang, Y.; Jiang, H.; Xu, Y.; Zhang, S.; Zhang, Y.; Xu, H.E. Structural basis for inhibition of the RNA-dependent RNA polymerase from SARS-CoV-2 by remdesivir. *Science*, **2020**, *368*(6498), 1499-1504.

[186] Trott, O.; Olson, A.J. AutoDock Vina: improving the speed and accuracy of docking with a new scoring function, efficient optimization, and multithreading. *J. Comput. Chem.*, **2010**, *31*(2), 455-461.

[187] Aftab, S.O.; Ghouri, M.Z.; Masood, M.U.; Haider, Z.; Khan, Z.; Ahmad, A.; Munawar, N. Analysis of SARS-CoV-2 RNA-dependent RNA polymerase as a potential therapeutic drug target using a computational approach. *J. Transl. Med.*, **2020**, *18*(1), 275.

[188] Kumar, D.T.; Shaikh, N.; Kumar, S.U.; Doss, C.G.; Zayed, H. Structure-Based Virtual Screening to Identify Novel Potential Compound as an Alternative to Remdesivir to Overcome the RdRp Protein Mutations in SARS-CoV-2. *Front. Mol. Biosci.*, **2021**, *8*, 645216.

[189] Pokhrel, R.; Chapagain, P.; Siltberg-Liberles, J. Potential RNA-dependent RNA polymerase inhibitors as prospective therapeutics against SARS-CoV-2. *J. Med. Microbiol.*, **2020**, *69*(6), 864-873.

[190] Jukic, M.; Janezic, D.; Bren, U. Potential Novel Thioether-Amide or Guanidine-Linker Class of SARS-CoV-2 Virus RNA-Dependent RNA Polymerase Inhibitors Identified by High-Throughput Virtual Screening Coupled to Free-Energy Calculations. *Int. J. Mol. Sci.*, **2021**, *22*(20), 11143.

[191] Newman, J.A.; Douangamath, A.; Yadzani, S.; Yosaatmadja, Y.; Aimon, A.; Brandao-Neto, J.; Dunnett, L.; Gorrie-Stone, T.; Skyner, R.; Fearon, D.; Schapira, M.; von Delft, F.; Gileadi, O. Structure, mechanism and crystallographic fragment screening of the SARS-CoV-2 NSP13 helicase. *Nat. Commun.*, **2021**, *12*(1), 4848.

[192] Zhao, Y.; Hongdu, B.; Ma, D.; Chen, Y. Really interesting new gene finger protein 121 is a novel Golgi-localized membrane protein that regulates apoptosis. *Acta Biochim. Biophys. Sin. (Shanghai)*, **2014**, *46*(8), 668-674.

[193] Grishin, N.V. Treble clef finger--a functionally diverse zinc-binding structural motif. *Nucleic Acids Res.*, **2001**, *29*(8), 1703-1714.

[194] Chen, J.; Malone, B.; Llewellyn, E.; Grasso, M.; Shelton, P.M.M.; Olinares, P.D.B.; Maruthi, K.; Eng, E.T.; Vatandaslar, H.; Chait, B.T.; Kapoor, T.M.; Darst, S.A.; Campbell, E.A. Structural Basis for Helicase-Polymerase Coupling in the SARS-CoV-2 Replication-Transcription Complex. *Cell*, **2020**, *182*(6), 1560-1573.

[195] Mirza, M.U.; Froeyen, M. Structural elucidation of SARS-CoV-2 vital proteins: Computational methods reveal potential drug candidates against main protease, Nsp12 polymerase and Nsp13 helicase. *J. Pharm. Anal.*, **2020**, *10*(4), 320-328.

[196] White, M.A.; Lin, W.; Cheng, X. Discovery of COVID-19 Inhibitors Targeting the SARS-CoV2 Nsp13 Helicase. *bioRxiv*, **2020**.

[197] Mesinele, J.; Ruffin, M.; Guillot, L.; Boelle, P.Y.; Corvol, H.; On Behalf Of The French Cf Modifier Gene Study, I. Factors Predisposing the Response to Lumacaftor/Ivacaftor in People with Cystic Fibrosis. *J. Pers. Med.*, **2022**, *12*(2), 252.

[198] Bailly, C. Cepharanthine: An update of its mode of action, pharmacological properties and medical applications. *Phytomedicine*, **2019**, *62*, 152956.

[199] Ahmad, S.; Waheed, Y.; Ismail, S.; Bhatti, S.; Abbasi, S.W.; Muhammad, K. Structure-Based Virtual Screening Identifies Multiple Stable Binding Sites at the RecA Domains of SARS-CoV-2 Helicase Enzyme. *Molecules*, **2021**, *26*(5).

[200] El Hassab, M.A.; Eldehna, W.M.; Al-Rashood, S.T.; Alharbi, A.; Eskandrani, R.O.; Alkahtani, H.M.; Elkaeed, E.B.; Abou-Seri, S.M. Multi-stage structure-based virtual screening approach towards identification of potential SARS-CoV-2 NSP13 helicase inhibitors. *J. Enzyme Inhib. Med. Chem.*, **2022**, *37*(1), 563-572.

[201] Vivek-Ananth, R.P.; Krishnaswamy, S.; Samal, A. Potential phytochemical inhibitors of SARS-CoV-2 helicase Nsp13: a molecular docking and dynamic simulation study. *Mol. Divers.*, **2022**, *26*(1), 429-442.

[202] Liu, C.; Zhu, X.; Lu, Y.; Zhang, X.; Jia, X.; Yang, T. Potential treatment with Chinese and Western medicine targeting NSP14 of SARS-CoV-2. *J. Pharm. Anal.*, **2021**, *11*(3), 272-277.

[203] Selvaraj, C.; Dinesh, D.C.; Panwar, U.; Abhirami, R.; Boura, E.; Singh, S.K. Structure-based virtual screening and molecular dynamics simulation of SARS-CoV-2 Guanine-N7 methyltransferase (nsp14) for identifying antiviral inhibitors against COVID-19. *J. Biomol. Struct. Dyn.*, **2021**, *39*(13), 4582-4593.

[204] Liu, C.; Shi, W.; Becker, S.T.; Schatz, D.G.; Liu, B.; Yang, Y. Structural basis of mismatch recognition by a SARS-CoV-2 proofreading enzyme. *Science*, **2021**, *373*(6559), 1142-1146.
[205] Frazier, M.N.; Dillard, L.B.; Krahn, J.M.; Perera, L.; Williams, J.G.; Wilson, I.M.; Stewart, Z.D.; Pillon, M.C.; Deterding, L.J.; Borgnia, M.J.; Stanley, R.E. Characterization of SARS2 Nsp15 nuclease activity reveals it's mad about U. *Nucleic Acids Res.*, **2021**, *49*(17), 10136-10149.
[206] Kim, Y.; Jedrzejczak, R.; Maltseva, N.I.; Wilamowski, M.; Endres, M.; Godzik, A.; Michalska, K.; Joachimiak, A. Crystal structure of Nsp15 endoribonuclease NendoU from SARS-CoV-2. *Protein Sci.*, **2020**, *29*(7), 1596-1605.
[207] Savale, R.U.; Bhowmick, S.; Osman, S.M.; Alasmary, F.A.; Almutairi, T.M.; Abdullah, D.S.; Patil, P.C.; Islam, M.A. Pharmacoinformatics approach based identification of potential Nsp15 endoribonuclease modulators for SARS-CoV-2 inhibition. *Arch. Biochem. Biophys.*, **2021**, *700*, 108771.
[208] Al-Rashedi, N.A.M.; Munahi, M.G.; Ah, A.L. Prediction of potential inhibitors against SARS-CoV-2 endoribonuclease: RNA immunity sensing. *J. Biomol. Struct. Dyn.*, **2020**, 1-14.
[209] Vijayan, R.; Gourinath, S. Structure-based inhibitor screening of natural products against NSP15 of SARS-CoV-2 revealed thymopentin and oleuropein as potent inhibitors. *J. Proteins Proteom.*, **2021**, *12*(2), 71-80.
[210] Motwalli, O.; Alazmi, M. Analysis of natural compounds against the activity of SARS-CoV-2 NSP15 protein towards an effective treatment against COVID-19: a theoretical and computational biology approach. *J. Mol. Model.*, **2021**, *27*(6), 160.
[211] Saeed, M.; Saeed, A.; Alam, M.J.; Alreshidi, M. Identification of Persuasive Antiviral Natural Compounds for COVID-19 by Targeting Endoribonuclease NSP15: A Structural-Bioinformatics Approach. *Molecules*, **2020**, *25*(23), 5657.
[212] Murugan, N.A.; Kumar, S.; Jeyakanthan, J.; Srivastava, V. Searching for target-specific and multi-targeting organics for Covid-19 in the Drugbank database with a double scoring approach. *Sci. Rep.*, **2020**, *10*(1), 19125.
[213] Dotolo, S.; Marabotti, A.; Facchiano, A.; Tagliaferri, R. A review on drug repurposing applicable to COVID-19. *Brief Bioinform.*, **2021**, *22*(2), 726-741.
[214] Tazeen, A.; Deeba, F.; Alam, A.; Ali, R.; Ishrat, R.; Ahmed, A.; Ali, S.; Parveen, S. Virtual Screening of Potential Therapeutic Inhibitors Against Spike, Helicase, and Polymerase of SARS-CoV-2 (COVID-19). *Coronaviruses*, **2021**, *2*(1), 89-105.
[215] Ginex, T.; Garaigorta, U.; Ramirez, D.; Castro, V.; Nozal, V.; Maestro, I.; Garcia-Carceles, J.; Campillo, N.E.; Martinez, A.; Gastaminza, P.; Gil, C. Host-Directed FDA-Approved Drugs with Antiviral Activity against SARS-CoV-2 Identified by Hierarchical In Silico/In Vitro Screening Methods. *Pharmaceuticals (Basel)*, **2021**, *14*(4), 332.
[216] Mishra, D.; Maurya, R.R.; Kumar, K.; Munjal, N.S.; Bahadur, V.; Sharma, S.; Singh, P.; Bahadur, I. Structurally modified compounds of hydroxychloroquine, remdesivir and tetrahydrocannabinol against main protease of SARS-CoV-2, a possible hope for COVID-19: Docking and molecular dynamics simulation studies. *J. Mol. Liq.*, **2021**, *335*, 116185.
[217] Nunes, V.S.; Paschoal, D.F.S.; Costa, L.A.S.; Santos, H.F.D. Antivirals virtual screening to SARS-CoV-2 non-structural proteins. *J. Biomol. Struct. Dyn.*, **2021**, 1-15.
[218] Barros, R.O.; Junior, F.; Pereira, W.S.; Oliveira, N.M.N.; Ramos, R.M. Interaction of Drug Candidates with Various SARS-CoV-2 Receptors: An in Silico Study to Combat COVID-19. *J. Proteome Res.*, **2020**, *19*(11), 4567-4575.
[219] Gupta, Y.; Maciorowski, D.; Zak, S.E.; Jones, K.A.; Kathayat, R.S.; Azizi, S.A.; Mathur, R.; Pearce, C.M.; Ilc, D.J.; Husein, H.; Herbert, A.S.; Bharti, A.; Rathi, B.; Durvasula, R.; Becker, D.P.; Dickinson, B.C.; Dye, J.M.; Kempaiah, P. Bisindolylmaleimide IX: A novel anti-SARS-CoV2 agent targeting viral main protease 3CLpro demonstrated by virtual screening pipeline and in-vitro validation assays. *Methods*, **2021**, *195*, 57-71.
[220] Kumar, S.; Sharma, P.P.; Upadhyay, C.; Kempaiah, P.; Rathi, B.; Poonam. Multi-targeting approach for nsp3, nsp9, nsp12 and nsp15 proteins of SARS-CoV-2 by Diosmin as illustrated by molecular docking and molecular dynamics simulation methodologies. *Methods*, **2021**, *195*, 44-56.
[221] Grahl, M.V.C.; Alcara, A.M.; Perin, A.P.A.; Moro, C.F.; Pinto, E.S.M.; Feltes, B.C.; Ghilardi, I.M.; Rodrigues, F.V.F.; Dorn, M.; da Costa, J.C.; Norberto de Souza, O.; Ligabue-Braun, R. Evaluation of drug repositioning by molecular docking of pharmaceutical resources available in the Brazilian healthcare system against SARS-CoV-2. *Inform. Med. Unlocked*, **2021**, *23*, 100539.
[222] Kadioglu, O.; Saeed, M.; Greten, H.J.; Efferth, T. Identification of novel compounds against three targets of SARS CoV-2 coronavirus by combined virtual screening and supervised machine learning. *Comput. Biol. Med.*, **2021**, *133*, 104359.
[223] Naik, B.; Mattaparthi, V.S.K.; Gupta, N.; Ojha, R.; Das, P.; Singh, S.; Prajapati, V.K.; Prusty, D. Chemical system biology approach to identify multi-targeting FDA inhibitors for treating COVID-19 and associated health complications. *J. Biomol. Struct. Dyn.*, **2021**, 1-25.
[224] Almeida, J.; Botelho, F.D.; de Souza, F.R.; Dos Santos, M.C.; Goncalves, A.D.S.; Rodrigues, R.L.B.; Cardozo, M.; Kitagawa, D.A.S.; Vieira, L.A.; Silva, R.S.F.; Cavalcante, S.F.A.; Bastos, L.D.C.; Nogueira, M.O.T.; de Santana, P.I.R.; Brum, J.O.C.; Nepovimova, E.; Kuca, K.; LaPlante, S.R.; Galante, E.B.F.; Franca, T.C.C. Searching for potential drugs against SARS-CoV-2 through virtual screening on several molecular targets. *J. Biomol. Struct. Dyn.*, **2021**, 1-14.
[225] Singh, J.; Malik, D.; Raina, A. Computational investigation for identification of potential phytochemicals and antiviral drugs as potential inhibitors for RNA-dependent RNA polymerase of COVID-19. *J. Biomol. Struct. Dyn.*, **2020**, 1-16.
[226] Rabie, A.M. CoViTris2020 and ChloViD2020: a striking new hope in COVID-19 therapy. *Mol. Divers.*, **2021**, *25*(3), 1839-1854.
[227] Thurakkal, L.; Singh, S.; Roy, R.; Kar, P.; Sadhukhan, S.; Porel, M. An in-silico study on selected organosulfur compounds as potential drugs for SARS-CoV-2

infection via binding multiple drug targets. *Chem. Phys. Lett.*, **2021**, *763*, 138193.
[228] Fayyazi, N.; Mostashari-Rad, T.; Ghasemi, J.B.; Ardakani, M.M.; Kobarfard, F. Molecular dynamics simulation, 3D-pharmacophore and scaffold hopping analysis in the design of multi-target drugs to inhibit potential targets of COVID-19. *J. Biomol. Struct. Dyn.*, **2021**, 1-22.
[229] Halgren, T.A.; Murphy, R.B.; Friesner, R.A.; Beard, H.S.; Frye, L.L.; Pollard, W.T.; Banks, J.L. Glide: a new approach for rapid, accurate docking and scoring. 2. Enrichment factors in database screening. *J. Med. Chem.*, **2004**, *47*(7), 1750-1759.
[230] SwissADME. http://www.swissadme.ch/
[231] Pharmacokinetic properties. http://biosig.unimelb.edu.au/pkcsm/prediction
[232] Esam, Z.; Akhavan, M.; Lotfi, M.; Bekhradnia, A. Molecular docking and dynamics studies of Nicotinamide Riboside as a potential multi-target nutraceutical against SARS-CoV-2 entry, replication, and transcription: A new insight. *J. Mol. Struct.*, **2022**, *1247*, 131394.
[233] Ayipo, Y.O.; Ahmad, I.; Najib, Y.S.; Sheu, S.K.; Patel, H.; Mordi, M.N. Molecular modelling and structure-activity relationship of a natural derivative of o-hydroxybenzoate as a potent inhibitor of dual NSP3 and NSP12 of SARS-CoV-2: in silico study. *J. Biomol. Struct. Dyn.*, **2022**, 1-19.
[234] Fan, L.; Feng, S.; Wang, T.; Ding, X.; An, X.; Wang, Z.; Zhou, K.; Wang, M.; Zhai, X.; Li, Y. Chemical composition and therapeutic mechanism of Xuanbai Chengqi Decoction in the treatment of COVID-19 by network pharmacology, molecular docking and molecular dynamic analysis. *Mol. Divers.*, **2022**, 1-22.
[235] Kumar, R.P.; Siddique, S. 22-Hydroxyhopane, a novel multitargeted phytocompound against SARS-CoV-2 from Adiantum latifolium Lam. *Nat. Prod. Res.*, **2021**, 1-6.
[236] Azim, K.F.; Ahmed, S.R.; Banik, A.; Khan, M.M.R.; Deb, A.; Somana, S.R. Screening and druggability analysis of some plant metabolites against SARS-CoV-2: An integrative computational approach. *Inform. Med. Unlocked*, **2020**, *20*, 100367.
[237] Gupta, S.; Singh, V.; Varadwaj, P.K.; Chakravartty, N.; Katta, A.; Lekkala, S.P.; Thomas, G.; Narasimhan, S.; Reddy, A.R.; Reddy Lachagari, V.B. Secondary metabolites from spice and herbs as potential multitarget inhibitors of SARS-CoV-2 proteins. *J. Biomol. Struct. Dyn.*, **2022**, *40*(5), 2264-2283.
[238] Prasanth, D.; Murahari, M.; Chandramohan, V.; Panda, S.P.; Atmakuri, L.R.; Guntupalli, C. In silico identification of potential inhibitors from Cinnamon against main protease and spike glycoprotein of SARS CoV-2. *J. Biomol. Struct. Dyn.*, **2021**, *39*(13), 4618-4632.
[239] Wong, F.C.; Ong, J.H.; Kumar, D.T.; Chai, T.T. In Silico Identification of Multi-target Anti-SARS-CoV-2 Peptides from Quinoa Seed Proteins. *Int. J. Pept. Res. Ther.*, **2021**, *27*(3), 1837-1847.
[240] Gao, L.Q.; Xu, J.; Chen, S.D. In Silico Screening of Potential Chinese Herbal Medicine Against COVID-19 by Targeting SARS-CoV-2 3CLpro and Angiotensin Converting Enzyme II Using Molecular Docking. *Chin. J. Integr. Med.*, **2020**, *26*(7), 527-532.
[241] Isidoro, C.; Chiung-Fang Chang, A.; Sheen, L.Y. Natural products as a source of novel drugs for treating SARS-CoV2 infection. *J. Tradit. Complement. Med.*, **2022**, *12*(1), 1-5.
[242] Ye, M.; Luo, G.; Ye, D.; She, M.; Sun, N.; Lu, Y.J.; Zheng, J. Network pharmacology, molecular docking integrated surface plasmon resonance technology reveals the mechanism of Toujie Quwen Granules against coronavirus disease 2019 pneumonia. *Phytomedicine*, **2021**, *85*, 153401.
[243] Wang, J.; Ge, W.; Peng, X.; Yuan, L.; He, S.; Fu, X. Investigating the active compounds and mechanism of HuaShi XuanFei formula for prevention and treatment of COVID-19 based on network pharmacology and molecular docking analysis. *Mol. Divers.*, **2021**, 1-16.
[244] Li, Y.; Chu, F.; Li, P.; Johnson, N.; Li, T.; Wang, Y.; An, R.; Wu, D.; Chen, J.; Su, Z.; Gu, X.; Ding, X. Potential effect of Maxing Shigan decoction against coronavirus disease 2019 (COVID-19) revealed by network pharmacology and experimental verification. *J. Ethnopharmacol.*, **2021**, *271*, 113854.
[245] Li, X.; Lin, H.; Wang, Q.; Cui, L.; Luo, H.; Luo, L. Chemical composition and pharmacological mechanism of shenfu decoction in the treatment of novel coronavirus pneumonia (COVID-19). *Drug Dev. Ind. Pharm.*, **2020**, *46*(12), 1947-1959.
[246] Dai, Y.J.; Wan, S.Y.; Gong, S.S.; Liu, J.C.; Li, F.; Kou, J.P. Recent advances of traditional Chinese medicine on the prevention and treatment of COVID-19. *Chin. J. Nat. Med.*, **2020**, *18*(12), 881-889.
[247] Alanazi, K.M.; Farah, M.A.; Hor, Y.Y. Multi-Targeted Approaches and Drug Repurposing Reveal Possible SARS-CoV-2 Inhibitors. *Vaccines (Basel)*, **2021**, *10*(1), 24.
[248] Schwede, T.; Kopp, J.; Guex, N.; Peitsch, M.C. SWISS-MODEL: An automated protein homology-modeling server. *Nucleic Acids Res.*, **2003**, *31*(13), 3381-3385.
[249] Jones, G.; Willett, P.; Glen, R.C.; Leach, A.R.; Taylor, R. Development and validation of a genetic algorithm for flexible docking. *J. Mol. Biol.*, **1997**, *267*(3), 727-748.
[250] de Leon, V.N.O.; Manzano, J.A.H.; Pilapil, D.Y.H.t.; Fernandez, R.A.T.; Ching, J.; Quimque, M.T.J.; Agbay, J.C.M.; Notarte, K.I.R.; Macabeo, A.P.G. Anti-HIV reverse transcriptase plant polyphenolic natural products with in silico inhibitory properties on seven non-structural proteins vital in SARS-CoV-2 pathogenesis. *J. Genet. Eng. Biotechnol.*, **2021**, *19*(1), 104.
[251] Pettersen, E.F.; Goddard, T.D.; Huang, C.C.; Couch, G.S.; Greenblatt, D.M.; Meng, E.C.; Ferrin, T.E. UCSF Chimera--a visualization system for exploratory research and analysis. *J. Comput. Chem.*, **2004**, *25*(13), 1605-1612.
[252] OSIRIS Property explorer - Cheminfo.org. http://www.cheminfo.org/Chemistry/Cheminformatics/Property_explorer/index.html
[253] Chourasia, R.; Padhi, S.; Chiring Phukon, L.; Abedin, M.M.; Singh, S.P.; Rai, A.K. A Potential Peptide From Soy Cheese Produced Using Lactobacillus delbrueckii WS4 for Effective Inhibition of SARS-CoV-2 Main Protease and S1 Glycoprotein. *Front. Mol. Biosci.*, **2020**, *7*, 601753.
[254] Minkiewicz, P.; Iwaniak, A.; Darewicz, M. BIOPEP-UWM Database of Bioactive Peptides: Current Opportunities. *Int. J. Mol. Sci.*, **2019**, *20*(23), 5978.

[255] ToxinPred - Open Source Drug Discovery. http://crdd.osdd.net/raghava/toxinpred
[256] Bioinformatics tool for allergenicity prediction.
[257] Haribabu, J.; Garisetti, V.; Malekshah, R.E.; Srividya, S.; Gayathri, D.; Bhuvanesh, N.; Mangalaraja, R.V.; Echeverria, C.; Karvembu, R. Design and synthesis of heterocyclic azole based bioactive compounds: Molecular structures, quantum simulation, and mechanistic studies through docking as multi-target inhibitors of SARS-CoV-2 and cytotoxicity. *J. Mol. Struct.*, **2022**, *1250*, 131782.
[258] Gorgulla, C.; Padmanabha Das, K.M.; Leigh, K.E.; Cespugli, M.; Fischer, P.D.; Wang, Z.F.; Tesseyre, G.; Pandita, S.; Shnapir, A.; Calderaio, A.; Gechev, M.; Rose, A.; Lewis, N.; Hutcheson, C.; Yaffe, E.; Luxenburg, R.; Herce, H.D.; Durmaz, V.; Halazonetis, T.D.; Fackeldey, K.; Patten, J.J.; Chuprina, A.; Dziuba, I.; Plekhova, A.; Moroz, Y.; Radchenko, D.; Tarkhanova, O.; Yavnyuk, I.; Gruber, C.; Yust, R.; Payne, D.; Naar, A.M.; Namchuk, M.N.; Davey, R.A.; Wagner, G.; Kinney, J.; Arthanari, H. A multi-pronged approach targeting SARS-CoV-2 proteins using ultra-large virtual screening. *iScience*, **2021**, *24*(2), 102021.
[259] Choudhary, S.; Silakari, O. Scaffold morphing of arbidol (umifenovir) in search of multi-targeting therapy halting the interaction of SARS-CoV-2 with ACE2 and other proteases involved in COVID-19. *Virus Res.*, **2020**, *289*, 198146.
[260] Freidel, M.R.; Armen, R.S. Mapping major SARS-CoV-2 drug targets and assessment of druggability using computational fragment screening: Identification of an allosteric small-molecule binding site on the Nsp13 helicase. *PLoS One*, **2021**, *16*(2), e0246181.
[261] Skariyachan, S.; Gopal, D.; Deshpande, D.; Joshi, A.; Uttarkar, A.; Niranjan, V. Carbon fullerene and nanotube are probable binders to multiple targets of SARS-CoV-2: Insights from computational modeling and molecular dynamic simulation studies. *Infect. Genet. Evol.*, **2021**, *96*, 105155.
[262] Veber, D.F.; Johnson, S.R.; Cheng, H.Y.; Smith, B.R.; Ward, K.W.; Kopple, K.D. Molecular properties that influence the oral bioavailability of drug candidates. *J. Med. Chem.*, **2002**, *45*(12), 2615-2623.
[263] Cheng, F.; Li, W.; Zhou, Y.; Shen, J.; Wu, Z.; Liu, G.; Lee, P.W.; Tang, Y. admetSAR: a comprehensive source and free tool for assessment of chemical ADMET properties. *J. Chem. Inf. Model.*, **2012**, *52*(11), 3099-3105.
[264] Verstraete, N.; Jurman, G.; Bertagnolli, G.; Ghavasieh, A.; Pancaldi, V.; De Domenico, M. CovMulNet19, Integrating Proteins, Diseases, Drugs, and Symptoms: A Network Medicine Approach to COVID-19. *Netw. Syst. Med.*, **2020**, *3*(1), 130-141.
[265] Nam, Y.; Yun, J.-S.; Lee, S.M.; Park, J.W.; Chen, Z.; Lee, B.; Verma, A.; Ning, X.; Shen, L.; Kim, D. Network reinforcement driven drug repurposing for COVID-19 by exploiting disease-gene-drug associations. *medRxiv* **2020**, *ppmedrxiv-20173120*.
[266] Fiscon, G.; Conte, F.; Farina, L.; Paci, P. SAveRUNNER: A network-based algorithm for drug repurposing and its application to COVID-19. *PLoS Comput. Biol.*, **2021**, *17*(2), e1008686.
[267] Mohapatra, S.; Nath, P.; Chatterjee, M.; Das, N.; Kalita, D.; Roy, P.; Satapathi, S. Repurposing therapeutics for COVID-19: Rapid prediction of commercially available drugs through machine learning and docking. *PLoS One*, **2020**, *15*(11), e0241543.